A bacteria-responsive drug release platform for the local treatment of bacterial vaginosis

by

Chuying Feng

A thesis

presented to the University of Waterloo

in fulfillment of the

thesis requirement for the degree of

Master of Science

in

Pharmacy

Waterloo, Ontario, Canada, 2022

© Chuying Feng 2022

Author's Declaration

I hereby declare that I am the sole author of this thesis. This is a true copy of the thesis, including any required final revisions, as accepted by my examiners. I understand that my thesis may be made electronically available to the public.

Abstract

Bacterial vaginosis (BV) is a common vaginal anaerobic dysbiosis affecting millions of women, with a high recurrence rate probably due to the stubborn existence of biofilms and *Gardnerella vaginalis* (*G. vaginalis*) as the primary pathogen. Antimicrobial therapy has been the standard treatment for BV for several decades, which includes oral and intravaginal therapy. However, the major drawback of using antibiotics extensively is drug resistance, leading to the ineffectiveness in killing bacterial pathogens. Stimuli-responsive systems are a promising solution to address bacterial resistance because they release drugs only in the presence of specific stimulus, e.g., changes in physical micro-environment and bacterial factors, which greatly avoids overdosing. In terms of treatment method, intravaginal formulations are superior to the conventional oral route with reduced side effects such as stomach irritation and more effective drug dose. This thesis focused on the development and characterization of a bacteria-responsive drug release platform that is aimed for intravaginal therapy to cure BV. Vaginolysin (VLY), a virulence factor produced specifically by *G. vaginalis,* was utilized as the stimulus to trigger drug release with the aim of achieving high specificity and improving antibacterial activity.

Series of liposome formulations were developed, optimized, and characterized in terms of preparation method, purification method, encapsulation efficiency, size distribution and zeta potential. We demonstrated that centrifugation was the optimal method to separate liposomes from the model free drug (calcein) while keeping liposomes stable without much aggregation. Increasing the initial calcein concentration and total amount of lipids facilitated a higher

encapsulation efficiency. All liposomes had an average diameter of around 300 nm with a polydispersity index (PDI) less than 0.3 and an average zeta potential of -60 mV.

Second, we optimized bacteria culture and evaluated the responsive calcein release in the presence of *G. vaginalis* and *Lactobacillus crispatus* (*L. crispatus*) supernatants. All liposome formulations showed sustained calcein release (cumulative release: 46.7%-51.8%) in response to *G. vaginalis* supernatant and very little calcein release (cumulative release: 1.1%) in the presence of *L. crispatus* supernatant, indicating that the responsive drug release platform had good specificity.

We then constructed an *Escherichia coli* (*E. coli*)-based recombinant protein expression system to express recombinant VLY which could be used as a standard to quantify VLY produced by *G. vaginalis*. After that, a series of optimizations in terms of host strain, cultivation conditions, cell lysis method, purification process optimization, etc. regarding recombinant VLY expression were carried out to promote soluble protein production. Unfortunately, we did not achieve the desired results as the recombinant VLY was expressed in the form of inclusion bodies.

Overall, the bacteria-responsive drug release platform has great potential, since it will be the first time to realize controlled drug release activated by a specific pathogen for BV prevention and treatment. This on-demand therapy can be potentially used by industry to provide millions of women patients with more sexual and reproductive health care.

Acknowledgements

I would like to express my sincere gratitude and appreciation to my supervisor Dr. Emmanuel A. Ho for his constant support and guidance. I am so grateful to him for offering me a precious opportunity to further my studies at the University of Waterloo and encouraging me to become a creative and self-motivated scientist. Without his trust and encouragement, I would not have been gone that far in a completely new research field that I was not familiar with.

I would like to thank my advisory and examination committee members, Dr. Shawn Wettig, Dr. Jonathan Blay, and Dr. Jean Duhamel for providing me with valuable insights in experiment design and thesis revision throughout the duration of my studies.

I would also like to express my thanks to Shirley Wong and Deborah Pushparajah for all the laboratory skills passed down to me and their friendship. Without their expertise in molecular biology, the completion of my project would not have been possible.

I feel so fortunate to have had wonderful lab mates: Yannick, Jin, Sihan, Derek, Nehil, Alistair and Calvin. I am sincerely thankful to all of them for offering me valuable suggestions and discussions. I will treasure the friendship and those memorable moments forever.

I would like to thank my family for their unconditional love, support and understanding. They motivated me to do my utmost in all aspects of my life and to become a woman with kindness, integrity, and diligence.

I am grateful to University of Waterloo scholarships, Canadian Society for Pharmaceutical Sciences and Gattefossé for their generous financial assistance that supports me to finish my studies.

Dedication

I would like to dedicate this thesis to my grandparents Naining Liu and Yanyu Chen, my mother Jian Liu, and my husband Zeyu Yang. Thank you for always standing by my side through all the ups and downs. Without your love and support I would have not been the person I am today.

Table of Contents

Author's Declaration ii

Abstract iii

Acknowledgements v

Dedication vi

List of Figures xi

List of Tables xx

List of Abbreviations xxii

Chapter 1 Introduction 1

1.1 Bacterial vaginosis 1

1.2 Treatment for bacterial vaginosis 4

1.3 Formulation strategies for treating bacterial vaginosis 7

1.3.1 Oral vs. intravaginal therapy 7

1.4 Bacteria-responsive drug release systems 12

1.4.1 pH-responsive systems 13

1.4.2 ROS-responsive systems 15

1.4.3 Enzyme/toxin-responsive systems 15

1.4.4 Combination therapies 21

1.5 Recombinant VLY protein expression 22

1.5.1 Recombinant protein expression in *Escherichia coli* 22

1.5.2 Expression plasmid selection 23

1.5.3 Host strain selection 27
1.5.4 Problems with recombinant protein production 27
1.6 Project rationale 30
1.7 Hypothesis and objectives 31
Chapter 2 Liposome preparation and characterization 32
2.1 Materials 32
2.2 Methods 32
2.2.1 Calcein calibration curve 32
2.2.2 Polyol dilution method 33
2.2.3 Encapsulation efficiency calculation and optimization 34
2.2.4 Characterization of size distribution and zeta potential 36
2.3 Results and discussion 36
2.3.1 Calcein calibration curve 36
2.3.2 Liposome preparation and purification 38
2.3.2 Liposome size distribution and zeta potential 43
Chapter 3 Bacteria-responsive drug release platform development 46
3.1 Materials 46
3.2 Methods 46
3.2.1 Bacteria culture 46
3.2.2 Bacteria counting 48
3.2.3 Calcein calibration curve 49
3.2.4 Bacteria-responsive calcein release of liposomes 49

3.3 Results and discussion 50
3.3.1 *G. vaginalis* culture optimization 50
3.3.2 Bacteria counting 54
3.3.3 Calcein calibration curve 56
3.3.4 Calcein fluorescence stability in different media 57
3.3.5 Responsive calcein release profile 58
Chapter 4 VLY gene cloning and recombinant protein expression system construction 61
4.1 Materials 61
4.2 Methods 62
4.2.1 *G. vaginalis* genomic DNA extraction and purification 62
4.2.2 VLY gene cloning 63
4.2.3 Construction of recombinant protein expression system 66
4.3 Results and discussion 72
4.3.1 *G. vaginalis* genomic DNA extraction and purification 72
4.3.2 VLY gene cloning 72
4.3.3 Construction of recombinant protein expression system 74
4.3.4 DNA sequencing of the recombinant plasmid 79
Chapter 5 Recombinant VLY expression and purification 81
5.1 Materials 81
5.2 Methods 81
5.2.1 Induction of recombinant VLY expression within the *E. coli* vector 81
5.2.2 *E. coli* cell lysis 83

5.2.3 Column purification of soluble recombinant VLY 84

5.2.4 Purification of inclusion bodies using the Bugbuster® reagent 85

5.2.5 Protein gel electrophoresis 85

5.2.6 Solubilization and column purification of inclusion body 86

5.3 Results and discussion 87

5.3.1 Induction within BL21(DE3) *E. coli* cells 87

5.3.2 Induction within BL21-CodonPlus (DE3)-RIPL *E. coli* cells 97

Chapter 6 Conclusions and future directions 104

Letters of Copyright Permissions 107

References 108

List of Figures

Figure 1.1 *G. vaginalis* (maroon) associated with the surface of a mouse vaginal epithelial cell (purple). Uranyl acetate staining was followed by transmission electron microscopy. Reprinted with permission from PubMed Central. 2

Figure 1.2 The process of polymicrobial biofilm formation in BV: secondary bacteria will incorporate the biofilm after the initial colonizer species has already adhered to the surface; a synergetic relationship can then be formed, allowing the biofilm to prosper. Created with BioRender.com. 3

Figure 1.3 Crystal structure of VLY in complex with hCD59. VLY interacts with hCD59 via the β-tongue located in D4. Loop L1 contains the Thr-Leu (TL) pair of CRM. Created with Swiss-Model. 4

Figure 1.4 Internal stimuli generated from micro-environmental changes in the presence of bacteria. Created with BioRender.com. 13

Figure 1.5 Schematic of two drug release mechanisms for designing enzyme-responsive systems: (A) direct release/activation; (B) indirect release/activation. Created with BioRender.com. 16

Figure 1.6 Schematic of the lipase-responsive drug delivery based on a polymeric triple-layered nanogel to treat bacterial infections. Created with BioRender.com. 18

Figure 1.7 Schematic of the hyaluronidase-responsive multilayer-based drug delivery system. Created with ChemDraw Professional 20.1 (PerkinElmer). 19

Figure 1.8 Schematic of phospholipase A2 (PLA_2)-responsive drug delivery based on chitosan-modified gold nanoparticles-stabilized liposomes to treat *H. pylori*. Created with BioRender.com. 19

Figure 1.9 Schematic of toxin-responsive drug release from gold nanoparticles-stabilized liposomes to treat *S. aureus*. Created with BioRender.com. 20

Figure 1.10 Schematic of recombinant protein expression in *E. coli*. Created with BioRender.com. 23

Figure 1.11 Genetic elements of a plasmid vector. Created with BioRender.com. 24

Figure 1.12 The mechanism of IPTG induction. When IPTG is absent, the *lac* repressor binds tightly to the operator preventing transcription by RNA polymerase. When IPTG is present, it binds to the repressor and separates it from the operator. This allows transcription by RNA polymerase. Created with BioRender.com. 26

Figure 2.1 Calcein calibration curve. Known concentrations of calcein (0 – 4 μg/mL) were used. Fluorescence emission was measured at 520 nm with excitation wavelength at 490 nm. Values represent mean +/- standard deviation (n=3). 37

Figure 2.2 The fluorescence spectra (500 – 650 nm) of calcein aqueous solutions with different concentration ranging from 0.1 to 4 μg/mL. (Excitation wavelength: 490 nm) 37

Figure 2.3 The absorption spectra (300 – 800 nm) of calcein aqueous solutions with concentrations of 1 μg/mL and 0.1 μg/mL. MilliQ water (pH 7.4) was set as blank. Note: the absorption spectrum of the 1 μg/mL calcein solution and the blank cannot be distinguished experimentally. 38

Figure 2.4 Comparison of liposome size distribution before and after centrifugation. Liposomes were prepared by sonication for 200 s at amplitude 3 using a sonicator. The liposomal suspension

was centrifuged at 40,000 g for 2 hours at 4 °C to remove non-encapsulated calcein. The liposomes harvested from centrifugation was completely resuspended in Milli-Q water (pH 7.4) prior to DLS measurement. The Z-average diameter values are the means +/- standard deviation of six repeat measurements (P value > 0.05). 40

Figure 2.5 EE of liposome formulations (F2_1-F2_6) calculated using direct method. F2_1: 0.11 mM lipids, 300 μL of 2 mg/mL initial calcein; F2_2: 0.22 mM lipids, 300 μL of 2 mg/mL initial calcein; F2_3: 0.33 mM lipids, 300 μL of 2 mg/mL initial calcein; F2_4: 0. 33 mM lipids, 300 μL of 4 mg/mL initial calcein; F2_5: 0.33 mM lipids, 2 mL of 2 mg/mL initial calcein; F2_6: 0.33 mM lipids, 2 mL of 4 mg/mL initial calcein. All values represent the means of three preparations +/- standard deviation. (P value < 0.05) 43

Figure 2.6 Size distribution of liposomes (Formulation 2) with varying sonication time lengths ranging from 80 s to 600 s without using PES filter. The Z-average diameter values are the means of six repeat measurements (+/- standard deviation). 44

Figure 3.1 *G. vaginalis* growth in liquid culture. 100 μL cells were inoculated into 10 mL broth and incubated at 37 °C. Alternatively, one CFU was scratched from the plate and inoculated into 10 mL broth and incubated at 37 °C. Values represent the mean of three recordings 52

Figure 3.2 Columbia agar plate. No bacteria growth was observed after one week of cultivation. 52

Figure 3.3 1685 NYC III agar plate (spreading). Bacteria lawn formed after 48 hours of cultivation. 53

Figure 3.4 1685 NYC III agar plate (streaking). Very few CFUs were found after 48 hours of cultivation. 53

Figure 3.5 Casman agar plate (streaking). CFUs were found after 36-48 hours of cultivation…...
…….56
Figure 3.6 CFUs of *G. vaginalis* grown on Casman agar plates (5% rabbit blood). a) 1,000-fold dilution; b) 10,000-fold dilution; c) 100,000-fold dilution. For each plate, 50 μL bacterial cells and 50 μL 1685 NYC III medium were spread. 55
Figure 3.7 *L. crispatus* growth (OD_{600}) in liquid culture. 100 μL cells were inoculated into 10 mL broth and incubated at 37 °C. Alternatively, one CFU was scratched from the plate and inoculated into 10 mL broth and incubated at 37 °C. Values represent the mean of three recordings. 55
Figure 3.8 CFUs of *L. crispatus* grown on MRS agar plates. a) 100-fold dilution; b) 1,000-fold dilution; c) 10,000-fold dilution; d)100,000-fold dilution. For each plate, 100 µL bacterial cells were spread. 56
Figure 3.9 Calcein calibration curve in 1685 NYC III medium. Known concentrations of calcein (0-10 μg/mL) were used. Fluorescence emission was measured at 520 nm with excitation wavelength at 490 nm. Values represent mean +/- standard deviation (n=3)..... 56
Figure 3.10 Calcein calibration curve in MRS medium. Known concentrations of calcein (0-4 μg/mL) were used. Fluorescence emission was measured at 520 nm with excitation wavelength at 490 nm. Values represent mean +/- standard deviation (n=3). 57
Figure 3.11 Calcein fluorescence stability in 1685 NYC III medium and *G. vaginalis* supernatant. The initial concentration of calcein is 10 μg/mL. 58
Figure 3.12 Comparison of cumulative calcein release stimulated by *G. vaginalis*. The values represent mean +/- standard deviation (n=3). 59

Figure 3.13 Cumulative calcein released from Formulation 2 in the presence of *G. vaginalis* supernatant or *L. crispatus* supernatant. The amount of calcein released from pure medium was subtracted to eliminate the difference caused by medium. The values represent mean +/-standard deviation (n=3). 60

Figure 4.1 Schematic of recombinant plasmid construction. 71

Figure 4.2 *G. vaginalis* genomic DNA concentration measured by Nanodrop™ 2000 spectrophotometer. 72

Figure 4.3 Agarose gel electrophoresis of DNA samples. Lane 2-lane 5 are the gene fragments amplified using primer pair 1, 2, 3, and 4 separately. Lane 6 is the control group using primer pair 1 without genomic DNA template. 73

Figure 4.4 Agarose gel electrophoresis of double digested DNA samples. Lane 2-lane 4 are the double digested gene fragments of vector pET-28a(+) (the linearized plasmid vector). Lane 5 and 6 are double digested VLY gene fragment_1 and double digested VLY gene fragment_2, respectively. 74

Figure 4.5 (a) The 5-α *E. coli* colonies grown on the LB selection plate (containing 50 μg/mL Kanamycin); (b) The 5-α *E. coli* colonies (concentrated) grown on the LB selection plate (containing 50 μg/mL Kanamycin). 75

Figure 4.6 Agarose gel electrophoresis of VLY gene fragments amplified using T7 primers. Lane 2-Lane 5 are the amplified DNA fragments using four CFUs scratched from the selection plates as PCR template. Lane 6 is the control group using T7 primers without template. 76

Figure 4.7 (a) The BL21 (DE3) *E. coli* colonies grown on the LB selection plate (containing 50 μg/mL Kanamycin); (b) The BL21 (DE3) *E. coli* colonies (concentrated) grown on the LB selection plate (containing 50 μg/mL Kanamycin)..... 77

Figure 4.8 Agarose gel electrophoresis of VLY gene fragments amplified using T7 primers. Lane 2-Lane 6 are the amplified DNA fragments using five CFUs scratched from the selection plates as PCR template. Lane 7 is the control group using T7 primers without template..... 78

Figure 4.9 (a) The BL21-CodonPlus (DE3)-RIPL *E. coli* colonies grown on the LB selection plate (containing 50 μg/mL Kanamycin and 50 μg/mL chloramphenicol); (b) The BL21-CodonPlus (DE3)-RIPL *E. coli* colonies (concentrated) grown on the LB selection plate (containing 50 μg/mL Kanamycin and 50 μg/mL chloramphenicol). 78

Figure 4.10 Agarose gel electrophoresis of VLY gene fragments amplified using T7 primers. Lane 1 is the ladder. Lane 2-9 are the amplified DNA fragments using eight CFUs scratched from the selection plates as PCR template. Lane 10 is the control group using T7 primers without template. 80

Figure 4.11 Schematic of the recombinant pET-28a(+) vector with the inserted VLY gene sequence. 80

Figure 5.1 SDS-PAGE gel image. BL21 (DE3) *E. coli* cells were induced with 0.1 mM IPTG at 30 °C for 20 hours. The cells were lysed by ultrasonication and BugBuster® reagent separately. Cell debris is the resuspended pellets after spinning down the lysate harvested by ultrasonication method at 16,000 g for 20 minutes at 4 °C. Loading sample 1 is the supernatant from the cell debris. Loading sample 2 is the supernatant from cell debris lysed with BugBuster® reagent (DNase and $MgCl_2$ added). Flow-through is the elute from the column with no imidazole present. Wash is

the elute from the column with 60 mM imidazole. Elution 1, 2 and 3 are the elutes of Culture 1 from the column with 100 mM imidazole, 200 mM imidazole and 500 mM imidazole respectively. 93

Figure 5.2 SDS-PAGE gel image. Three cultures of BL21 (DE3) *E. coli* cells were induced with 0.1 mM IPTG at 20 °C for 20 hours. The cells were lysed by BugBuster® Master Mix. Cell debris is the resuspended pellets after spinning down the lysate at 16,000 g for 20 m minutes at 4 °C. Loading sample is the supernatant from the cell debris. 94

Figure 5.3 SDS-PAGE gel image. Three cultures of BL21 (DE3) *E. coli* cells were induced with 0.1 mM IPTG at 20 °C for 20 hours. Two of the cultures were lysed with BugBuster® Master Mix and purified using HisTrap™ HP. Loading sample is the supernatant from the cell debris diluted 5 fold. Flow-through is the elute from the column with no imidazole present. Wash is the elute from the column with 60 mM imidazole. Elution 1 and 2 are the elutes from the column with 200 mM imidazole and 500 mM imidazole respectively. 96

Figure 5.4 SDS-PAGE gel image. Four cultures of BL21-CondonPlus (DE3)-RIPL *E. coli* cells were induced with 1 mM IPTG at 37 °C for 2 hours. The cells were lysed with BugBuster® Master Mix in the presence of 1:200 diluted protease inhibitor cocktail. Culture 8 was kept at control group without adding IPTG while keeping other conditions the same with other three cultures. 99

Figure 5.5 SDS-PAGE gel image. Culture 9 was induced with 0.1 mM IPTG at 20 °C for 20 hours. Culture 10 was induced with 1 mM IPTG at 20 °C for 20 hours. Culture 11 was induced with 0.5 mM IPTG at 20 °C for 20 hours. Culture 12 was cultivated at 20 °C for 20 hours without adding IPTG. The insoluble materials spun down at 16,000 g for 20 minutes at 4 °C were purified with BugBuster® Master Mix before loaded onto the gel (culture 9, 10 and 11). The non-induced

soluble is the cell debris after cell lysis of culture 12. The non-induced load is the supernatant from the cell debris of culture 12. 100
Figure 5.6 SDS-PAGE gel image. The culture was induced with 1 mM IPTG at 20 °C for 20 hours. After cell lysis, the IBs were collected, solubilized, and purified using HisTrap™ HP. Flow-through is the elute from the column with no imidazole present. Wash is the elute from the column with 60 mM imidazole and 25 mM Empigen BB®. Elution 1 and 2 are the elutes from the column with 300 mM imidazole and 500 mM imidazole with 25 mM Empigen BB®, respectively. 101
Figure 5.7 SDS-PAGE gel image. Culture 13 was set as non-induced control group. Culture 14 (150 mL) was induced with 1 mM IPTG and 0.5 M sorbitol at 20 °C for 20 hours. Culture 14 induced cell lysate is the mixture harvested after lysed with BugBuster® Master Mix. Culture 14 induced load is the supernatant from the cell debris. Culture 14 induced flow-through is the elute from the column with no imidazole present. Culture 14 induced wash is the elute from the column with 70 mM imidazole. Culture 14 induced elution 1 is the elute from the column with 300 mM imidazole. Culture 14 induced elution 2 is the elute from the column with 500 mM imidazole. Culture 14 before cell lysis is the supernatant from the 150 mL cell culture. 102
Figure 5.8 SDS-PAGE gel image. Culture 15 was induced with 0.5 mM IPTG and incubated at 20 °C for 20 hours as control. Culture 16 was induced with 0.5 mM IPTG at 47 °C for 20 minutes before incubated at 20 °C for 20 hours. Culture 16 cell lysate 2x dilution is diluted mixture harvested after lysed with BugBuster® Master Mix. Culture 16 2x dilution of loading sample is the supernatant from the cell debris. Culture 16 flow-through is the elute from the column with no imidazole present. Culture 16 wash is the elute from the column with 70 mM imidazole. Culture

16 elution 1 is the concentrated elute from the column with 300 mM imidazole. Culture 16 elution 2 is the elute from the column with 500 mM imidazole. 103

List of Tables

Table 1.1 Alternative options for treating BV. 5

Table 1.2 Combination therapies utilizing dual stimuli for bacteria-responsive drug release systems. 21

Table 2.1 Liposome formulation design. 34

Table 2.2 Parallel formulations aimed for EE optimization. 35

Table 2.3 Liposome size distribution before and after centrifugation. 40

Table 2.4 Comparison of EE of liposome formulations. 42

Table 2.5 EE of liposome formulations 1-4. 42

Table 2.6 Size distribution and zeta potential of Formulations 1-4. 45

Table 3.1 Solid culture optimization of *G. vaginalis*. 52

Table 4.1 Primers for VLY gene amplification. 64

Table 4.2 Optimal PCR formulation (the test group). 64

Table 4.3 Optimal PCR formulation (the control group). 65

Table 4.4 Optimal PCR program (gradient annealing process). 65

Table 4.5 Optimal double digestion reaction formulation for pET-28a(+). 67

Table 4.6 Optimal double digestion reaction formulation for VLY gene 67

Table 4.7 Optimal ligation reaction formulation. 67

Table 4.8 Optimal colony PCR formulation (the test group) 69

Table 4.9 Optimal colony PCR formulation (the control group). 69

Table 4.10 DNA concentration and A260/A280 ratio after gel extraction. 73

Table 4.11 DNA concentration and A260/A280 ratio after gel extraction. 74

Table 4.12 Plasmid DNA concentration and A260/A280 ratio after isolation and purification... 76

Table 5.1 Ultrasonication method to lyse cells. 89

Table 5.2 Summary of *E. coli* cell culture conditions for recombinant VLY expression..... 90

List of Abbreviations

AgNCs: silver nanoparticle clusters

ATCC: American Type Culture Collection

bp: base pair

BHI: brain heart infusion

BPO: benzoyl peroxide

BV: bacterial vaginosis

CAI: Codon Adaptation Index

CDCs: cholesterol-dependent cytolysins

CFU: colony-forming unit

CHOL: cholesterol

CLIN: clindamycin

CRM: cholesterol recognition motive

CS: chitosan

DLS: dynamic light scattering

E. coli: *Escherichia coli*

EPC: egg L-α-phosphatidylcholine

EPG-Na: egg L-α-phosphatidylglycerol (sodium salt)

FDA: Food and Drug Administration

G. vaginalis: *Gardnerella vaginalis*

hCD59: human complement glycoprotein CD59

HEC: hydroxyethylcellulose

HEPES: 4-(2-Hydroxyethyl)piperazine-1-ethanesulfonic acid

HIV: human immunodeficiency virus

HPMC: hydroxypropyl methycellulose

H. pylori: *Helicobacter pylori*

IBs: inclusion bodies

IPTG: isopropyl β-D-1 thiogalactopyranoside

IVRs: intravaginal rings

Lactobacillus crispatus: *L. crispatus*

LB: lysogeny broth

MET: metronidazole

MPCS: methylpyrrolidinone-chitosan

mPEG-TK: thioketal grafted methoxy poly(ethylene glycol)

MRS: Man-Rogosa-Sharpe

MSN: mesoporous silica nanoparticles

MW: molecular weight

OD: optical density

PAE: poly (β-amino ester)

PBS: phosphate buffered saline

PCL: poly (ε-caprolactone)

PCR: polymerase chain reaction

PDI: polydispersity index

PEG: poly (ethylene glycol)

PES: polyethersulfone

PFTs: pore-forming toxins

PID: pelvic inflammatory disease

PLA_2: phospholipase A2

PLGA: polylactic-co-glycolic acid

PMX: polymyxin B

PPG: propylene glycol

ROS: reactive oxygen species

S. aureus: *Staphylococcus aureus*

SD: Shine-Dalgarno

SDS-PAGE: sodium dodecyl-sulfate polyacrylamide gel electrophoresis

Sec: General Secretory System

SPC: soybean phosphatidylcholine

STIs: sexually transmitted infections

TAE: tris-acetate-EDT

TL: Thr-Leu

VFS: vaginal fluid simulant

VLY: vaginolysin

Chapter 1 Introduction

1.1 Bacterial vaginosis

Bacterial vaginosis (BV, also known as vaginal bacteriosis) is one of the most prevalent vaginal infections affecting more than one fifth of the world population, with an estimated annual economic burden of $4.8 billion globally[1]. Although the aetiology has not been fully understood yet, BV is believed to be a common vaginal anaerobic dysbiosis that occurs when the *Lactobacillus spp*.-dominated flora in the healthy vagina is replaced by certain overgrown anaerobes such as *Gardnerella vaginalis (G. vaginalis)*, *Atopobium vaginae*, *Prevotella spp*., *Mobiluncus spp*., and *Mycoplasma spp*.[2]. According to the gold standard proposed by Amsel[3], BV is diagnosed when at least three out of four criteria are present: i) an abnormal vaginal pH >4.5; ii) a homogenous, milk-like vaginal discharge; iii) a fishy odor released by volatile amines; iv) presence of clue cells (vaginal epithelial cells heavily coated with bacteria). With a high reoccurrence rate (50% of women experience recurrence after treatment within 1 year), BV also severely impacts the overall quality of life of childbearing women by inducing preterm delivery and increasing the risks of pelvic inflammatory disease (PID) and sexually transmitted infections (STIs) including human immunodeficiency virus (HIV)[4, 5].

The unknown etiopathogenesis of BV owing to the diversity and complexity of the microbes involved results in a big challenge to eradicate this infection. Previous studies revealed that biofilms play a pivotal role in both BV etiology and relapse treatment failure[6, 7]. The biofilm presented in BV is a dense, structured multispecies community of bacteria that strongly adhere to vaginal epithelial cells, among which *Gardnerella vaginalis (G. vaginalis)* is the initial and major

colonizer (Figure 1.1)[8]. This strain is able to initiate the formation of biofilm that serves as a scaffold for other pathogenic bacteria (or secondary bacteria) such as *Prevotella bivia*, *Actinomyces neuii*, and *Brevibacterium ravenspurgense* to cling to the surface of vaginal epithelial cells, enabling the formation of a synergistic bacterial relationship to develop into a prosperous biofilm (Figure 1.2)[9-11]. Moreover, *G. vaginalis* is the only anaerobe that is capable to exhibit three virulence factors in BV[9]: i) the adherence to vaginal epithelial cells; ii) the capacity to produce biofilms; iii) the cytotoxic activity of producing pore-forming toxins (PFTs), i.e. vaginolysin (VLY). The fact that *G. vaginalis* is isolated from almost all women carrying BV[12], the ability to facilitate biofilm establishment, and the high virulence potential, together contribute to the reason why *G. vaginalis* has been identified as a primary pathogen among various BV-associated bacteria.

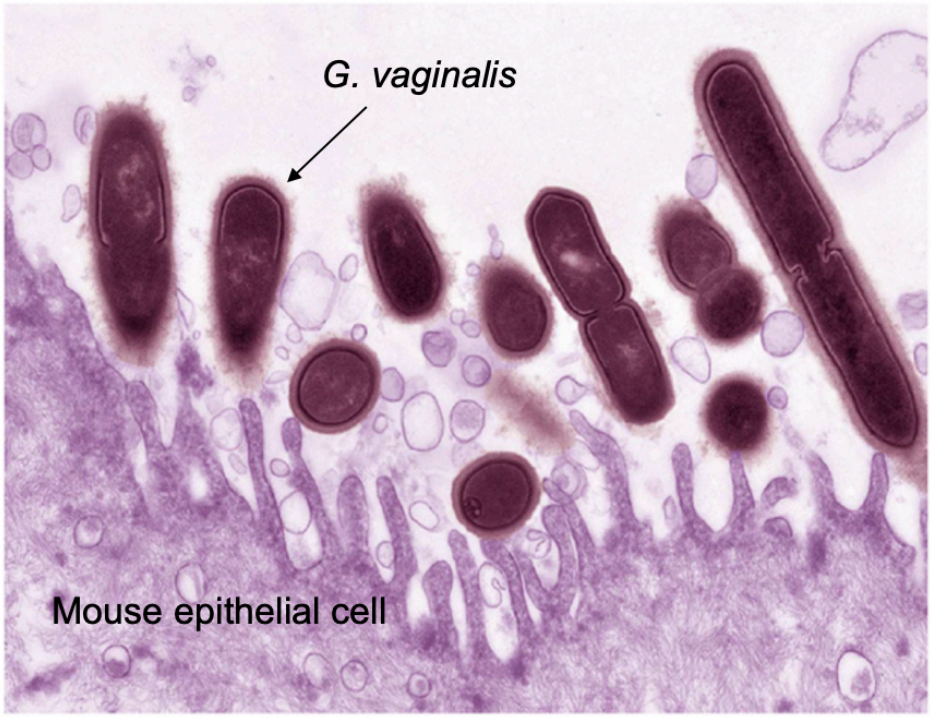


Figure 1.1 *G. vaginalis* (maroon) associated with the surface of a mouse vaginal epithelial cell (purple)[8]. Uranyl acetate staining was followed by transmission electron microscopy. Reprinted with permission from PubMed Central.

VLY produced by *G. vaginalis*, a virulence factor that has been extensively studied and related to BV pathogenesis, is a member of cholesterol-dependent cytolysin (CDCs) family[12, 13]. CDCs are capable of binding to cell membranes in the presence of cholesterol (CHOL), forming large and oligomeric complexes, and then inserting into the bilayer to form water-filled pores[14]. Studies have demonstrated that VLY induces cell lysis by two pathways[14, 15]: i) binding to CHOL using the CHOL-recognition motif in Loop L1 and oligomerization to form pore complexes (Figure 1.3)[14]; ii) binding to human complement glycoprotein CD59 (hCD59) via the β-tongue in the domain D4 to form prepores followed by transition to pores in the presence of CHOL (Figure 1.3)[15]. It is also shown that VLY significantly impairs the integrity of CHOL-rich synthetic membranes with a CHOL threshold of 50 mol% and at a higher pH specific for BV[15, 16].

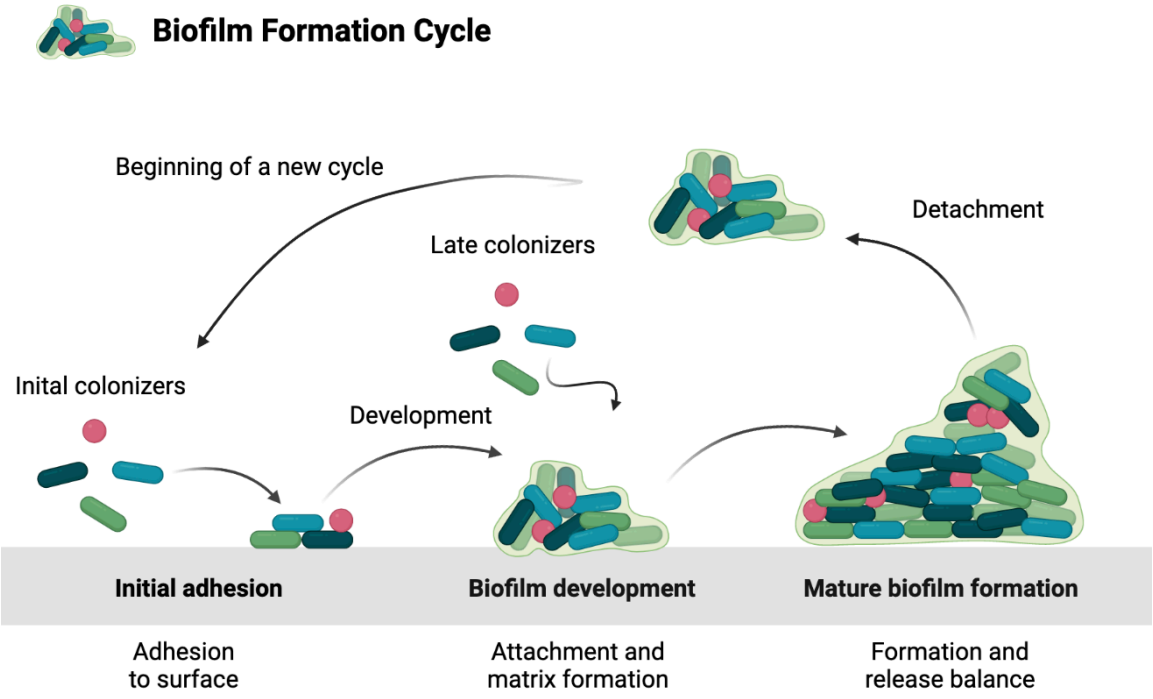


Figure 1.2 The process of polymicrobial biofilm formation in BV: secondary bacteria will incorporate the biofilm after the initial colonizer species has already adhered to the surface; a

synergetic relationship can then be formed, allowing the biofilm to prosper. Created with BioRender.com.

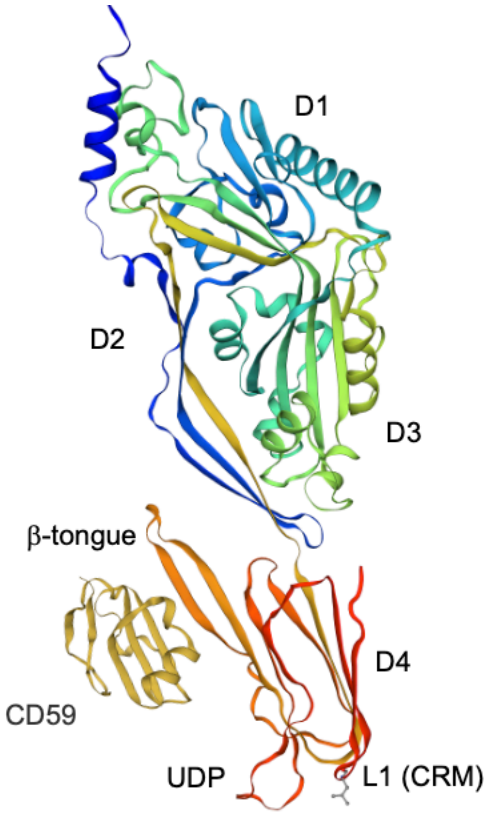


Figure 1.3 Crystal structure of VLY in complex with hCD59. VLY interacts with hCD59 via the β-tongue located in D4. Loop L1 contains the Thr-Leu (TL) pair of CRM. Created with Swiss-Model.

1.2 Treatment for bacterial vaginosis

Antibiotics or antimicrobials remain the international standard protocol for the treatment of BV, among which metronidazole (MET) and clindamycin (CLIN) are the most common agents. MET is regarded as the drug of choice for BV and has been extensively used in clinical practice for years. Its cytotoxicity against bacteria might derive from the unique intermediate metabolites that target DNA, e.g., the reduced product of MET from reductive activation[17]. CLIN interferes with

bacterial protein synthesis by binding to the 50S ribosome subunit, leading to decreased adherence of bacteria to host cells and increased intracellular killing of bacteria[18]. MET is more effective for *Prevotella spp*. with no cytotoxicity to beneficial microorganisms, e.g., *Lactobacilli*[19], while CLIN has greater activity against most BV-associated bacteria such as *G. vaginalis*, *Atopobium vaginae* and *Mobiluncus spp*[19, 20]. In general, MET and CLIN have identical therapeutic efficacy in the treatment of BV with a cumulative cure rate of 82%. CLIN tends to result in more severe adverse effects even in the form of vaginal preparations e.g., *Clostridium difficile* associated diarrhea[18-20]. Apart from the two front-line choices, alternative options have also been studied as replacement or combined agents with the standard therapies, such as other antimicrobials, antiseptics, surfactants, acidifying agents, probiotics, prebiotics, etc. (Table 1.1)[19, 21]. However, due to the mixed results of various studies and the great diversity of experimental designs, the treatment efficacy of these alternative strategies still needs to be confirmed further in follow-up trials and examinations.

Table 1.1 Alternative options for treating BV[19, 21].

Category	Examples	Main Function	Approval
Antimicrobials	• Rifaximin • Secnidazole • Retrocyclin	• Inhibit BV-associated bacteria growth and toxin activity • Inhibit biofilm formation	Rifaximin: early phase 2 Secnidazole: FDA approved
Antiseptics	• Dequalinium chloride • Povidone iodide • Chlorhexidine	• Promote bacteria death by damaging cell membranes	Dequalinium chloride: licensed in UK

Surfactants	• Cocoamphopropionate	• Damage existing biofilms	No
Natural compounds	• *Prangos ferulacea* • *Thymbra capitata* • *Artemisia princeps Pamp*.	• Inhibit bacteria growth • Inhibit biofilm formation • Alleviate BV symptoms	No
Acidifying agents	• Vitamin C • Lactic acid • Polycarbophil • Boric acid	• Re-establish the acidic environment in the vagina	No
Probiotics	• *Lactobacillus* strains	• Re-establish beneficial microbiome in the vagina	No
Prebiotics	• Sugar alcohols • Fructooligosaccharides • Lactulose	• Promote the growth of beneficial microbiome in the vagina	No
Others	• Benzoyl peroxide • Nifuratel • DNase	• Inhibit bacteria growth • Inhibit biofilm formation	No

1.3 Formulation strategies for treating bacterial vaginosis

1.3.1 Oral vs. intravaginal therapy

The general formulation strategies to treat BV are oral drug therapy and intravaginal drug administration. A typical example of the former is the 7-day regimen of oral MET (500 mg twice daily for 7 days)[20]. Although it is the most convenient treatment, it suffers from the harsh gastrointestinal environment and hepatic first-pass metabolism greatly reduces the effective drug dose and limits therapeutic efficacy, not to mention the severe side effects associated with oral intake such as nausea and vomiting[7]. In contrast, topical drug administration via the vaginal route is superior in improving therapeutic effects due to better permeability to many drugs, higher local drug concentrations and minimized adverse reactions, e.g., 0.75% MET vaginal gel (5 g gel, twice daily for 5 days) and 2% CLIN vaginal cream (5 g gel, once daily for 7 days) are found as efficacious as oral therapy but at a lower total dose[20].

Traditional intravaginal drug administration for BV falls into two categories: semi-solid systems and solid systems. As the primary dosage form, semi-solid systems are normally applied using a vaginal applicator and are available in the form of gels, ointments, and creams, while solid systems include suppositories, tablets, films, and delivery devices designed specifically for intravaginal use. The most common type of delivery devices are intravaginal rings (IVRs), a kind of flexible and elastomeric polymeric device inserted into the vaginal lumen to achieve sustained drug release. Currently, these IVRs are approved for contraception and hormone replacement therapy[22].

1.3.1.1 Semi-solid systems

The formulations of semi-solid systems are in most cases based on bioadhesive polymers such as chitosan (CS), polyacrylates, cellulose derivatives, sodium alginate etc. to prevent leakage and undesired elimination caused by self-cleansing mechanism of the vaginal tract. One common example is the commercial carbomer-based MET gel (Carbopol® 974P) which provides good muco-adhesion and helps re-establish a healthy, acidic vaginal pH[23]. Perioli et al. prepared a gel by combining hydroxyethylcellulose (HEC) and CS or CS derivatives, 5-methylpyrrolidinone-chitosan (MPCS), to load MET with increased muco-adhesion force compared with the commercial gel[24]. The HEC-MPCS gel was even better than the HEC-CS gel in prolonging MET-mucosa contact due to its increased ability to form hydrogen bonds with mucins.

Another example of polyacrylate-based gels for treating BV is the polycarbophil and Carbopol® 934P hydrogel encapsulating benzoyl peroxide (BPO) developed by Xu et al[25]. BPO is an antibacterial approved by Food and Drug Administration (FDA) for the topical treatment of acne. It has a selective antibacterial profile against *G. vaginalis* owing to its ability to generate benzoate free radicals under a homolytic fission (a chemical process that is also utilized by hydrogen peroxide produced by *Lactobacilli* to inhibit other bacteria in the vagina). According to the well diffusion assays, the BPO-loaded hydrogel could effectively inhibit *G. vaginalis* growth at a low concentration of 0.01%, with a tolerance concentration of 2.5% for *Lactobacillus spp.*, demonstrating its biosafety. Moreover, the hydrogel also exhibited desired rheological properties with high viscosity and low shear rate, enabling a long duration within the vaginal cavity. All these results suggest that this formulation qualifies as a suitable candidate for BV local treatment.

In addition, Carbopol® 934P has been applied in a novel formulation of bigels to achieve sustained release of MET. Bigels are the proportioned mixture of hydrogel and organogel, with the former containing aqueous solvents while the latter containing apolar solvents. Singh et al. fabricated a bigel combining Carbopol® 934P and sorbitan monostearate-sesame oil organogel[26]. The developed bigel was smooth and biocompatible, appearing as an oil-in-water type of emulsion gel with the droplets ranging from 10 to 35 μm. The shear-thinning behavior and viscoelastic property of the bigel make it applicable to adhere to vaginal mucosa. The release of MET is shown to be diffusion mediated and is influenced by the proportion ratio of organogel and the aqueous layer. When the proportion of the former increases, MET is released in a controlled fashion, while the proportion of the latter dominates, MET release is accelerated.

Apart from bioadhesive formulations, stimuli-responsive systems are also applied in intravaginal drug delivery. Stimuli-responsive systems are able to achieve conditional drug release by undergoing physicochemical or pharmaceutical changes triggered by changes to the physiological environment. In terms of treating BV, thermo, ion and pH-sensitive systems have been developed. Ibrahim et al. designed an *in situ* gel formulation based on poloxamers (Pluronic® F127 and/ or Pluronic® F68), a triblock copolymer that can go through a reversible sol-gel transition at a certain temperature[27]. By adjusting the composition ratios of Pluronic® F127 and Pluronic® F68, the gelation temperature can be tuned to around 37 ºC, facilitating accurate dosing as a form of liquid and good spreadability within the vagina while avoiding leakage. Moreover, Pluronic also serves as a rate-controlling barrier by forming micelles and raising viscosity, to control MET release.

Patel et al. prepared another kind of *in situ* gel containing CLIN based on hydroxypropyl methycellulose (HPMC) and gellan gum with good bioadhesion and stimuli-responsiveness[28]. HPMC can decrease the gelation temperature while gellan gum gels upon contact with ions in the vaginal fluid, both contributing to *in situ* gel formation. Formulated together, HPMC and gellan gum exert a synergistic effect on muco-adhesion to maintain constant CLIN release for 12 hours.

A pH-responsive calcium alginate hydrogel loaded with polymyxin B (PMX) was developed by Ferreira et al. to achieve sustained drug release for six days[29]. The hydrogel is formed through self-assembling of negatively charged alginate and cationic drug PMX, followed by cross-linking with Ca^{2+} ions. The formation of polyelectrolyte complexes facilitates controlled PMX release at pH 4.5 by preventing the burst. At pH 7.4, the release rate is improved due to increased polymer chain flexibility resulting from weakened supramolecular interactions.

The third formulation strategy is to combine vaginal gels with nanotechnology to obtain enhanced BV therapies, e.g., liposomes-in-gel. Liposomes have been extensively studied as drug delivery systems for over 40 years, with minimized system absorption and side effects, and excellent biocompatibility. By embedding liposomes in gels, liposome gels possess synergistic properties of bioadhesion and prolonged drug release to greatly improve intravaginal therapeutic efficacy. Pavelic et al. synthesized liposomes composed of egg phosphatidylcholine and egg phosphatidylglycerol-sodium entrapping MET and incorporated them into Carbopol® 974P[30]. The results of *in vitro* release studies showed that more than 50% of the originally entrapped MET was still retained in the gel even after 24 hours incubation with vaginal fluid simulant (VFS), demonstrating the improved stability and prolonged drug release upon incorporation into the gel.

Another unique characteristic of liposomes is deformability, which enables them to penetrate into deeper layers of the skin. Vanic et al. developed deformable propylene glycol-containing liposomes encapsulating MET or clotrimazole that penetrate more rapidly than conventional liposomes, to achieve more efficient MET delivery to deeper vaginal epithelial cells affected by BV[31]. This novel nano-delivery system based on liposome-in-gel is very promising for increasing drug permeation while maintaining controlled and sustained release for eradicating vaginal infections.

1.3.1.2 Solid systems

Solid formulations against BV involve tablets and films, which are not very commonly found in dosage forms probably due to difficulties in spreading homogenously and extensively within the vaginal tract compared with gels. However, they do have unique advantages: i) less concerns related to leakage and messiness due to rapid dissolution; ii) no need of multiple daily administrations. Similar to the gel formulation, the base compositions of tablets and films are bioadhesive polymers.

Machado et al. prepared a novel vaginal sheet capable of swelling to absorb excess vaginal discharge formulated by gelatin and propylene glycol (used as a plasticizer)[32]. The sheet showed efficient absorption of vaginal fluid at pH 5, the typical pH for a vagina carrying BV, due to the hygroscopic property of gelatin, and high acid-buffering capacity at pH 4. Easily inserted and removed, this new form of solid formulation has potentials in incorporating drugs to treat BV, though further *in vitro* and clinical studies are needed to evaluate its applicability and patient compliance.

Other film formulations for BV treatment include the alginate/chitosan membrane containing MET and the xanthan gum/hydroxypropyl cellulose film loading CLIN[33, 34]. These films made from aqueous polymers can remain in the vaginal mucosa for 8 hours before final dissolution in the vaginal fluid, Therefore, they are more suitable for one-time treatment instead of fighting against BV relapse. Similarly, the tablet formulation of glutaraldehyde-crosslinked alginate/chitosan vaginal tablet loading MET[35] is also aimed for one-time release.

IVRs can be regarded as a special type of solid formulation. Unlike tablets and films, IVRs are not bioadhesive-based; instead, they are made of elastomers such as polyurethane and poly(ε-caprolactone) (PCL). Verstraete et al. developed a thermoplastic polyurethane-based IVR to promote lactic acid release over 28 days and MET release over 4-7 days[36]. In another research, an IVR made from porous PCL was able to release MET rapidly over 24 hours (35-55%) followed by a gradual release of 80% MET over 12 days when immersed in simulated vaginal fluid[37].

1.4 Bacteria-responsive drug release systems

As an increasingly popular stimuli-responsive system, the bacteria-responsive drug release system has been explored as an antimicrobial therapy for bacterial infections. Unlike the common external triggers such as light, temperature and magnetic field utilized in stimuli-responsive systems, the stimuli that bacteria-responsive therapeutic systems use are generated internally because of micro-environmental changes in the presence of bacteria. These changes include variations in pH, elevated levels of reactive oxygen species (ROS), and overexpression of enzymes or toxins. Not confined to monotherapy, bacteria-responsive systems can be designed to be more complicated to

release drugs with higher precision and greater therapeutic effect in the presence of multiple stimuli.

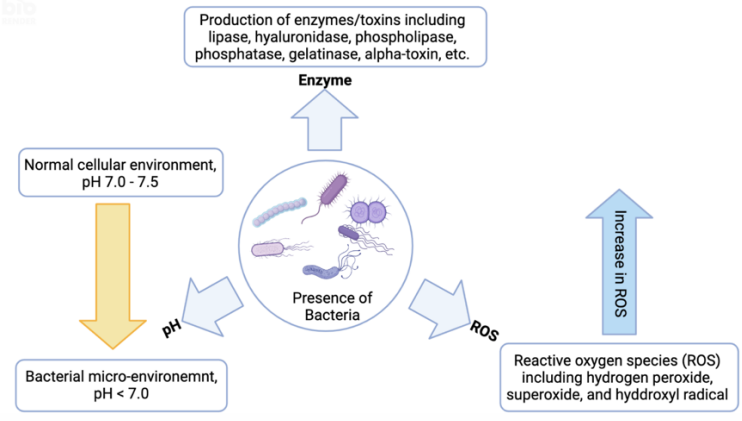


Figure 1.4 Internal stimuli generated from micro-environmental changes in the presence of bacteria. Created with BioRender.com.

1.4.1 pH-responsive systems

Among internal stimuli-responsive systems, pH-responsive systems have been mostly studied in that the pH of the micro-environment in which bacterial infections occur can be easily altered (certain bacteria secret acidic metabolites) and that there are a couple of pH-sensitive polymer materials available as drug carriers. Generally, there are two strategies to realize pH-responsive drug release. One is based on the solubility, morphological or volume transitions of ionizable polymers/surfactants during protonation/deprotonation process, while the other is based on the cleavage of dynamic covalent bonds that lead to the direct break down or dissociation of drug carriers.

In the first strategy, drug carriers with ionizable functional groups can achieve better bacteria targeting in acidic micro-environment because they accept protons and thus become positively charged. Prolonged *in vitro* vancomycin delivery has been achieved by utilizing a

charge-adaptive triblock polymer composed of poly (ethylene glycol) (PEG), PCL and poly(*β*-amino ester) (PAE)[38]. At acidic infections sites, the nanoparticles were able to undergo charge alteration from slightly negative to positive because of PAE protonation, resulting in enhanced binding capacity to the negatively charged cell wall of the bacteria. Vancomycin-loaded chitosan nanoparticles stabilized with an anionic gemini surfactant has demonstrated significantly greater *in vitro* antimicrobial activity at acidic pH[39]. A pH-switchable antimicrobial nanofiber based on amphipathic peptides capable of biofilm elimination was also prepared by incorporating octapeptide into a supramolecular hydrogel followed by cypate and proline loading[40]. The hydrogel showed a broad spectrum of antimicrobial effect and facilitated rapid wound healing in an *in vivo* mouse model. Similarly, poly(L-histidine) containing imidazole groups was introduced into a triblock polymer consisting of polylactic-co-glycolic acid (PLGA), polyhistidine and PEG to form pH-sensitive nanoparticles[41]. The local uptake of the nanoparticles by Gram-positive and Gram-negative bacteria was greatly improved due to the strong electrostatic interactions under acidic conditions. Liposomes coated with quaternary ammonium chitosan were used to deliver doxycycline hydrochloride for eradication of multi-resistant biofilms[42]. At low pH, the residual amines could be protonated and target liposomes to negatively charged biofilm surfaces.

In the second strategy, antibacterial nanoparticles instead of antibiotics were released as a result of chemical bond hydrolysis activated under acidic environment. For example, silver nanoparticle clusters (AgNCs) were synthesized and functionalized with polymers containing ortho ester segments[43]. Once the ortho ester was hydrolyzed, the AgNCs collapsed, reassembled into Ag nanoparticles, and then released Ag^+, resulting in the damage of bacteria membrane and interference with DNA/RNA replication.

1.4.2 ROS-responsive systems

ROS such as hydrogen peroxide and superoxide are produced at inflammatory sites to combat pathogenic bacteria. ROS can inhibit pathogen growth by oxidatively damaging DNA. However, with a high level of production at infection sites they can also be detrimental to healthy tissues and cells as the oxidation reaction is non-specific. On the other hand, a couple of bacteria-responsive drug release systems has been reported to utilize the overexpressed ROS as stimulus to trigger "smart" release of antibiotics in treating bacterial infections.

Thioketal is one of the most used functional groups as ROS-responsive linkers. Mesoporous silica nanoparticles (MSN) functionalized with thioketal grafted methoxy poly(ethylene glycol) (mPEG-TK) has been designed to encapsulate vancomycin[44]. When hydrogen peroxide accumulated at the active site, mPEG-TK could be degraded to allow vancomycin to escape easily. A multifunctional nanotherapy based on boronic ester modified cyclodextrin carrying moxifloxacin was developed by Sun et al. to treat pulmonary bacterial infection[44]. In the presence of 0.5 mM hydrogen peroxide, moxifloxacin release from the core-shell nanoparticles was accelerated. Koo et al. developed biocompatible ferumoxytol nanoparticles to catalyze *in situ* generation of free radicals from hydrogen peroxide to disrupt oral biofilms and prevent tooth decay[45].

1.4.3 Enzyme/toxin-responsive systems

Compared to pH and ROS-responsive systems that utilize physical changes as stimuli, enzyme/toxin-responsive systems are more promising as virulence factors produced by bacteria are highly specific. Generally, bacterial infection sites are characterized with abnormal expression

of enzymes, among which lipase, hyaluronidase, phospholipase, and phosphatase are the most common[46]. These enzymes can break down certain chemical bonds and thus are used for designing enzyme-responsive drug release systems to treat bacterial infections. Basically, the drug release mechanisms for enzyme-activated systems are divided into two categories (Figure 1.5): i) direct release through chemical bond cleavage; ii) indirect release induced by physicochemical transitions, both of which are realized in the presence of enzymes[46].

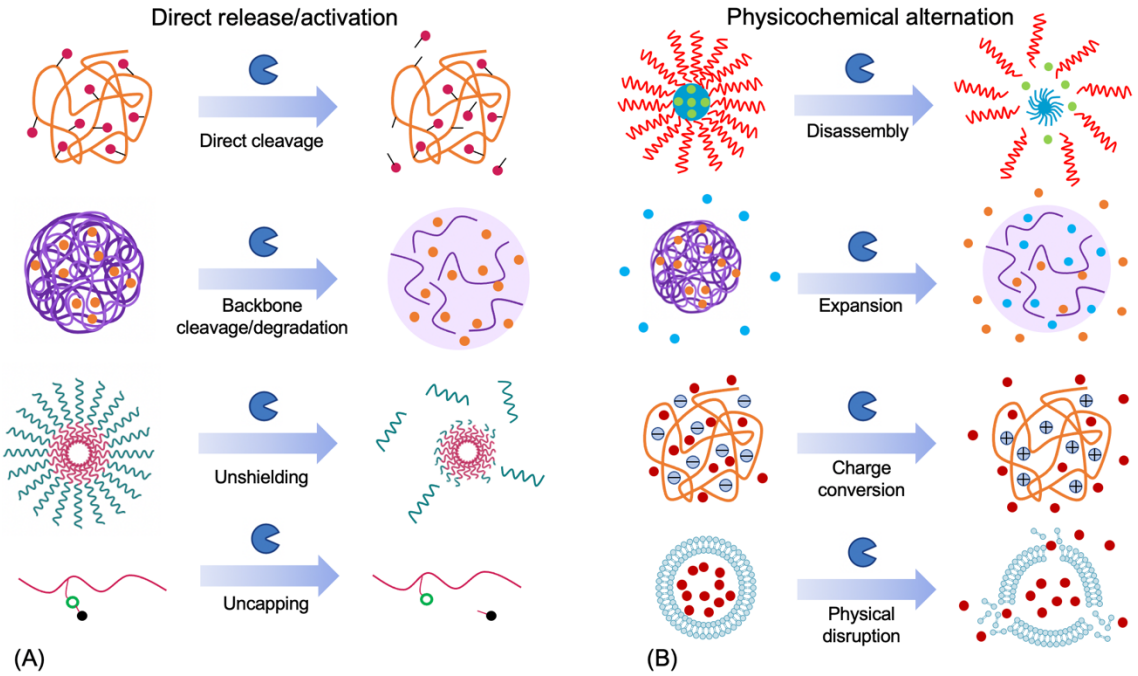


Figure 1.5 Schematic of two drug release mechanisms for designing enzyme-responsive systems: (A) direct release/activation; (B) indirect release/activation. Created with BioRender.com.

Lipase is produced abundantly at the infection site[46]. A core-shell structure composed of MSN loaded with gentamicin and modified lipid bilayers has been developed to release drug rapidly in the presence of lipase produced by *Staphylococcus aureus* (*S. aureus*) in an extracellular model[47]. Polymers containing lipase-labile bonds such as esters have also been explored as drug

carriers used in enzyme-responsive systems, one of which is PCL. Liu et al. developed PCL/poly(ethylene succinate)-based core-shell nanofiber membranes whose shell could be broken down in the presence of lipase and then presented on-demand biocide release[48]. Wang et al. fabricated a triple layered nanogel composed of PCL interlayered between the cross-linked polyphosphoester and PEG triggered by lipase to release vancomycin[49] (Figure 1.6).

Hyaluronidase is secreted by many Gram-positive bacteria. Therefore, hyaluronic acid has been incorporated in enzyme-responsive systems as a capping agent in response to hyaluronidase produced at the infectious site. Hyaluronic acid capped graphene-mesoporous silica nanosheets anchored with ferromagnetic nanoparticles on the outer surface have been synthesized as drug carrier for the prodrug ascorbic acid[50]. Upon degradation of hyaluronic acid, ascorbic acid could be converted to hydroxyl radicals catalyzed by magnetic nanoparticles to kill the bacteria. Wu et al. developed a cross-linked multilayer surface via layer-by-layer assembly of poly(acrylic acid) and chitosan quaternary ammonium salt with hyaluronic acid as the topmost layer[51] (Figure 1.7). Accelerated antibacterial release could be achieved once the top layer was degraded by the hyaluronidase secreted by bacteria.

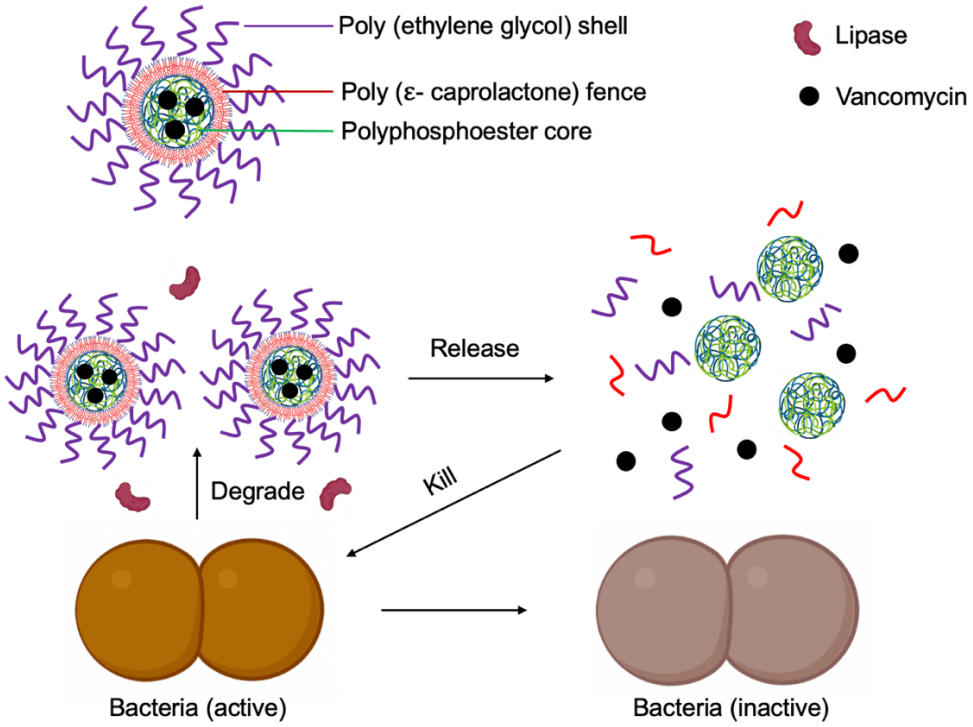


Figure 1.6 Schematic of the lipase-responsive drug delivery based on a polymeric triple-layered nanogel to treat bacterial infections. Created with BioRender.com.

A mannosylated nanogel with PEG shell and crosslinked polyphosphoester core was synthesized with vancomycin loading[52]. Triggered by phosphatase, the nanogel was able to release drugs to macrophages and then kill the bacteria ingested. Zhang et al. formulated chitosan-modified gold nanoparticles-stabilized liposomes which were susceptible to phospholipase A2 produced by *Helicobacter pylori* (*H. pylori*)[53] (Figure 1.8). The liposomes were very effective in preventing drug leakage and inhibiting bacteria growth.

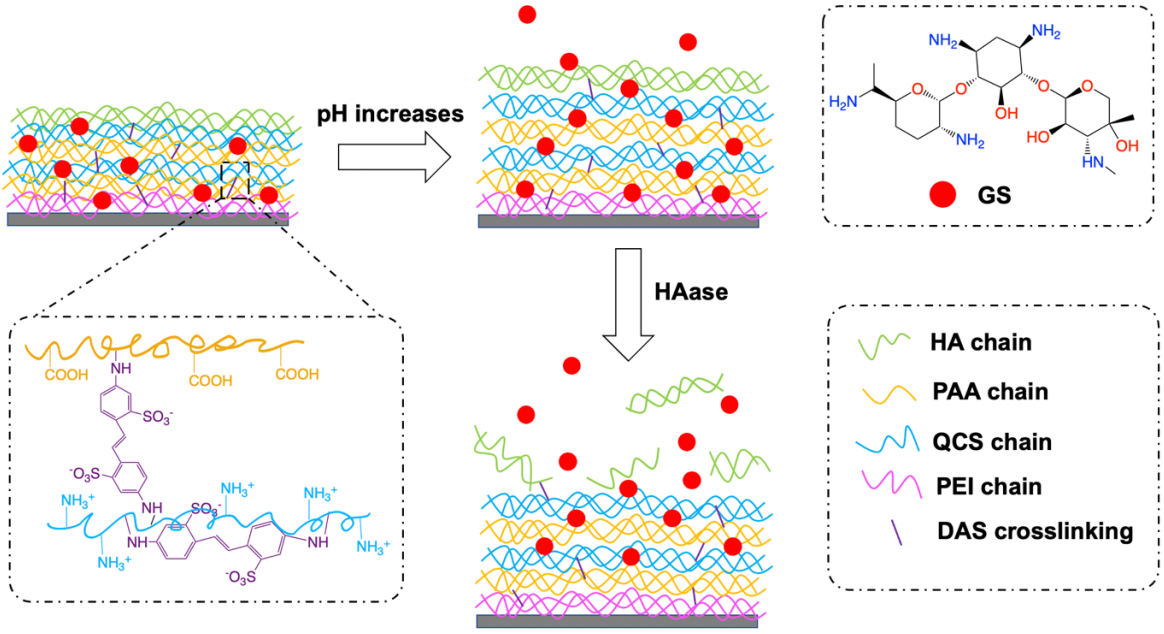


Figure 1.7 Schematic of the hyaluronidase-responsive multilayer-based drug delivery system. Created with ChemDraw Professional 20.1 (PerkinElmer).

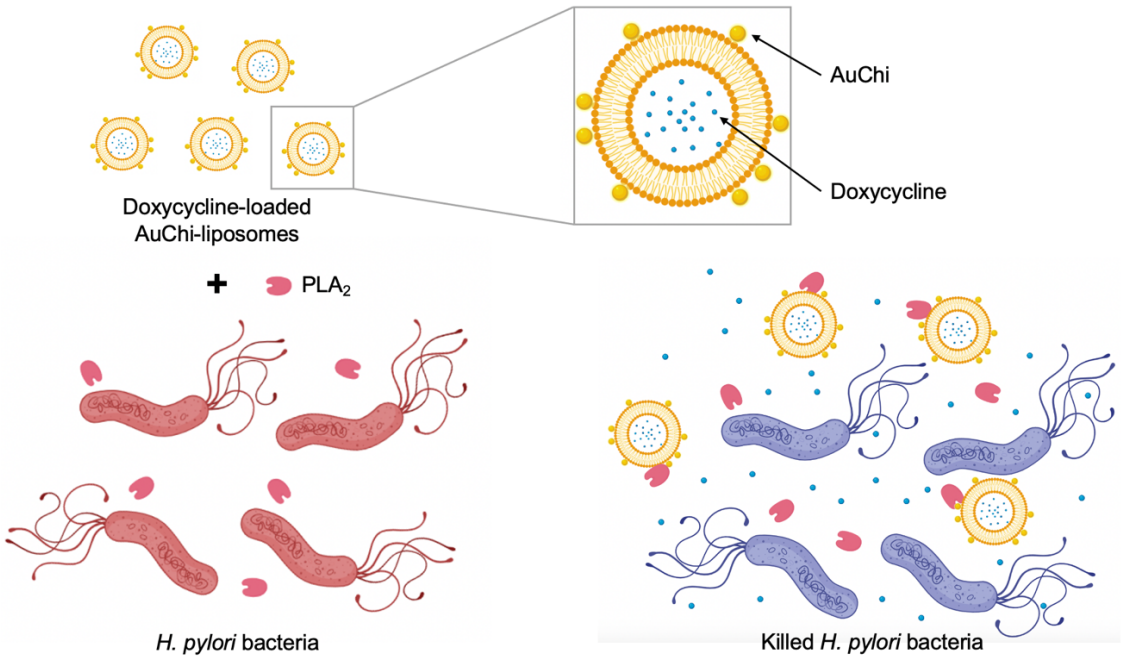


Figure 1.8 Schematic of phospholipase A2 (PLA_2)-responsive drug delivery based on chitosan-modified gold nanoparticles-stabilized liposomes to treat *H. pylori*. Created with BioRender.com.

Apart from the above-mentioned common enzymes, gelatinase is also secreted by a broad spectrum of bacteria. Hence, gelatin nanoparticles coated with red blood cell membrane were designed by Liu et al. to deliver Ru-complex-modified selenium nanoparticles upon degradation by gelatinase secreted by *S. aureus*[54]. Camouflaged with red blood cell membrane, the nanosystem could also escape the phagocytosis of macrophages and effectively neutralize bacterial exotoxins.

Toxins other than enzymes produced by bacteria are less commonly used to trigger drug release, although there have been a few examples. Chitosan-modified gold nanoparticles were used to modify liposomes that released vancomycin in the presence of α-toxin, a pore-forming toxin produced by *S. aureus*[55]. The toxin was demonstrated to insert into lipid membranes and create pores, leading to 100% drug release and effective bacteria inhibition in 24 hours.

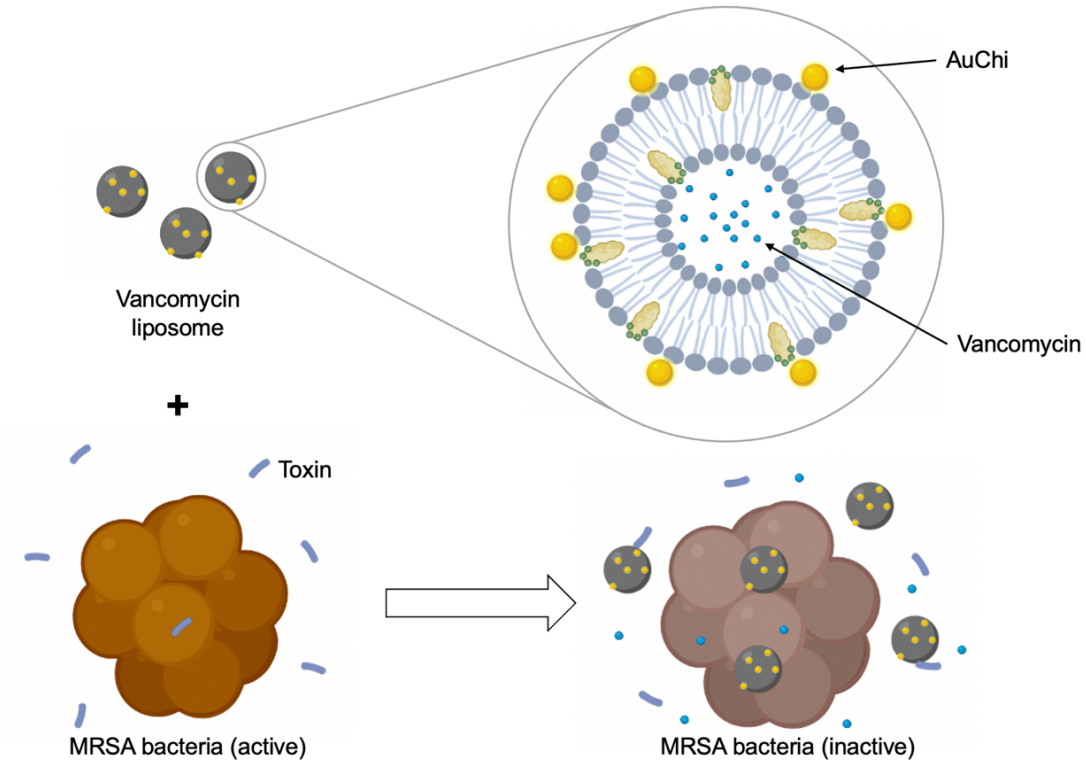


Figure 1.9 Schematic of toxin-responsive drug release from gold nanoparticles-stabilized liposomes to treat *S. aureus*. Created with BioRender.com.

1.4.4 Combination therapies

Bacteria-responsive drug release systems aimed for a higher level of drug delivery precision have been developed based on multiple micro-environment factors (pH, ROS, enzymes)[56]. Table 1.2 provides a few examples related to dual-stimuli responsive systems for antibacterial combination therapies, including the responsive materials, active substances, type of stimulus and target bacteria.

Table 1.2 Combination therapies utilizing dual stimuli for bacteria-responsive drug release systems.

Responsive materials	Antibacterial agent	Stimulus	Target bacteria	References
Block copolymers of PEG, poly(aspartamide), and 2-(diisopropylamino)ethylamine	D-tyrosine and azithromycin	Acidic pH and lipase	*Pseudomonas aeruginosa* biofilm	Li et al. 2019[57]
Ferumoxytol nanoparticles	Iron oxide	Acidic pH and ROS	*Streptococcus mutans* oral biofilm	Koo et al. 2018[45]
Mannoslated nanogel with polyphosphoester core	Vancomycin	Phospholipase and phosphatase	*S. aureus*	Wang et al. 2012[52]

1.5 Recombinant VLY protein expression

1.5.1 Recombinant protein expression in *Escherichia coli*

Obtaining sufficient quantities of purified proteins is crucial to study their structures, functions and interactions with other biomolecules. However, the low native expression level and difficulties in separating the target protein from the mixture of other proteins, nucleic acids and impurities make it nearly impossible. Hence, recombinant protein expression is the most applicable solution with easy accessibility and straightforward genetic manipulation. So far, *Escherichia coli* (*E. coli*) has been the most popular host organism for recombinant protein production, especially for those proteins of bacteria origin[58]. There are many advantages regarding the use of *E. coli* as cloning host including but not limited to i) fast growth kinetics with high cell density easily achieved; ii) inexpensive rich complex media available; iii) fast and easy DNA transformation[58].

The procedures of performing recombinant protein expression in *E. coli* are straight forward, if all basic elements are ready at hand (Figure 1.10). Basically, the gene of interest is amplified using polymerase chain reaction (PCR) and then cloned into an expression vector to form a construct, followed by transformation of the construct into a host strain. Then, expression is induced to produce the recombinant protein within the host strain before protein purification and characterizations (e.g., purity, quantification, activity). However, in industrial applications, recombinant protein expression is not always successful and there are a number of options in terms of host strains, expression vectors, induction and cultivation strategies. To obtain the target protein, multiple trial-and-error studies must be carried out to find a successful combination.

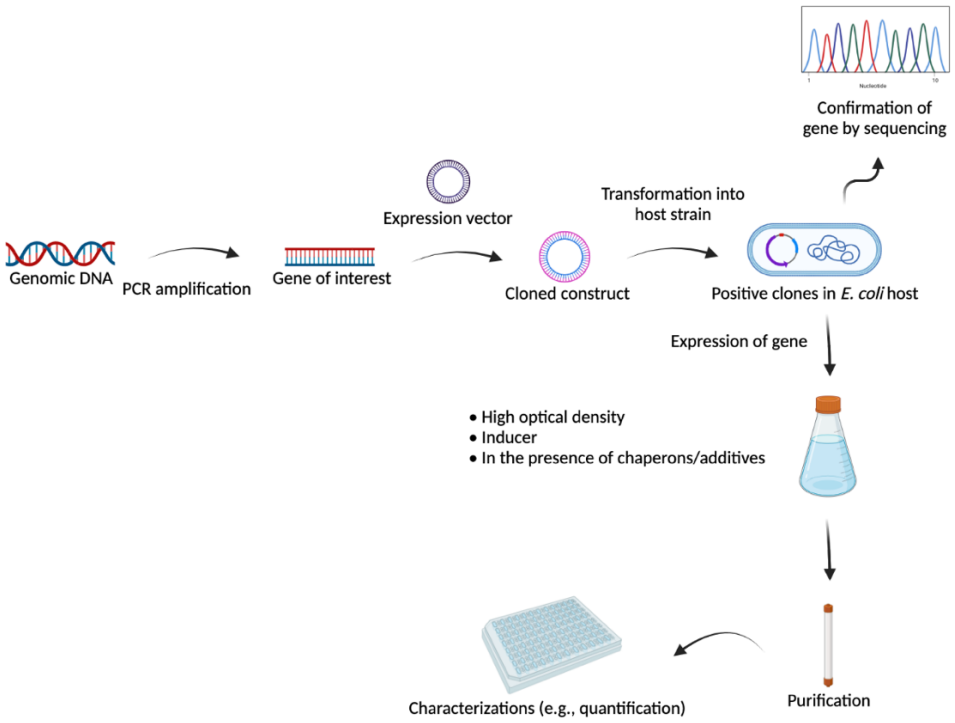


Figure 1.10 Schematic of recombinant protein expression in *E. coli*. Created with BioRender.com.

1.5.2 Expression plasmid selection

Expression plasmid, or expression vector, is a vector in which a cloned gene will be transcribed and translated[59]. It is used for foreign gene cloning and expression in *E. coli*. The most commonly used vectors are the pET series. The essential elements they contain will be discussed in the following paragraphs.

The genetic components of plasmid vectors include an origin of replication (*ori*), a promoter, a multi-cloning site, affinity tags, a terminator and selection markers (Figure 1.11)[58].

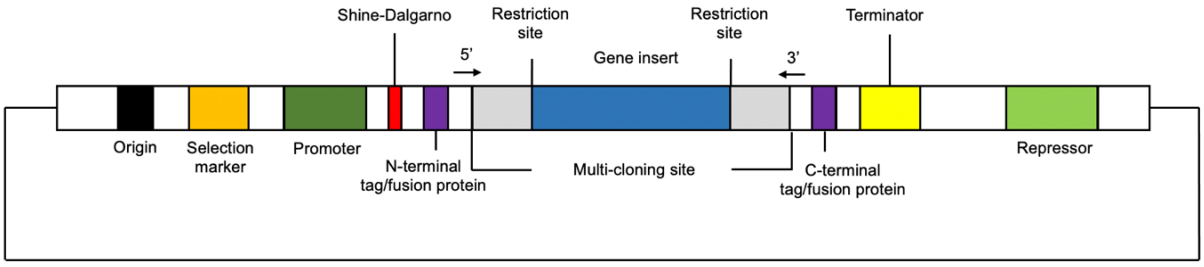


Figure 1.11 Genetic elements of a plasmid vector. Created with BioRender.com.

1.5.2.1 Replicon

The replicon of plasmid vectors consists of the *ori* and its associated *cis* acting elements[60]. The *ori* controls the plasmid copy number, an important parameter when selecting expression vectors. Most plasmids used in recombinant protein expression possess the ColE1 (15-20 copies per cell) or the p15A (10-12 copies per cell) replicon[60, 61]. The pET series possesses the pMB1 origin, a derivative of COlE1 with 15-60 copies[60, 61].

1.5.2.2 Promoter

A strong promoter in expression vectors is crucial to promote high-level gene expression. Generally, promoters in different expression systems have two origins, namely bacteria and bacteriophage[59]. The former origin includes the lactose operon promoter (*lac* promoter) and the arabinose operon promoter (*araBAD* promoter). The *Lac* promoter and its derivatives are weak and thus rarely used for recombinant protein production, while the *araBAD* promoter is suitable for facilitating soluble toxic protein expression by reducing leaky expression. The latter origin includes T7 promoter, which is extremely popular in the pET vector-based expression system. In

this system, the gene of interest is cloned behind the T7 promoter recognized by the phage T7 RNA polymerase which is under the translational control of the *lac*UV5 promoter (a mutant of the *lac* promoter) in *E. coli* BL21(DE3). In the absence of isopropyl β-D-1 thiogalactopyranoside (IPTG), a non-hydrolyzable analog of allolactose, the repressor protein LacI binds to the *lac* operator, blocking RNA polymerase and preventing the transcription of the gene. In the presence of IPTG, the repressor binds to IPTG and is released from the *lac* operator. Consequently, RNA polymerase binds to the T7 promoter and gene transcription starts (Figure 1.12).

However, the T7 promoter-based expression system has its disadvantage, e.g., the basal expression of T7 RNA polymerase in the absence of inducer (also called leaky expression)[59]. This can be addressed by co-expression of T7 lysozyme that helps control unintended expression under the T7 promoter, in which a replication compatible plasmid such as pLYsS must be involved in the system.

1.5.2.3 Affinity tags

Affinity tags are incorporated into the target protein for a couple of reasons. For example, small peptide tags such as poly-His- can be introduced at either the N-terminal or C-terminal to allow for affinity purification from other proteins produced by *E.coli*. Proteins bearing the His-tag are easily recovered by immobilized metal ion affinity chromatography using Ni (II) or Co (II)-loaded nitrilotriacetic acid agarose resins due to the strong interaction between polyhistidine groups and metal ions[61]. Another type is the non-peptide fusion tag used for improving protein solubility, e.g., the maltose-binding protein and N-utilization substance protein A, although the mechanism is still unclear[62, 63].

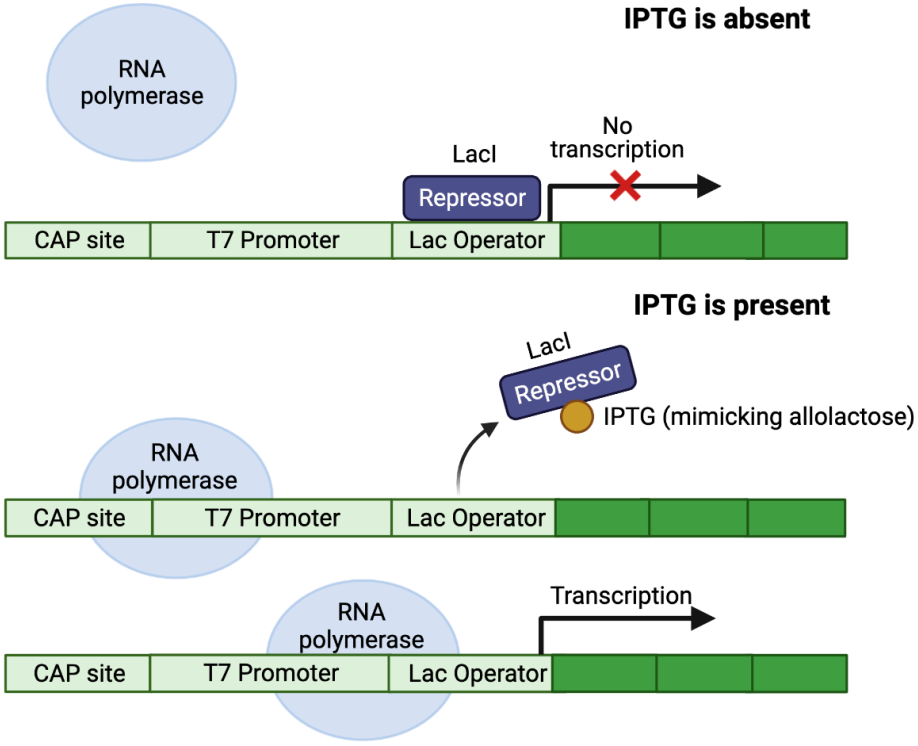


Figure 1.12 The mechanism of IPTG induction. When IPTG is absent, the *lac* repressor binds tightly to the operator preventing transcription by RNA polymerase. When IPTG is present, it binds to the repressor and separates it from the operator. This allows transcription by RNA polymerase. Created with BioRender.com.

1.5.2.4 Selection markers

The expression vectors carry antibiotic resistance markers to inhibit the growth of plasmid-free bacterial cells. In this way, successfully transformed cells containing the plasmid construct can be selected out. Common markers encoded in the pET series are ampicillin and kanamycin, although there are also other markers such as chloramphenicol and tetracycline[60]. However, in most cases, colony PCR stills needs to be performed to verify transformation to avoid false positives.

1.5.3 Host strain selection

BL21(DE3) and its derivatives are the most popular strains used for heterologous protein expression. BL21(DE3) is engineered as protease-deficient without Lon protease and OmpT protease gene coding[58]. In addition, it contains λDE3 prophage that encodes T7 RNA polymerase gene under the control of the *lac*UV5 promoter, which directs the expression of cloned genes under the control of the T7 promoter, as mentioned before[58].

Apart from the regular BL21(DE3) strain, there are other commercially available strains tailored for difficult expression scenarios. For example, the Rosetta (DE3) strain (Novagen) and BL21-CodonPlus strain (Agilent) both carry tRNA genes for rare codons to compensate the tRNA pool of *E. coli*[58, 64]. BL21(DE3) pLysS/E (Novagen) is able to reduce basal expression of the target gene by producing T7 lysozyme[58]. BL21-AI strain (Invitrogen) can also address the leaky expression problem by utilizing the *araBAD* promoter, which does not belong to the T7 promoter-based expression system[59].

1.5.4 Problems with recombinant protein production

1.5.4.1 Protein toxicity

If the heterologous protein is toxic to the host cells, it can negatively affect the normal proliferation and homeostasis of *E. coli*, leading to expression failure. One possible reason is the basal expression of the toxic protein[61]. In this case, host strains such as BL21-AI or BL21(DE3) pLysS/E can be used to tightly control transcription and translation.

1.5.4.2 Codon bias

Codon bias occurs when the frequency of codons used in foreign DNA is significantly different from that in the host cells. Codons abundant in the heterologous genes are very likely to be rare in *E. coli*. During the translation process, *E. coli*'s internal rRNA pool will be depleted, resulting in early termination of translation and thus expression failure[65].

Generally, there are two approaches to solve this issue. One is to perform codon optimization to the gene of interest. This involves adapting rare codons of the gene to the commonly used codons in the host without altering the amino acid sequence (often achieved by site-directed mutagenesis) followed by whole gene synthesis. This method is very time-consuming and expensive. More importantly, previous studies have found that codon optimization suffer from a series of problems including mRNA instability, protein improper folding, etc[66-68]. The other is to perform co-expression of the expression vector and a functional plasmid that encodes rare tRNAs within the host. Typical strains carrying such plasmids are the BL21-CodonPlus strain and Rosetta (DE3) strain, both of which possess the p15A replicon that is compatible with the ColE1 and ColE1 derivative replicons in expression vectors. The use of these strains can improve recombinant protein production but is very likely to cause protein aggregation due to the increased translation speed[61].

1.5.4.3 Inclusion body formation

Inclusion bodies (IBs) are protein aggregates formed without proper post-translational modifications or folding during foreign gene expression in the host cells. This happens when the heterologous protein expression rate exceeds the capacity of host cells in managing precise three-

dimensional structures. The mis-folded protein does not have biological activity in most cases. A number of strategies have been developed to mitigate IB formation, but none of them is perceived as panacea for all expression systems as every protein is different. Therefore, troubleshooting IB is very challenging.

One simple way to minimize IB formation is to optimize culture conditions including culture temperature, inducer concentration, additives, etc. In most cases, decreasing culture temperature to 15-20 °C and decreasing inducer concentration to less than 1.0 mM can reduce the protein production rate and thus help ease the cellular stress, thereby promoting the expression of soluble fractions[69]. There have also been several studies that utilized bacteria's own defense mechanism to produce molecular chaperons to help produce more soluble foreign proteins. For example, heat shock cultivation at 47 °C for 30 minutes prior to *E. coli* induction might mitigate IB formation in that the bacteria can synthesize heat shock proteins that help with protein folding[70, 71]. Similarly, the addition of additives such as sorbitol and ethanol into the expression system can also facilitate soluble protein formation by increasing the osmotic stress[69]. The second strategy is the co-expression of molecular chaperones through host engineering, which is more complicated and provides no guarantee to improve protein solubility[72, 73]. The third strategy is the introduction of a fusion tag at the N- or C-terminal of the protein to aid in improving solubility. Typical examples include the maltose-binding protein and Spheroplast Protein Y[74, 75].

In contrast to the above stated strategies aiming to minimize IB formation, another way is to recover protein through IB solubilization which normally involves using detergents or chaotropes, and *in vitro* refolding, though it is very challenging given the uncertainties in the protein re-folding process[69, 76, 77]. It is very likely that the protein is inactivated upon exposure to

detergents. One of the few successful cases is the recovery of recombinant human growth hormone using ion-exchange and gel filtration chromatography reported by Panda et al[78].

1.6 Project rationale

Two major problems exist among the current vaginal formulations against BV:

i) They are not designed for on-demand therapy: Despite dominating in the commercial drug market, semi-solids are actually for one-time treatment, since they require multiple administrations on a regular basis. Solid dosage forms such as tablets or films have similar problems owing to the short retention time within the vaginal cavity as a result of their dissolution-controlled release mechanism, which is unfavorable to sustained drug release. Appling an IVR can mitigate this problem with prolonged drug release and more effective dosing, but it is not "smart" by design, continuously releasing the drug even when it is not needed. Besides, the formulation based on IVRs is highly acceptable for women who have previous user experience, but not a prioritized choice for many other women with vaginal infections probably due to comfort issues[79].

ii) They are not preventive therapies. A common issue is that 50% of women with BV are asymptomatic and are unaware that they have the disease, making it difficult to treat them in time[19]. However, it is often the case that the applied treatments to realize sustained or controlled drug release during the course of symptomatic BV are neither helpful in promoting a rapid recovery nor inhibiting possible recurrence. Therefore, such methods are not ideal for BV prevention and relapse treatment.

In this case, stimuli-responsive systems capable of achieving "smart" release of drugs might be a promising solution. However, studies on smart systems aiming to treat BV are very

limited, with only a few publications focusing on thermo, ion and pH-sensitive drug delivery. In other studies, targeting bacterial infections, enzymes secreted by the target bacteria such as lipase and hyaluronidase have been utilized as stimuli to trigger drug release. Compared to those physical stimuli, these virulence factors are preferable in achieving bacteria-responsive drug release due to specificity. As a result, such drug delivery systems have much better therapeutic efficacy. In this study, a liposome-based bacteria-responsive drug release platform will be designed in response to one of the virulence factors of *G. vaginalis*, namely VLY. This will be the first on-demand therapy for the prophylaxis and relapse treatment of BV.

1.7 Hypothesis and objectives

Hypothesis

Our bacteria-responsive drug delivery platform will significantly release drug in the presence of VLY in comparison to the control group.

Objectives

Objective 1: To prepare and characterize liposomes.

Objective 2: To develop the bacteria-responsive drug release platform.

Objective 3: To construct the recombinant VLY expression system.

Objective 4: To perform recombinant VLY expression and purification.

Chapter 2 Liposome preparation and characterization

2.1 Materials

Egg L-α-Phosphatidylcholine (EPC), cholesterol (CHOL) and calcein were purchased from Sigma Aldrich. Egg L-α-phosphatidylglycerol (sodium salt) (EPG-Na) was purchased from Sigma Aldrich (Avanti Polar Lipids). Propylene glycol (PPG) was purchased from TCI. Dialysis devices (Spectra-Por® Float-A-Lyzer®G2, molecular weight cutoff 20 kDa) were purchased from Sigma Aldrich. Dialysis tubing (molecular weight cutoff 14 kDa) was purchased from VWR. 0.45 μm polyethersulfone (PES) syringe filter was purchased from Froggabio. Sodium hydroxide was purchased from Sigma Aldrich. Amicon® Ultra-15 centrifugal filters (molecular weight cutoff 3 kDa and 10 kDa) were purchased from Sigma Aldrich. Triton X™-100 was purchased from Sigma Aldrich.

2.2 Methods

2.2.1 Calcein calibration curve

Calcein stock solution was prepared by dissolving 80 mg calcein powder in 20 mL Milli-Q water. The pH of calcein in water was adjusted to 7.4. The stock solution was serially diluted to 1000, 100, 10, 8, 6, 4, 2, 1, 0.8, 0.6, 0.4, 0.2 and 0.1 μg/mL. The fluorescence was measured using a Varioskan™ LUX multimode microplate reader (Thermo Fisher Scientific) (excitation wavelength 490 nm, emission wavelength 520 nm). Linear regression was used to generate a calibration curve. Values were normalized to a blank sample. To eliminate the possible effect of calcein absorption

has on its fluorescence, the absorption spectrum of calcein was scanned from 300 to 800 nm using a Varioskan™ LUX multimode microplate reader (Thermo Fisher Scientific).

2.2.2 Polyol dilution method

Liposomes were prepared using the polyol dilution method. Four formulations were designed with different composition ratios of EPC, EPG-Na, and CHOL (Table 2.1). Briefly, EPC and EPG-Na were dissolved in PPG at 60 °C and cholesterol was dissolved in propylene glycol at 120 °C. Once the two solutions were well mixed, the calcein stock solution was quickly poured into the mixture and stirred at 60 °C for a few minutes. The suspension was diluted with Milli-Q water (pH adjusted to 7.4), preheated to 60 °C, and stirred for 30 minutes. The volume percentage of PPG in the final suspension was 3% (v/v). Then, liposomes were sonicated for 5 s on/off for different time periods (80 s, 100 s, 200 s, 400 s) at an amplitude level of 3 using an ultrasonicator (Qsonica S-4000) before being stirred at 60 °C for 1 hour. The suspension was cooled down to room temperature. Finally, all liposomes were passed through a 0.45 μm PES membrane filter twice.

Three methods were applied to separate non-encapsulated calcein from liposomal calcein: centrifugation, ultrafiltration, and dialysis. For centrifugation, the liposomes were centrifuged at 40,000 g for 2 hours at 4 °C and washed four times with Milli-Q water (pH 7.4). For ultrafiltration, the liposomes were washed seven times using Amicon® Ultra-15 centrifugal filter (3 kDa and 10 kDa cutoff) at 4 °C. For dialysis, the liposomes were dialyzed against 2 L Milli-Q water (pH 7.4) for five days using Spectra-Por® Float-A-Lyzer®G2 dialysis cassette with a molecular weight cutoff (MWCO) of 20 kDa.

2.2.3 Encapsulation efficiency calculation and optimization

The concentration of solutions of calcein of known concentrations (0 – 4 μg/mL) were used to generate the calibration curve. Calcein of unknown concentrations was quantified using the calibration curve. The encapsulation efficiency (EE) was calculated both directly and indirectly using Equation 2.1.

$$Encapsulation\ efficiency\ (indirect)(\%) = \frac{Amount\ of\ initial\ calcein\ added - Amount\ of\ unencapsulated\ calcein}{Amount\ of\ initial\ calcein\ added} \times 100\%$$

$$Encapsulation\ efficiency\ (direct)(\%) = \frac{Amount\ of\ encapsulated\ calcein}{Amount\ of\ initial\ calcein\ added} \times 100\%$$

Equation (2.1)

Table 2.1 Liposome formulation design.

Component	Molar ratio			
	Formulation 1	Formulation 2	Formulation 3	Formulation 4
EPC	10	10	10	10
EPG-Na	1	1	1	1
CHOL	9	10	11	12
Mol% of CHOL	45%	47.6%	50%	52%

For the indirect method, the fluorescence intensity of the supernatants from the liposomes encapsulating calcein harvested from centrifugation was measured using a Varioskan™ LUX

multimode microplate reader (excitation wavelength 490 nm, emission wavelength 520 nm). For the direct method, the liposomes were treated with Triton™ X-100 to dissolve the phospholipids and were then diluted with Milli-Q water (pH 7.4) to achieve a final concentration of Triton™ X-100 of 3%. The mixture was incubated at room temperature for 30 minutes prior to the measurements. The fluorescence spectra were background corrected by using 3% Triton™ X-100 aqueous solution (pH 7.4) as the blank.

To study the influence of total lipids and initial calcein concentration on EE, parallel formulations were designed (Table 2.2). The composition ratio of parallel formulations was based on Formulation 2. EE values are presented as the mean ± standard deviation. One-way analysis of variance was performed with P values of <0.05 considered to be significant.

Table 2.2 Parallel formulations aimed for EE optimization.

Formulation	Total lipids (mM)	Amount of initial calcein	PPG amount (μL)	Liposomal suspension
F2_1	0.11	2 mg/mL, 300 μL	100	5 mL
F2_2	0.22	2 mg/mL, 300 μL	200	10 mL
F2_3	0.33	2 mg/mL, 300 μL	300	20 mL
F2_4	0.33	4 mg/mL, 300 μL	300	20 mL
F2_5	0.33	2 mg/mL, 2 mL	300	20 mL
F2_6	0.33	4 mg/mL, 2 mL	300	20 mL

2.2.4 Characterization of size distribution and zeta potential

The average diameter, size distribution and zeta potential of liposomes were measured by dynamic light scattering (DLS) using a Zetasizer Nano ZS (ZEN3600, Malvern Instruments). For zeta potential measurements, liposome samples were diluted in Milli-Q water and placed in a DTS1070 cuvette (Malvern Panalytical). Each sample was measured by making six recordings at 25 °C.

2.3 Results and discussion

2.3.1 Calcein calibration curve

Calcein was chosen as a model drug to be encapsulated into liposomes as its concentration is relatively easy to quantify by spectroscopy due to its strong fluorescence. In addition, calcein is a hydrophilic molecule that can be encapsulated inside liposomes instead of inserted into lipid bilayers. This will result in low phospholipid permeation that helps avoid possible drug leakage. The absorbance of calcein was also studied from 300 to 800 nm. The results show that calcein has very low absorbance at low concentrations (0.1 – 1 μg/mL), indicating that the impact of absorbance on calcein's fluorescence can be neglected (Figure 2.3).

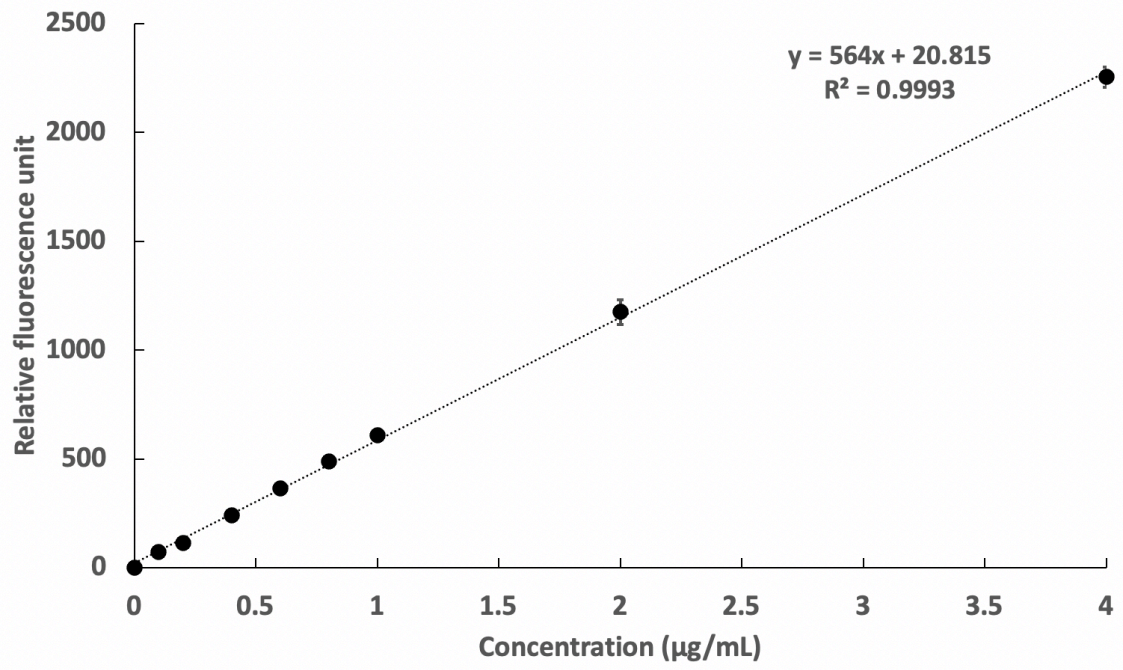


Figure 2.1 Calcein calibration curve. Known concentrations of calcein (0 – 4 µg/mL) were used. Fluorescence emission was measured at 520 nm with excitation wavelength at 490 nm. Values represent mean +/- standard deviation (n=3).

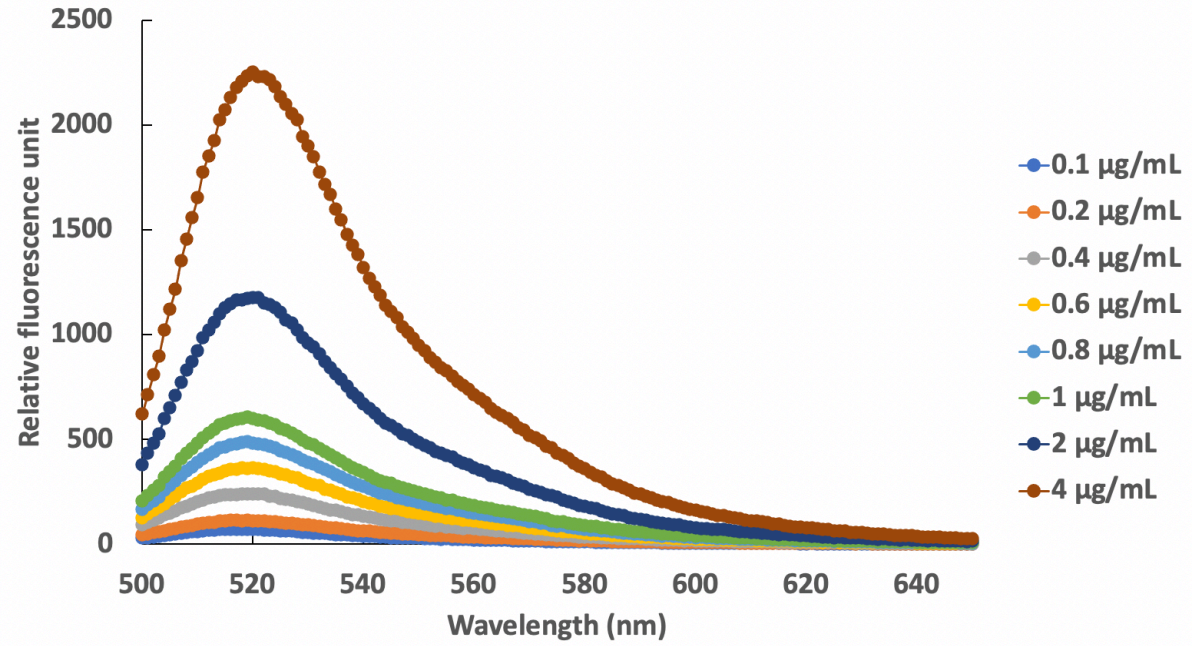


Figure 2.2 The fluorescence spectra (500 – 650 nm) of calcein aqueous solutions with different concentration ranging from 0.1 to 4 µg/mL. (Excitation wavelength: 490 nm)

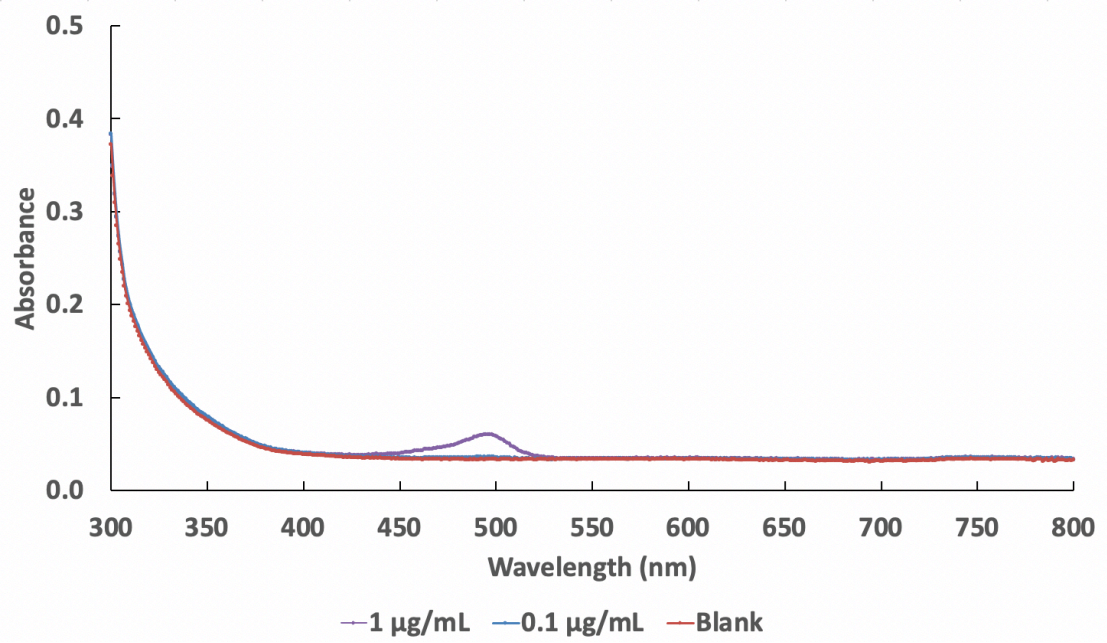


Figure 2.3 The absorption spectra (300 – 800 nm) of calcein aqueous solutions with concentrations of 1 µg/mL and 0.1 µg/mL. MilliQ water (pH 7.4) was set as blank. Note: the absorption spectrum of the 1 µg/mL calcein solution and the blank cannot be distinguished experimentally.

2.3.2 Liposome preparation and purification

The polyol dilution method was chosen to prepare liposomes due to its unique advantages over other conventional strategies such as thin film hydration and reverse-phase evaporation. Propylene glycol is water-soluble and non-toxic compared to volatile organic solvents such as chloroform. Thus, there is no need to remove solvents from the final liposomal suspension because propylene glycol does not harm human tissues or cells once the formulation is applied in women vagina. Moreover, propylene glycol also helps improve liposome stability during long-term storage due to the interaction between polyols and lipid membrane[80]. Therefore, polyol dilution is a simple and valuable method of preparing liposomes encapsulating drugs.

The components for liposome formulations were selected as follows. EPC was chosen as the structural component in terms of cost-effectiveness, stability and superior drug carrying ability over other types of phospholipids. First, phospholipids from natural sources such as plants (e.g. soybean) and animals (e.g. egg yolk) have a lower product cost than synthetic phospholipids. Second, phospholipids isolated from egg yolk has better oxidation stability compared to those isolated from soybeans due to the relatively high saturation level of egg yolk lecithin, resulting in more controlled quality production of liposomes[81]. In addition, it has been shown that liposomes made from EPC demonstrate higher EE and lower drug leakage rate than those made from soybean phosphatidylcholine (SPC) when it comes to drug loading[81].

CHOL was incorporated into liposomes with different molar ratios ranging from 45% to 52% as the bacteria-responsive component to evaluate liposome drug release performance in the presence of VLY. Another function of CHOL is to increase bilayer rigidity of liposomes and reduce membrane permeability[82]. EPG-Na was introduced at a relatively low molar ratio as a negatively charged lipid to prevent potential liposome aggregation by creating electrostatic repulsion between particles.

Three purification methods were compared in terms of effectiveness and efficiency to determine an optimal condition to separate non-encapsulated calcein from liposomes. It is found that centrifugation at a moderate centrifugal force (40,000 g) is the best option without sacrificing liposome stability compared to ultrafiltration and dialysis. After four successive washes, the calcein concentration of the supernatant from liposomes is less than 0.1%. The average diameters and size distributions of liposomes before and after purification through centrifugation were measured by DLS (Figure 2.4). There is no significant difference in size distribution, indicating

that liposomes remain relatively stable without much aggregation. The slight decrease in the PDI of the liposomes after centrifugation is probably due to the exclusion of the fractions with much smaller size by centrifugation, resulting in a liposomal suspension with a narrow distribution of hydrodynamic diameters (Table 2.3).

Table 2.3 Liposome size distribution before and after centrifugation.

Sample	Z-average diameter and polydispersity index (PDI)
Liposomes before centrifugation	341 ± 12 nm, PDI 0.336
Liposomes after centrifugation	331 ± 9 nm, PDI 0.327

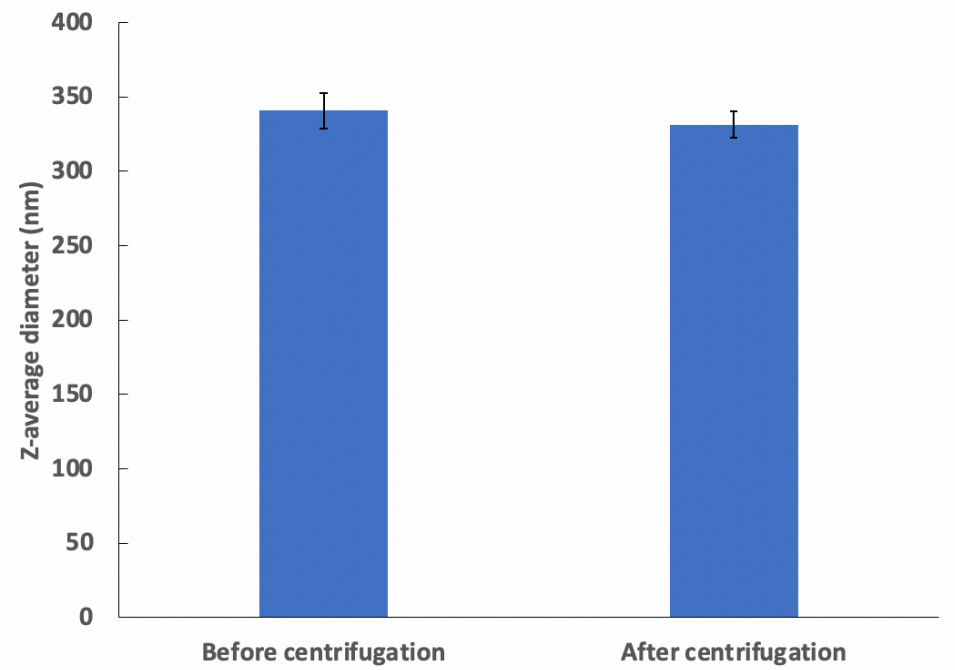


Figure 2.4 Comparison of liposome size distribution before and after centrifugation. Liposomes were prepared by sonication for 200 s at amplitude 3 using a sonicator. The liposomal suspension was centrifuged at 40,000 g for 2 hours at 4 °C to remove non-encapsulated calcein. The liposomes harvested from centrifugation was completely resuspended in Milli-Q water (pH 7.4) prior to DLS measurement. The Z-average diameter values are the means +/- standard deviation of six repeat measurements (P value > 0.05).

Ultrafiltration was applied as the second purification method, but it turned out that it was not very effective in achieving complete separation. Liposomal suspension was filtrated with a 10 kDa cutoff membrane filter under centrifugation conditions of 5000 g at 4 °C followed by seven washes conducted sequentially. However, the calcein concentration of the filtrate was still more than 5% even after multiple washing steps. More important, increasing washing times results in unnecessary loss of liposomes, as liposomes could be forced to squeeze through the membrane and migrate into the filtrate. This assumption was further proved by DLS that the filtrate had an average size of less than 200 nm indicating that some small liposomes had passed through. To prevent liposomes migration, a membrane filter with a 3 kDa cutoff was used for filtration. However, the filtration efficiency was greatly compromised, with a near tripling of the centrifugation time. Increasing centrifugal force was not applicable either, as the membrane could be damaged. Similarly, dialysis was also not the ideal purification method as it took as long as a week to remove the non-encapsulated calcein as completely as possible, with frequent changes of the dialysis medium to ensure molecular diffusion caused by concentration gradient.

It was found that the EE depends on the total amount of lipids and initial calcein concentration. Comparisons were made among EE calculated using the direct method, as the indirect method is more questionable considering possible calcein loss during the purification process. Generally, the EE increases as the total amount of lipids increases (Figure 2.5). In addition, a higher EE can be achieved if the initial calcein solution is more concentrated, as there is a significant difference between 2 and 4 mg/mL. Although increasing the amount of initial calcein (e.g., from 300 μL of 2 mg/mL to 2 mL of 2 mg/mL or from 300 μL of 4 mg/mL to 2 mL of 4 mg/mL) does not result in a significant difference in terms of EE, it helps increase the amount

of calcein encapsulated. In this study, the formulation parameters (amounts of initial calcein and PPG) of F2_6 were chosen for Formulation 1-4, as it favors a larger amount of encapsulated calcein instead of a higher EE, since the former conditions help better evaluate the performance of bacteria-responsive calcein release in the following chapter. Therefore, 2 mL of 4 mg/mL calcein stock solution was added to Formulations 1-4 as the initial dose. In Formulation 2, the total amount of lipids was set at 0.33 mM, whereas in Formulation 1, 3 and 4 the composition ratio of EPC to EPG-Na was kept the same as that in Formulation 2 with varying amounts of CHOL.

Table 2.4 Comparison of EE of liposome formulations.

Formulation	Total lipids (mM)	Amount of initial calcein	EE (indirect, %)	EE (direct, %)
F2_1	0.11	2 mg/mL, 300 μL	6 $\pm$ 3	5 $\pm$ 2
F2_2	0.22	2 mg/mL, 300 μL	9$\pm$ 3	7 $\pm$ 3
F2_3	0.33	2 mg/mL, 300 μL	10 $\pm$ 3	9 $\pm$ 2
F2_4	0.33	4 mg/mL, 300 μL	16 $\pm$ 2	14 $\pm$ 2
F2_5	0.33	2 mg/mL, 2 mL	10 $\pm$ 3	9 $\pm$ 2
F2_6	0.33	4 mg/mL, 2 mL	15 $\pm$ 2	13 $\pm$ 2

EE values represent the means of three preparations $\pm$ standard deviation.

Table 2.5 EE of liposome formulations 1-4.

Formulation	EE (%)		Component molar ratio
	Indirect method	Direct method	
1	15 $\pm$ 3	13 $\pm$ 2	EPC:EPG-Na:CHOL = 10:1:9
2	15 $\pm$ 2	13 $\pm$ 2	EPC:EPG-Na:CHOL = 10:1:10
3	13 $\pm$ 3	12 $\pm$ 2	EPC:EPG-Na:CHOL = 10:1:11
4	11 $\pm$ 3	11 $\pm$ 1	EPC:EPG-Na:CHOL = 10:1:12

All values represent the means of three preparations $\pm$ standard deviation.

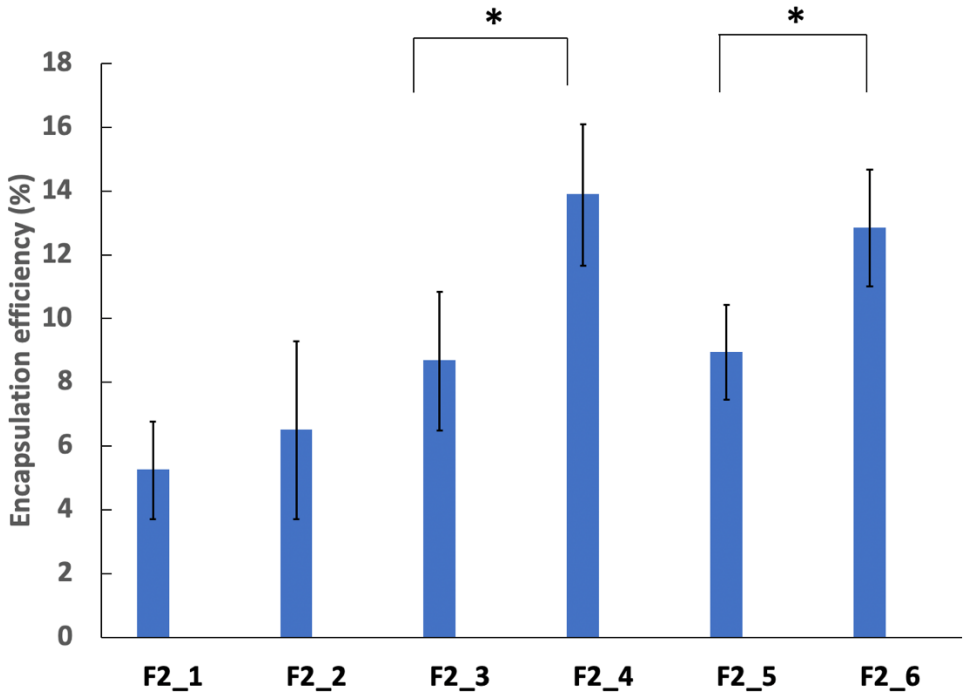


Figure 2.5 EE of liposome formulations (F2_1-F2_6) calculated using direct method. F2_1: 0.11 mM lipids, 300 µL of 2 mg/mL initial calcein; F2_2: 0.22 mM lipids, 300 µL of 2 mg/mL initial calcein; F2_3: 0.33 mM lipids, 300 µL of 2 mg/mL initial calcein; F2_4: 0. 33 mM lipids, 300 µL of 4 mg/mL initial calcein; F2_5: 0.33 mM lipids, 2 mL of 2 mg/mL initial calcein; F2_6: 0.33 mM lipids, 2 mL of 4 mg/mL initial calcein. All values represent the means of three preparations +/- standard deviation. (P value < 0.05)

2.3.2 Liposome size distribution and zeta potential

The size distributions of liposomes (using Formulation 2 as an example) treated with varying sonication times were measured by DLS to study the effect of sonication on size (Figure 2.6). The liposome dispersions were not filtered with the PES membrane filter. In general, the average diameter of liposomes decreases as sonication time increases. However, liposomes with a relatively large diameter (> 500 nm) were less stable according to the quality report of the Zetasizer measurement results, with wider size distributions, larger standard deviations and varying zeta potential values. This is probably because large particles are prone to aggregate under gravity

force, which may negatively affect the homogeneity of the liposomal suspension. In contrast, smaller particles tend to be more stable and the results for size distribution and zeta potential are relatively more consistent. But the purification efficiency was greatly sacrificed. For example, particles as small as 100 nm were very hard to spin down even with a centrifugal force of 100,000 g. Considering that the liposome formulation will not be applied internally in the human body, there is no need to reduce the size of the liposomes too much. Hence, the sonication time was fixed at 200 s to prepare liposomes with an average diameter ranging from 300 nm to 400 nm, so that the liposomes could be purified through centrifugation at 40,000 g without compromising the drug loading amount and stability too much. Once the sonication time was determined, Formulations 1-4 were filtered with a 0.45 μm PES membrane filter to further narrow the size distribution prior to the measurement.

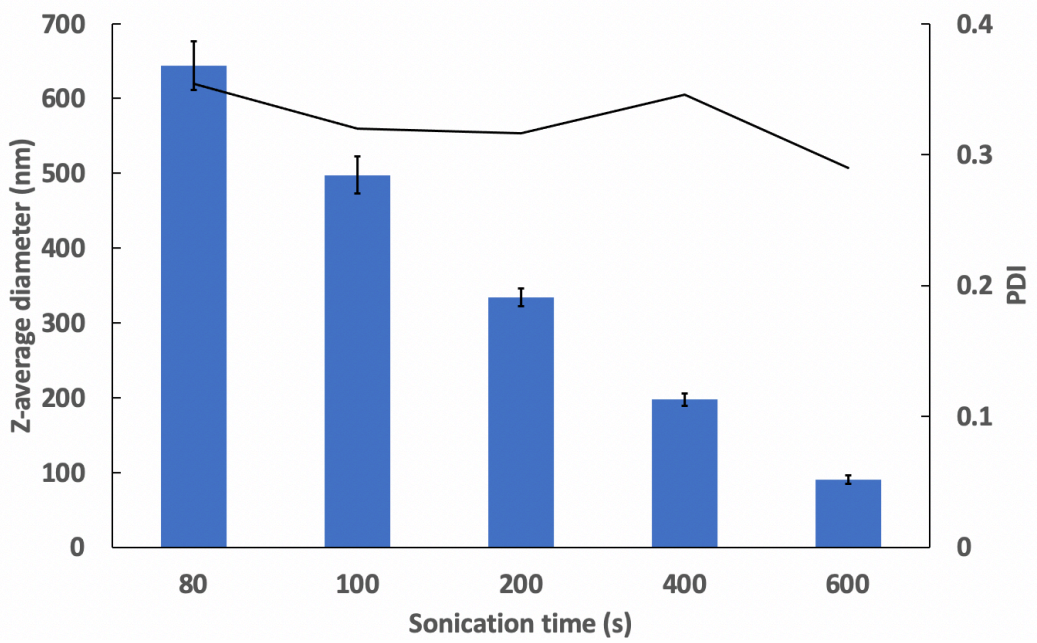


Figure 2.6 Size distribution of liposomes (Formulation 2) with varying sonication time lengths ranging from 80 s to 600 s without using PES filter. The Z-average diameter values are the means of six repeat measurements (+/- standard deviation).

Liposomes of Formulation 1 – 4 have an average diameter of about 300 nm with a relatively narrow PDI of less than 0.3, indicating that the amount of CHOL in the formulation does not affect particle size much. In addition, all liposomes have a negative zeta potential that is attributed to the presence of the negatively charged EPG-Na.

Table 2.6 Size distribution and zeta potential of Formulations 1-4.

Formulation	Size distribution	Zeta potential
1	319 ± 5 nm, PDI 0.252	-64 ± 1 mV
2	324 ± 4 nm, PDI 0.255	-56 ± 2 mV
3	330 ± 3 nm, PDI 0.286	-59 ± 1 mV
4	319 ± 4 nm, PDI 0.284	-65 ± 1 mV

Chapter 3 Bacteria-responsive drug release platform development

3.1 Materials

Brain heart infusion (BHI) (GranuCult®) and Columbia agar were purchased from Sigma Aldrich. *Gardnerella vaginalis* (ATCC 14018) *Lactobacillus crispatus* (ATCC 33820) were purchased from American Type Culture Collection (ATCC). Lactobacilli Man-Rogosa-Sharpe (MRS) agar (BD Difco™) and MRS broth were purchased from Thermo Fisher Scientific. Sheep blood (sterile, defibrinated) was purchased from Cedarlane. Yeast extract (Gibco™) and proteose peptone No. 3 (Gibco™) were purchased from Thermo Fisher Scientific. Casman agar base was purchased from BD. N-(2-Hydroxyethyl)piperazine-N′-(2-ethanesulfonic acid), 4-(2-Hydroxyethyl)piperazine-1-ethanesulfonic acid (HEPES) was purchased from Sigma Aldrich. Horse serum (Gibco™, heat inactivated, New Zealand origin) was purchased from Thermo Fisher Scientific. Rabbit blood (sterile, defibrinated) was purchased from Thermo Fisher Scientific. Penicillin/streptomycin solution (Gibco™) was purchased from Thermo Fisher Scientific. Polyethersulfone (PES, 0.22 μm) syringe filter (sterile) was purchased from Froggabio. Sodium chloride, glucose, agar and glycerol were purchased from Sigma Aldrich.

3.2 Methods

3.2.1 Bacteria culture

G. vaginalis strain 14018 was cultured in liquid media, i.e., BHI medium and ATCC medium 1685 NYC III, and solid media (agar plate) separately. Once prepared, the media and agar plates were stored at 4 °C. The strain was stored in 10% sterile glycerol at – 80 °C.

BHI was prepared by adding 37 g to 1 L Milli-Q water and autoclaved at 121 °C for 15 minutes. 1685 NYC III was prepared by adding 4 g HEPES, 15 g proteose peptone No. 3 and 5 g sodium chloride to 875 mL Milli-Q water. The pH of the solution was adjusted to 7.3. The solution was then autoclaved at 121 °C for 15 minutes and cooled down to room temperature. The solution of 5 g glucose, 25 mL fresh yeast extract and 100 mL heat inactivated horse serum was filter-sterilized using a 0.22 μm PES filter and then added to the above autoclaved solution. For each liquid culture, 100 μL of preserved strain was thawed on ice and inoculated into 10 mL broth. The culture was incubated at 37 °C with 5% CO_2 overnight.

1685 NYC III agar plates were prepared by adding 4 g HEPES, 15 g Proteose Peptone No. 3, 5 g sodium chloride and 15 g agar to 875 mL Milli-Q water. The solution was autoclaved at 121 °C for 15 minutes and cooled down for a while before adding the filter-sterilized solution of glucose, fresh yeast extract and heat inactivated horse serum. Then the solution was quickly poured onto sterilized petri dishes and solidified at room temperature.

Columbia agar plates were prepared by adding 42 g Columbia agar to 1 L Milli-Q water. The solution was autoclaved at 121 °C for 15 minutes and cooled down to 50 – 60 °C before adding 5% (v/v) sterile sheep blood. Then the solution was quickly poured onto sterilized petri dishes and solidified at room temperature.

Casman agar plates were prepared by adding 43 g Casman agar base to 950 mL Milli-Q water. The solution was autoclaved at 121 °C for 15 minutes and cooled down to 45 – 50 °C before adding 5% (v/v) sterile rabbit blood. Then the solution was quickly poured onto sterilized petri dishes and solidified at room temperature.

For each solid culture, a sterile inoculation loop was dipped into a liquid culture and then streaked on the agar plate. The plate was incubated at 37 °C with 5% CO_2 for at least 48 hours to show completely isolated colonies. The optical density (OD) of *G. vaginalis* was measured using a SpectraMax M5 Multimode Plate Reader (Molecular Devices Inc.) at the wavelength of 600 nm.

L. crispatus strain 33820 was cultured in liquid media and solid media separately. Once prepared, the media and agar plates were stored at 4 °C. The strain was stored in 10% sterile glycerol at – 80 °C.

The MRS broth was prepared by adding 55 g of powder to 1 L Milli-Q water. The solution was autoclaved at 121 °C for 15 minutes and cooled down to room temperature. For each liquid culture, 30 µL of preserved strain was thawed on ice and inoculated into 10 mL broth. The culture was incubated at 37 °C with 5% CO_2 overnight.

MRS agar was prepared by adding 70 g of powder to 1 L Milli-Q water. The solution was autoclaved at 121 °C for 15 minutes and cooled down for a while. Then the solution was quickly poured onto sterilized petri dishes and solidified at room temperature. For each solid culture, a sterile inoculation loop was dipped into a liquid culture and then streaked on the agar plate. The plate was incubated at 37 °C with 5% CO_2 for 36 – 48 hours to show completely isolated colonies. The OD of *L. crispatus* was measured using SpectraMax M5 Multimode Plate Reader (Molecular Devices Inc.) at the wavelength of 600 nm.

3.2.2 Bacteria counting

For *G. vaginalis* counting, one colony-forming unit (CFU) was scratched from a fresh agar plate and inoculated into 10 mL broth. 50 µL of the cells was drawn from the broth and diluted 10, 100,

1,000, 10,000 and 100,000-fold separately with 1685 NYC III. Four agar plates were spread with 50 µL of the diluted cells (100x, 1,000x, 10,000x and 100,000x dilution) and 50 µL 1685 NYC III. The plates were incubated at 37 °C and 5% CO_2 for 48 hours. The number of the CFUs counted from the 100,000-fold dilution plate was counted three times and averaged. The concentration of the original broth is calculated using Equation 3.1.

$$Bacteria\ concentration\ (numbers/mL) = \frac{The\ number\ of\ the\ CFUs\ counted\ from\ the\ 100{,}000x\ dilution\ plate \times 1000\ \mu L \times 100{,}000}{50\ \mu L \times 1\ mL}$$

$$Equation\ (3.1)$$

For *L. crispatus* counting, the method was similar to that for *G. vaginalis*. Four agar plates were inoculated with 100 uL cells and incubated at 37 °C and 5% CO_2 for 36 – 48 hours.

3.2.3 Calcein calibration curve

The stock solutions of calcein in the 1685 NYC III and MRS media were prepared using a method similar to that stated in Chapter 2. Briefly, 20 mg calcein was dissolved in 20 mL medium, followed by a serial dilution to 100, 10, 8, 6, 4, 2, 1, 0.8, 0.6, 0.4, 0.2, 0.1, 0.08, 0.06, 0.04 and 0.02 µg/mL. Linear regression was used to generate a calibration curve and the value of the blank was subtracted from the value of each point of the curve.

3.2.4 Bacteria-responsive calcein release of liposomes

The stability of calcein in different media was evaluated by measuring its fluorescence intensity that varied with time in the 1685 NYC III medium and *G. vaginalis* supernatant. Briefly, calcein was dissolved in the medium to reach a concentration of 10 µg/mL (with 1% v/v

penicillin/streptomycin) added. The solution was incubated at 37 °C and shaken at 100 rpm (avoid light). Samples were taken at different time intervals and changes in fluorescence intensity were monitored.

G. vaginalis and *L. crispatus* were inoculated into 10 mL 1685 NYC III and 10 mL MRS broth, respectively, and incubated overnight. The concentrations (CFUs/mL) of *G. vaginalis* and *L. crispatus* were kept constant. Bacterial cells were removed through centrifugation at 8,000 g for 10 minutes. 4 mL bacterial supernatant was mixed with purified liposomes and penicillin/streptomycin (1% v/v) to reach a total volume of 5 mL. A same volume (4 mL) of either 1685 NYC III or MRS broth mixed with equal amounts of purified liposomes and penicillin/streptomycin (1% v/v) was kept as control group. The mixtures were incubated at 37 °C and shaken at 100 rpm (avoid light). Aliquots (400 μL) of mixtures were taken at different time intervals (0-150 hours) and centrifuged at 40,000 g for 2 hours at 4 °C to remove the pellets. The fluorescence intensity of the supernatant was measured to determine the calcein concentration with the calibration curve. To compare the responsive release from *G. vaginalis* and *L. crispatus* supernatants, the amount of calcein released from the control group (pure medium) was subtracted from the experiment group.

3.3 Results and discussion

3.3.1 *G. vaginalis* culture optimization

Optimizations were performed to both liquid culture and solid culture. It is found that *G. vaginalis* was found to be unable to grow in BHI probably due to the lack of nutrients such as serum, whereas it grew well in the 1685 NYC III medium. In addition, the growth rate of *G. vaginalis* also depends

on the total amount of inoculation. The more cells are inoculated, the faster *G. vaginalis* grows. Finally, 100 μL of preserved cells was determined as the optimal inoculation amount to allow for a suitable growth rate in broth culture (Figure 3.1).

The growth of *G. vaginalis* on agar plates was found to be very poor at the beginning. Therefore, a series of optimization studies were carried out to determine an optimal cultivation condition for *G. vaginalis*, including agar plate selection, inoculation method and inoculation amount (Table 3.1). No bacteria growth was observed on Columbia agar plates even after a week's incubation (Figure 3.2), whereas growth was observed in varying degrees on both 1685 NYC III and Casman agar plates. The results showed that the spreading method could facilitate a heavy and confluent growth, resulting in a bacteria lawn (Figure 3.3), while the streaking method resulted in separately grown colonies (Figure 3.4 and 3.5). Apart from the inoculation method, bacteria growth also depends on the inoculation amount. Too much inoculation is very likely to bring about fierce competition among bacteria colonies, leading to very little or no growth. Overall, Casman agar was considered more suitable than Columbia agar and 1685 NYC III agar. Thus, for bacteria counting, *G. vaginalis* was cultured on Casman agar with the streaking method and incubated at 37 °C for 48 hours.

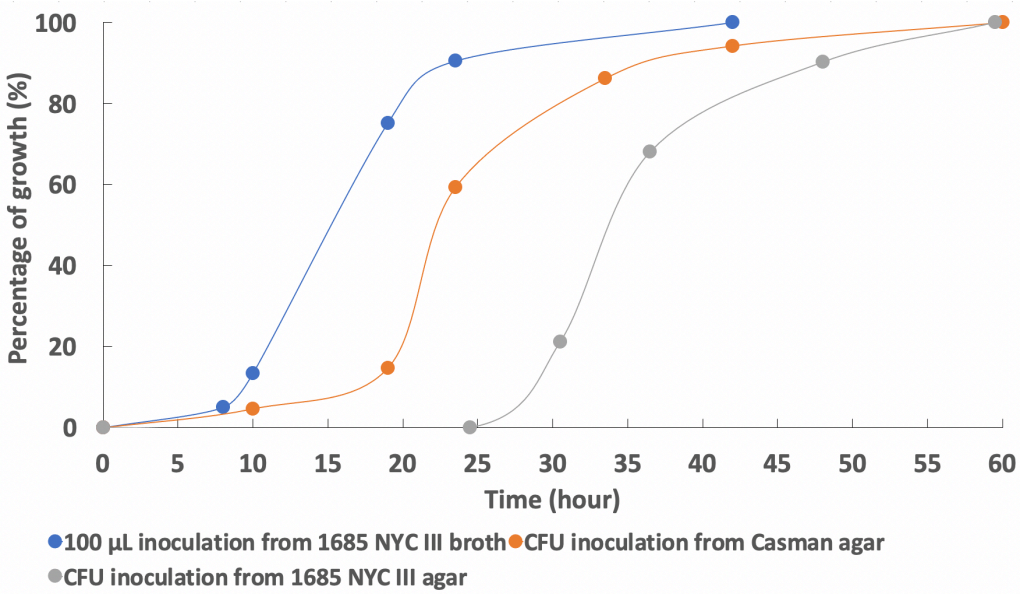
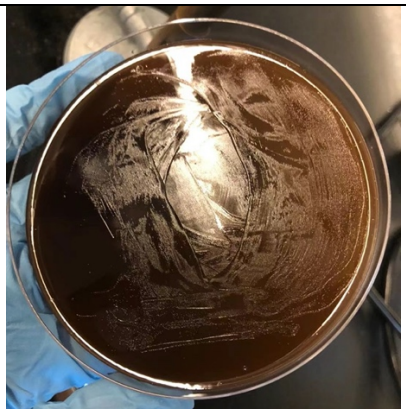
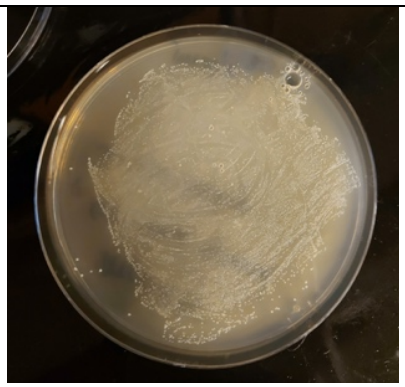
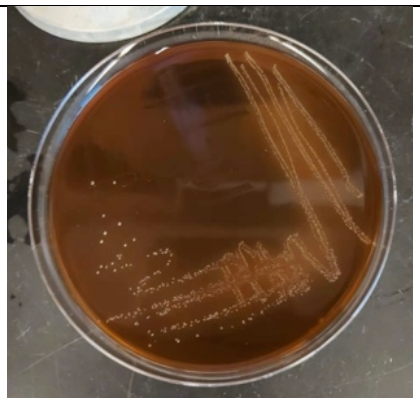


Figure 3.1 *G. vaginalis* growth in liquid culture. 100 µL cells were inoculated into 10 mL broth and incubated at 37 °C. Alternatively, one CFU was scratched from the plate and inoculated into 10 mL broth and incubated at 37 °C. Values represent the mean of three recordings.

Table 3.1 Solid culture optimization of *G. vaginalis*.

Agar plate type	Inoculation method	Inoculation volume (μL)	Bacteria growth
Columbia agar (5% sheep blood)	Spreading	100	 **Figure 3.2** Columbia agar plate. No bacteria growth was observed after one week of cultivation.
Columbia agar (5%	Spreading	50	No growth.

sheep blood)			
Columbia agar (5% sheep blood)	Streaking	N/A	No growth
1685 NYC III agar	Spreading	30 μL	 **Figure 3.3** 1685 NYC III agar plate (spreading). Bacteria lawn formed after 48 hours of cultivation.
1685 NYC III agar	Streaking	N/A	 **Figure 3.4** 1685 NYC III agar plate (streaking). Very few CFUs were found after 48 hours of cultivation.

Casman agar (5% rabbit blood)	Streaking	N/A	 **Figure 3.5** Casman agar plate (streaking). CFUs were found after 36-48 hours of cultivation.
Casman agar (5% rabbit blood)	Spreading	100 μL	No growth.

3.3.2 Bacteria counting

Both *G. vaginalis* and *L. crispatus* were counted on the 100,000-fold dilution plates.

i) *G. vaginalis*: The number of the 100,000-fold dilution plate was counted to be 249. Hence, the original concentration of the broth was 4.97×10^8/mL, which corresponded to 78.6% of the total bacteria growth (20 hours of cultivation); ii) *L. crispatus*: The number of the 100,000-fold dilution plate was counted to be 325. Hence, the original concentration of the broth was 6.5×10^8/mL, which corresponded to 56.3% of the total bacteria growth (16 hours of cultivation).

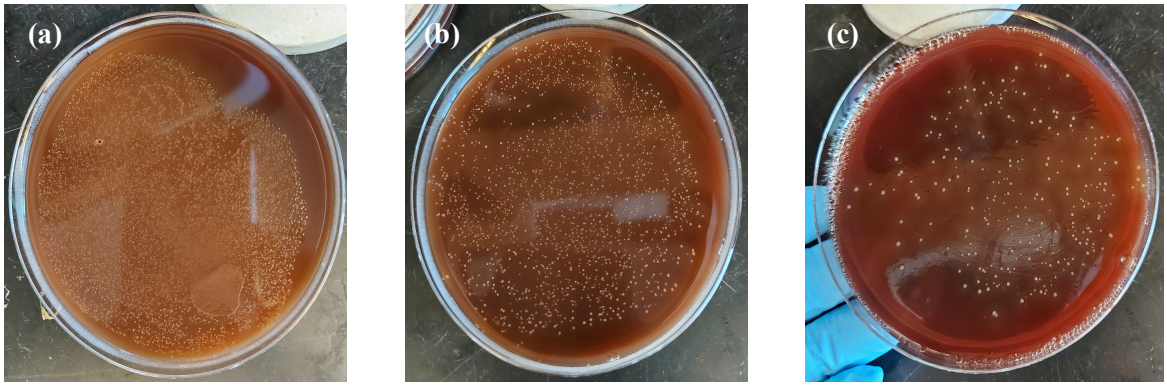


Figure 3.6 CFUs of *G. vaginalis* grown on Casman agar plates (5% rabbit blood). a) 1,000-fold dilution; b) 10,000-fold dilution; c) 100,000-fold dilution. For each plate, 50 µL bacterial cells and 50 µL 1685 NYC III medium were spread.

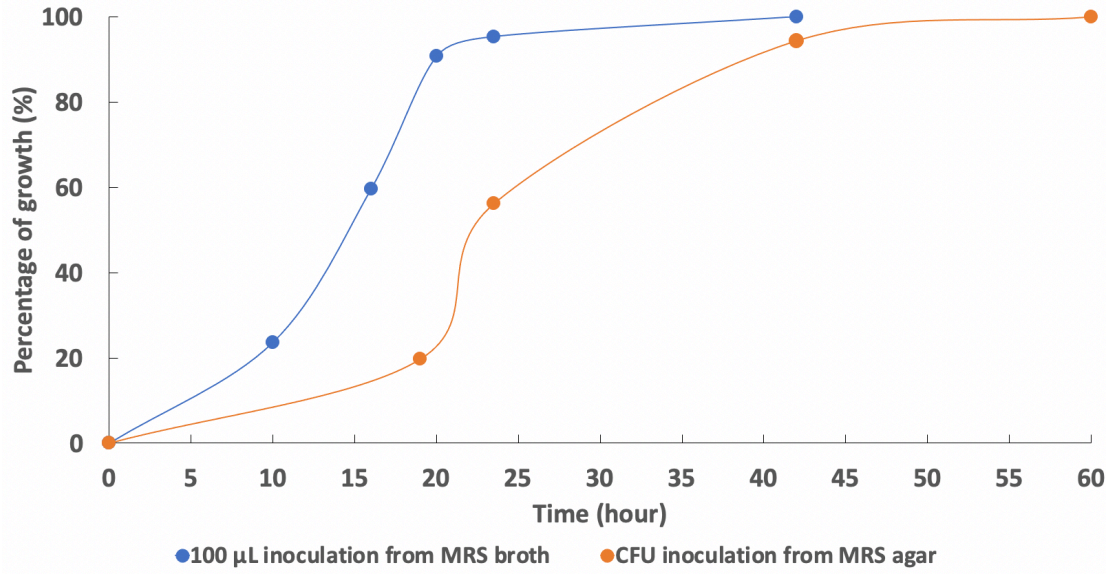


Figure 3.7 *L. crispatus* growth (OD_{600}) in liquid culture. 100 µL cells were inoculated into 10 mL broth and incubated at 37 °C. Alternatively, one CFU was scratched from the plate and inoculated into 10 mL broth and incubated at 37 °C. Values represent the mean of three recordings.

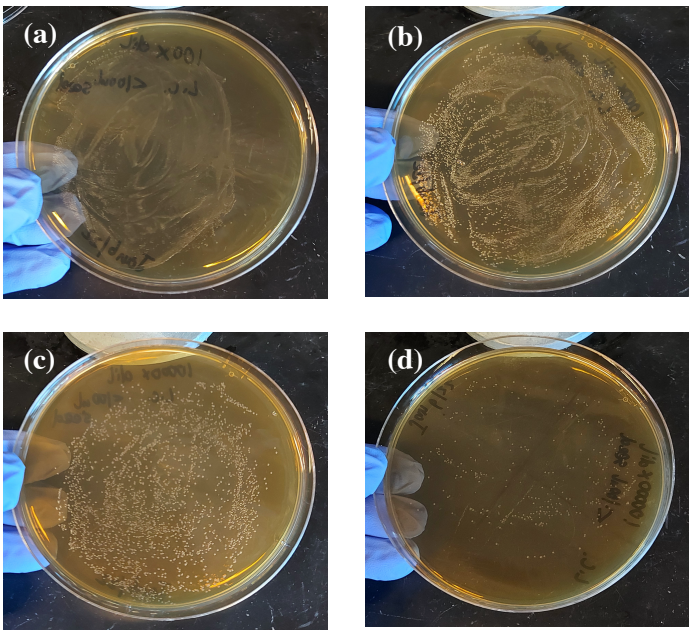


Figure 3.8 CFUs of *L. crispatus* grown on MRS agar plates. a) 100-fold dilution; b) 1,000-fold dilution; c) 10,000-fold dilution; d)100,000-fold dilution. For each plate, 100 µL bacterial cells were spread.

3.3.3 Calcein calibration curve

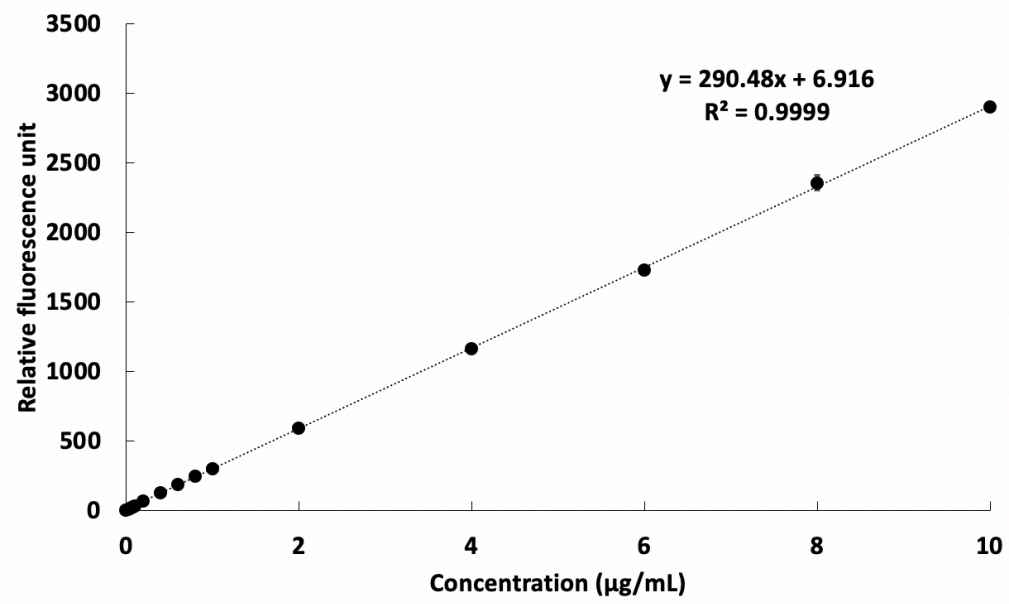


Figure 3.9 Calcein calibration curve in 1685 NYC III medium. Known concentrations of calcein (0-10 µg/mL) were used. Fluorescence emission was measured at 520 nm with excitation wavelength at 490 nm. Values represent mean +/- standard deviation (n=3).

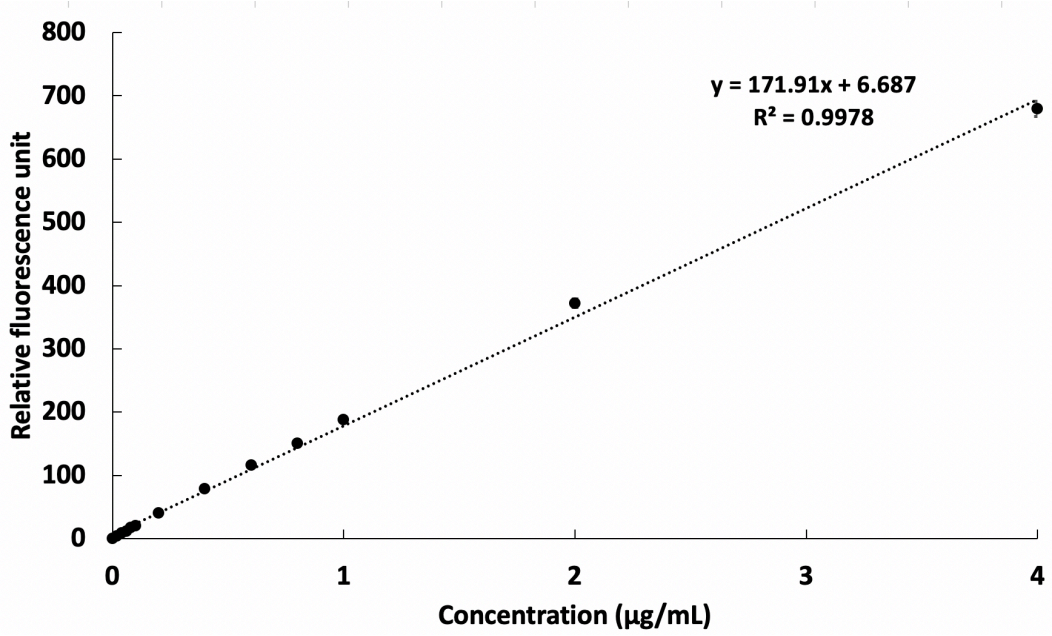


Figure 3.10 Calcein calibration curve in MRS medium. Known concentrations of calcein (0-4 µg/mL) were used. Fluorescence emission was measured at 520 nm with excitation wavelength at 490 nm. Values represent mean +/- standard deviation (n=3).

3.3.4 Calcein fluorescence stability in different media

Calcein was dissolved in the 1685 NYC III medium and *G. vaginalis* supernatant separately. The fluorescence intensity was monitored for 140 hours (Figure 3.11). To prevent potential contamination during the course of the study, penicillin and streptomycin were added to the medium to inhibit microorganism growth.

After 140 hours, 1685 NYC III medium and *G. vaginalis* supernatant with 1% penicillin/streptomycin were both clear without turbidity, indicating that 1% penicillin/streptomycin was effective enough to prevent bacterial growth. Therefore, 1% penicillin/streptomycin addition was adopted in the following studies. Moreover, an 11 – 15 % of calcein fluorescence decrease was found during the process. This quenching was deemed reasonable considering the very long exposure time and indicated that calcein was a suitable

indicator of responsive release from liposomes.

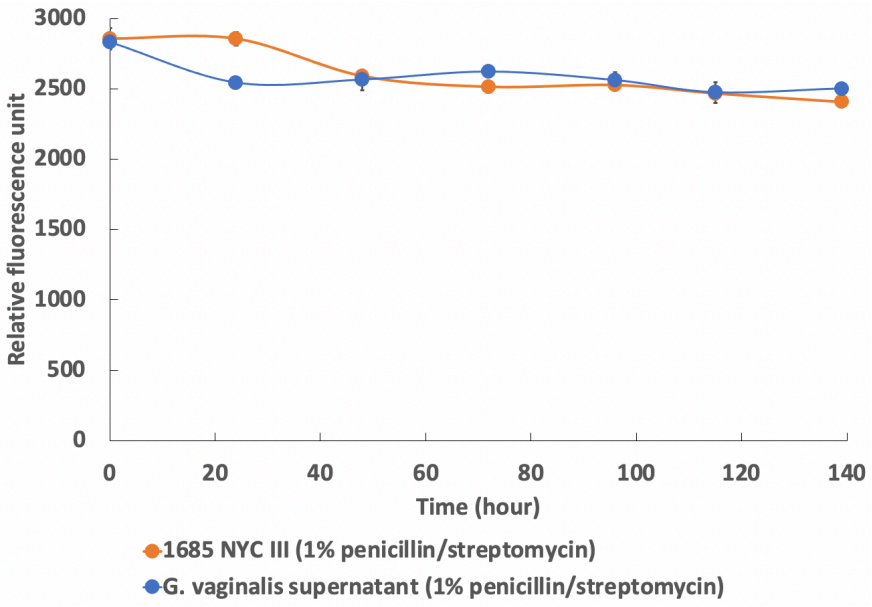


Figure 3.11 Calcein fluorescence stability in 1685 NYC III medium and *G. vaginalis* supernatant. The initial concentration of calcein is 10 µg/mL.

3.3.5 Responsive calcein release profile

The calcein release profiles of Formulations 1 – 4 were studied to evaluate the responsiveness of the liposomes to *G. vaginalis*. The bacteria were grown to achieve around 78% of total growth before the supernatant was collected and mixed with liposomes. During this period, the bacteria are in the late stage of the exponential phase where the production of VLY is supposed to be maximized. As is shown in Figures 3.12, four formulations were able to achieve a 3 – 5 days' sustained release in the presence of *G. vaginalis* supernatant, whereas four control groups demonstrated negligible release. The responsive release is attributed to the damage of the liposome structure caused by VLY produced by *G. vaginalis*.

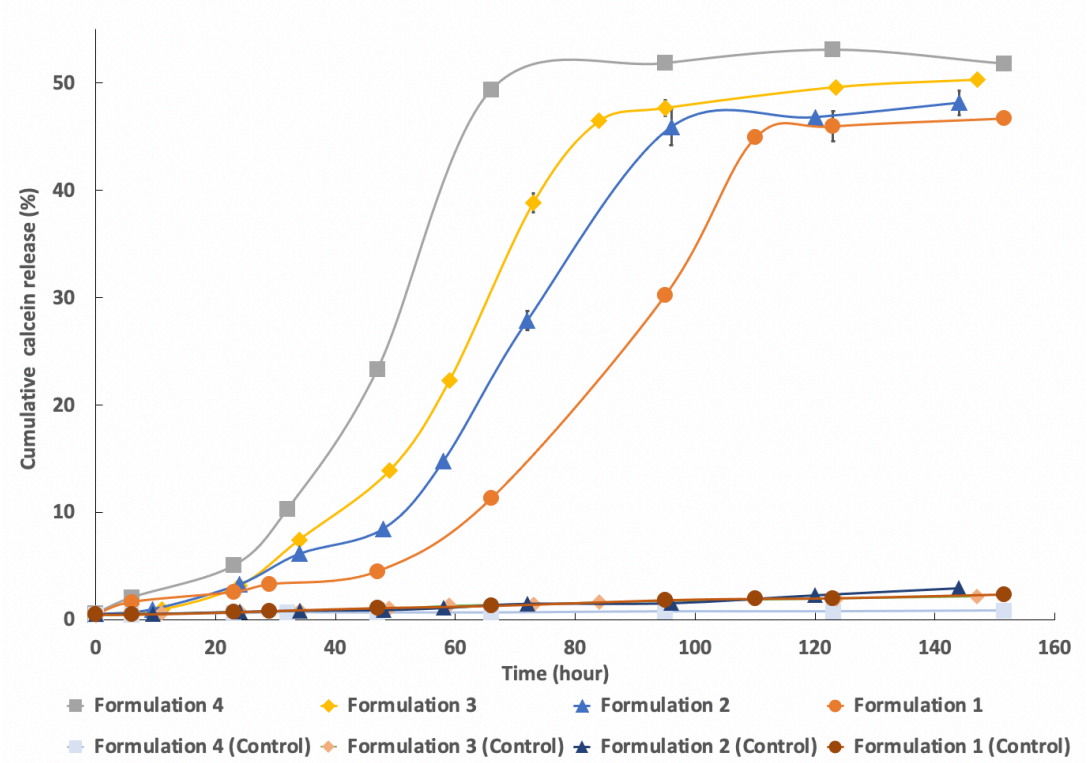


Figure 3.12 Comparison of cumulative calcein release stimulated by *G. vaginalis*. The values represent mean +/- standard deviation (n=3).

The calcein release rate depends on the amount of CHOL in the liposomes, as more CHOL promotes VLY binding to the bilayer and thus pore formation, resulting in calcein discharge. The average cumulative calcein release percentage of the experiment groups is slightly different among the four formulations, ranging from 46.7% to 51.8%, while that of the control group ranges from 0.85% to 2.94% (Figure 3.12). It is plausible that Formulation 4 demonstrates the largest accumulative release percentage as more liposomes are disrupted by VLY with CHOL concentration as high as 52 mol%. However, as shown in Figure 3.12, the differences in the cumulative calcein release from four formulations are not significant, which is probably attributed to drug saturation (the released calcein level is sufficiently high in the medium). In future, one

possible solution is to perform the responsive release studies under sink conditions to avoid saturation and calculate cumulative drug release percentage more accurately.

The calcein release profile in the presence of *L. crispatus* supernatant was also evaluated to assess the liposomes' inertness to *L. crispatus*. *L. crispatus* were cultivated to reach around 56% of total growth to make sure that the *L. crispatus* broth had a similar concentration to the *G. vaginalis* broth based on the number of colonies per milliliter prior to responsive calcein release studies. As is shown in Figure 3.13, the liposomes hardly showed any responsive release in the presence of *L. crispatus* supernatant (the average cumulative calcein release: 1.1%). This means that liposomes will not harm normal microbiota in women vagina.

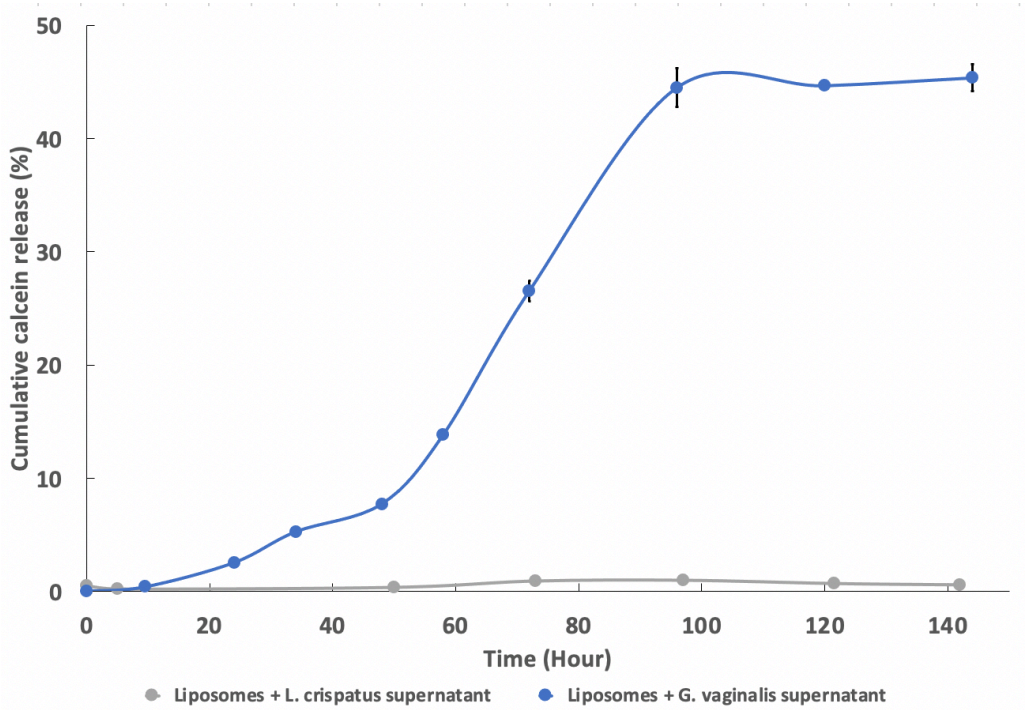


Figure 3.13 Cumulative calcein released from Formulation 2 in the presence of *G. vaginalis* supernatant or *L. crispatus* supernatant. The amount of calcein released from pure medium was subtracted to eliminate the difference caused by medium. The values represent mean +/-standard deviation (n=3).

Chapter 4 VLY gene cloning and recombinant protein expression system construction

4.1 Materials

E.Z.N.A Bacterial DNA Kit was purchased from Omega Bio-Tek. 1 kb DNA ladder, Quick-Load® purple 1 kb DNA ladder, gel loading dye, Monarch® DNA Gel Extraction Kit and Monarch® Plasmid Miniprep Kit were purchased from New England Bio Labs Inc. Agarose and ethidium bromide solution were purchased from Sigma Aldrich. Phusion flash high-fidelity PCR master mix, fastdigest NdeI, fastdigest BamHI and T4 DNA ligase were purchased from Thermo Fisher Scientific. Tris acetate-EDTA (TAE) buffer 50x concentrate and tris-EDTA buffer solution were purchased from Sigma Aldrich. Kanamycin solution (50-60 mg/mL) and isopropyl β-D-thiogalactopyranoside (IPTG) solution were purchased from Sigma Aldrich. pET-28a(+) DNA (Novagen) was purchased from Millipore Sigma. 5-α competent *E. coli* cells (NEB®) and BL21(DE3) competent *E. coli* cells were purchased from New England Bio Labs Inc. BL21-CodonPlus-RIPL competent cells were purchased from Agilent. Chloramphenicol was purchased from Sigma Aldrich. Ethanol was purchased from Sigma Aldrich. Nuclease-free water was purchased from Thermo Fisher Scientific. Lysogeny broth (LB) was purchased from Sigma Aldrich.

4.2 Methods

4.2.1 *G. vaginalis* genomic DNA extraction and purification

G. vaginalis genomic DNA was isolated and purified with E.Z.N.A Bacterial DNA Kit by the centrifugation protocol. HiBind® DNA mini columns, HBC buffer, TL buffer, DNA wash buffer, elution buffer, proteinase K solution, RNase A and lysozyme were included in the kit. Before use, HBC buffer and DNA wash buffer were diluted with 100% ethanol, whereas lysozyme was resuspended with elution buffer. The elution buffer was heated at 65 °C before use. Centrifugation was carried out by Avanti® J-E centrifuge (Beckman Coulter). Purified genomic DNA concentration was measured with a Nanodrop™ 2000 spectrophotometer (Thermo Scientific).

G. vaginalis was cultured in ATCC 1685 media at 37 °C and 5% CO_2 overnight. A 5 mL volume of culture was centrifuged at 4,000 g for 10 minutes at room temperature before the supernatant was aspirated and discarded. Then, 100 µL of TE buffer was added to completely resuspend the pellets before 40 µL lysozyme was added. After that, the reaction was incubated at 37 °C for 20 minutes. After TL buffer (100 µL) and proteinase K solution (20 µL) were added, the reaction was incubated at 55 °C for 1 hour and vortexed every 20 minutes. RNase A (5 µL) was added. The reaction tube was inverted several times to mix well and was left at room temperature for 5 minutes. Then the reaction was centrifuged at 10,000 g for 2 minutes to pellet any undigested material. The supernatant was carefully transferred to a new 1.5 mL microcentrifuge tube without disturbing the pellets. 220 µL BL buffer was added and the mixture was vortexed to mix thoroughly before being incubated at 65 °C for 10 minutes. 220 µL 100% ethanol was added and the reaction was vortexed to mix thoroughly. The entire sample was then transferred to a HiBind®

DNA mini column inserted into a 2 mL collection tube and centrifuged at 10,000 g for 1 minute and then the filtrate was discarded. HBC buffer (500 µL) was added to the HiBind® DNA mini column after it was inserted into a new 2 mL collection tube. The column was centrifuged at 10,000 g for 1 minute and then the filtrate was discarded. Then the column was washed twice with 700 µL DNA wash buffer followed by centrifugation at 10,000 g for 1 minute. The empty HiBind® DNA mini column was centrifuged at 19,000 g for 2 minutes to remove residue ethanol, and then inserted into a new nuclease-free 1.5 mL microcentrifuge tube. The column was washed with 100 µL preheated elution buffer and then left for 5 minutes at room temperature, followed by centrifugation at 10,000 g for 1 minute to elute DNA. Finally, the column was washed again with 100 µL preheated elution buffer, incubated at room temperature and then centrifuged to obtain the purified genomic DNA.

4.2.2 VLY gene cloning

4.2.2.1 Primer design

Four pairs of primers used for cloning VLY gene were designed by the Primer 5 software based on the complementary base pairing rule using the VLY gene (GenBank: *Gardnerella vaginalis* strain 14018) as template (Table 4.1) and purchased from Thermo Fisher Scientific. The restriction site of NdeI (CATATG) was included in the forward primers, whereas the restriction site of BamHI (GGATCC) was included in the reverse primers. The primers were centrifuged at 10,000 g for 5 minutes. Nuclease-free water was added to make a final concentration of 20 µM for each primer.

4.2.2.2 Optimal PCR system

Five reactions (4 reactions with 4 pairs of primers and 1 reaction as control) were performed with a C1000^{TM} Thermal Cycler (Bio-Rad) using the optimal reaction formulation and the optimal PCR reaction program shown in Table 4.2-4.4.

Table 4.1 Primers for VLY gene amplification.

# of Primer pair	Forward primer; Reverse primer
1	5'– GGAATTCCATATGAAGAGTACAAAGTTCTACCGTAATG – 3'; 5'– CGCGGATCCTCAGTCGTTCTTTACAGTTTCAGCA – 3'
2	5'– GGAATTCCATATGAAGAGTACAAAGTTCTACCGTAATGC – 3'; 5'– CGCGGATCCTCAGTCGTTCTTTACAGTTTCAGCA – 3'
3	5'– GGAATTCCATATGAAGAGTACAAAGTTCTACCGTAATG – 3'; 5'– CGCGGATCCTCAGTCGTTCTTTACAGTTTCAGC – 3'
4	5'– GCCGCCGCCCATATGAAGAGTACAAAG – 3'; 5'– GCCGGATCCTCAGTCGTTCTTTACAGT – 3'

Table 4.2 Optimal PCR formulation (the test group).

Component	50 µL reaction	Final concentration
2x Phusion Flash High-Fidelity PCR Master Mix	25 µL	1x
Forward primer	20 µM, 2 µL	0.8 µM
Reverse primer	20 µM, 2 µL	0.8 µM
Template DNA (Purified *G. vaginalis* genomic DNA)	50 ng/µL, 4 µL	4 ng/µL
Nuclease-free water	17 µL	N/A

Table 4.3 Optimal PCR formulation (the control group).

Component	50 µL reaction	Final concentration
2x Phusion Flash High-Fidelity PCR Master Mix	25 µL	1x
Forward primer	20 µM, 2 µL	0.8 µM
Reverse primer	20 µM, 2 µL	0.8 µM
Nuclease-free water	21 µL	N/A

Table 4.4 Optimal PCR program (gradient annealing process).

Steps	Temperature (°C)	Time (s)	Cycle
Initial denaturation	98	10	1
Denaturation	98	1	15
Annealing	65 (-1/cycle)	5	
Extension	72	30 (15 s/kb)	
Denaturation	98	1	20
Annealing	50	5	
Extension	72	30 (15 s/kb)	
Final extension	72	60	1
	4	Hold	

4.2.2.3 DNA gel electrophoresis and DNA purification

Amplified VLY gene fragments were identified by DNA agarose gel electrophoresis. Briefly, agarose was dissolved in 60 mL 1x TAE buffer to obtain a final concentration of 0.8% (w/v). An ethidium bromide solution (2 μL) was then added and mixed well. The DNA samples were prepared by adding 6x DNA gel loading dye to the PCR products, whereas the DNA ladder sample

was prepared either by mixing 2 μL 1 kb DNA ladder, 2 μL gel loading dye (6x, no SDS) and 8 μL nuclease-free water gently or by directly loading onto the gel (Quick-load® 1 kb DNA ladder, 10 µL/gel lane). Once solidified, the agarose gel was run at 86 V for 1 hour 30 minutes. The DNA fragments were visualized by Alphaimager® HP (Alpha Innotech) at 365 nm.

Gel slices that contained amplified VLY gene fragments (visualized by Spectroline™ ultraviolet transilluminator (Fisher Scientific)) were cut and extracted by Mornach® DNA Gel Extraction Kit (New England Biolabs Inc.). The concentration of purified VLY gene fragments was measured with a Nanodrop™ 2000 spectrophotometer (Thermo Scientific).

4.2.3 Construction of recombinant protein expression system

4.2.3.1 Restriction digest of the cloned vaginolysin gene and plasmid vector

pET-28a(+) was chosen as the plasmid vector. Both pET-28a(+) and purified VLY gene were cut by the restriction enzymes NdeI and BamHI. The reactions were incubated at 37 °C overnight (Table 4.5 and Table 4.6).

4.2.3.2 Ligation of the linearized plasmid vector and double-digested VLY gene

The linearized pET-28a(+) and double-digested VLY gene bearing the same sticky ends were ligated to obtain the recombinant plasmid. The reaction was incubated at 16 °C overnight (Table 4.7).

Table 4.5 Optimal double digestion reaction formulation for pET-28a(+).

Component	25 µL reaction
Restriction enzyme NdeI	1.25 µL
Restriction enzyme BamHI	1.25 µL
Green buffer	2.5 µL
Vector pET-28a(+)	20 µL

Table 4.6 Optimal double digestion reaction formulation for VLY gene.

Component	25 μL reaction
Restriction enzyme NdeI	1.25 μL
Restriction enzyme BamHI	1.25 μL
Green buffer	2.5 μL
VLY gene fragment	20 μL

Table 4.7 Optimal ligation reaction formulation.

Component	10 µL reaction
T4 DNA ligase	1 µL
T4 DNA ligase buffer	1 µL
VLY gene fragment	4 µL
Linearized vector pET-28a(+)	4 µL

4.2.3.3 Transformation of the recombinant plasmid into a cloning host

E. coli was chosen as the host organism. The recombinant plasmid was transferred via the heat shock method to *E. coli* cells to construct the recombinant bacterial expression system.

The recombinant plasmid was first transformed into 5-α competent *E. coli* cells. LB medium was prepared by adding 25 g of powder to 1 L Milli-Q water. The solution was then autoclaved at 121 ℃ for 15 minutes. Antibiotic selection plates (kanamycin) were prepared by adding 25 g of LB powder and 15 g of agar to 1 L Milli-Q water. The solution was then autoclaved at 121 ℃ for 15 minutes and allowed to cool down to around 55 ℃ before adding kanamycin stock solution (50 mg/mL). The solution was finally poured into petri dishes to obtain antibiotic selection plates (50 μg/mL kanamycin).

A tube of 5-α competent *E. coli* cells was thawed on ice for 10 minutes. The ligation product (10 μL) was added to the cell mixture. The tube was then carefully flicked 4-5 times to mix well before the reaction was placed on ice for 30 minutes. Then the reaction was heat shocked at exactly 42 °C for exactly 30 seconds and placed on ice for 5 minutes. SOC medium at room temperature (950 μL) was added. The reaction was then incubated at 37 °C, 200 rpm for 60 minutes. 100 μL of the reaction was spread onto a selection plate (50 μg/mL Kanamycin). The plate was incubated overnight at 37 °C. The leftovers (900 μL) was centrifuged at 8,000 g for 2 minutes. An 800 μL volume of the supernatant was removed. The rest cells were then resuspended. The concentrated 100 μL reaction was spread onto another selection plate (50 μg/mL Kanamycin). The plate was incubated overnight at 37 °C.

Colony PCR and DNA agarose gel electrophoresis were performed for validation in case some CFUs contained the plasmids that did not encode the gene of interest successfully. CFUs from the selection plate were scratched and each CFU was resuspended in 10 μL nuclease-free water. Each suspension was used as the template for each colony PCR. T7 primers were incorporated into the reaction to avoid false positives. The optimal reaction formulations (the test

group and the control group) are shown in Tables 4.8 and 4.9. The optimal PCR program is the same as that in the section of VLY gene cloning.

Table 4.8 Optimal colony PCR formulation (the test group).

Component	25 µL reaction	Final concentration
2x Phusion Flash High-Fidelity PCR Master Mix	12.5 µL	1x
T7 forward primer	20 µM, 1 µL	0.8 µM
T7 reverse Primer	20 µM, 1 µL	0.8 µM
CFU suspended in nuclease-free water	2 µL	N/A
Nuclease-free water	8.5 µL	N/A

Table 4.9 Optimal colony PCR formulation (the control group).

Component	25 µL reaction	Final concentration
2x Phusion Flash High-Fidelity PCR Master Mix	12.5 µL	1x
T7 forward primer	20 µM, 1 µL	0.8 µM
T7 reverse Primer	20 µM, 1 µL	0.8 µM
Nuclease-free water	10.5 µL	N/A

Colony PCR results were validated by DNA gel electrophoresis. The successfully verified CFUs were then inoculated into 5 mL LB medium (50 µg/mL Kanamycin) and incubated at 37 °C and 250 rpm overnight. Recombinant plasmid DNA was isolated from the 5 mL culture and purified by Monarch® Plasmid Miniprep Kit for further transformation into BL21 (DE3) competent *E. coli* cells. The purified plasmid DNA was stored at -20 °C.

The purified plasmid DNA was then transformed into BL21 (DE3) competent *E. coli* cells using the same protocol of transformation into 5-α competent *E. coli* cells. Colony PCR and DNA

agarose gel electrophoresis were performed for validation. The validated CFUs were inoculated into LB medium (50 µg/mL kanamycin and 50 µg/mL chloramphenicol) and stored at -80 °C with 10% sterile glycerol as cryoprotectant.

Similarly, the recombinant plasmid was transformed into BL21-CodonPlus (DE3)-RIPL competent *E. coli* cells. Chloramphenicol stock solution (50 mg/mL) was prepared by dissolving 1 g of chloramphenicol powder in 20 mL ethanol. The solution was then filter-sterilized by a 0.22 µm PES syringe filter and stored at -20 °C. Antibiotic selection plates (kanamycin and chloramphenicol) were prepared by adding 25 g of LB powder and 15 g of agar to 1 L Milli-Q water. The solution was then autoclaved at 121 °C for 15 minutes and allowed to cool down to around 55 °C before adding kanamycin stock solution (50 mg/mL) and chloramphenicol stock solution (50 mg/mL). The solution was finally poured into petri dishes to obtain antibiotic selection plates (50 µg/mL kanamycin and 50 µg/mL chloramphenicol).

A tube of BL21-CodonPlus (DE3)-RIPL competent *E. coli* cells was thawed on ice. XL10-gold β-mercaptoethanol mix was diluted 10 times with autoclaved Milli-Q water. A 2 uL volume of the 1:10 diluted XL10-gold β-mercaptoethanol mix was added to the cells. The tube was swirled gently and incubated on ice for 10 minutes with swirling every 2 minutes. The purified plasmid DNA was added to the mixture. The tube was then carefully flicked 4-5 times to mix well and incubated on ice for 30 minutes. The mixture was transferred quickly to a prechilled 14-mL Falcon tube, heat shocked at 42 °C for 20 seconds, and placed on ice for 2 minutes. SOC medium (900 µL) preheated at 42 °C was added, and the reaction was incubated at 37 °C and 250 rpm for 60 minutes. A 200 µL volume of the mixture was spread onto a selection plate (50 µg/mL Kanamycin

and 50 µg/mL chloramphenicol). The plate was incubated overnight at 37 °C. The leftovers (800 µL) was centrifuged at 200 g for 5 minutes at 4 °C. A 600 µL volume of the supernatant was removed. The rest cells were then resuspended. The concentrated 200 µL reaction was spread onto another selection plate (50 µg/mL Kanamycin and 50 µg/mL chloramphenicol). The plate was incubated overnight at 37 °C. Colony PCR and DNA agarose gel electrophoresis were performed for validation.

4.2.3.4 DNA sequencing of the recombinant plasmid

BL21 (DE3) *E. coli* cells carrying recombinant plasmids were cultured in 5 mL LB medium (50 µg/mL Kanamycin) and BL21-CodonPlus (DE3)-RIPL *E. coli* cells carrying recombinant plasmids were cultured in 5 mL LB medium (50 µg/mL Kanamycin and 50 µg/mL chloramphenicol) at 37 °C and 250 rpm overnight. The plasmid DNA from two types of cells were isolated and purified separately by Mornach® Plasmid Miniprep Kit to obtain a final concentration of 50 µg/µL. A 8 µL volume of the purified plasmid DNA was sequenced by the Centre for Applied Genomics from The Hospital for Sick Children using T7 primers via Sanger Sequencing.

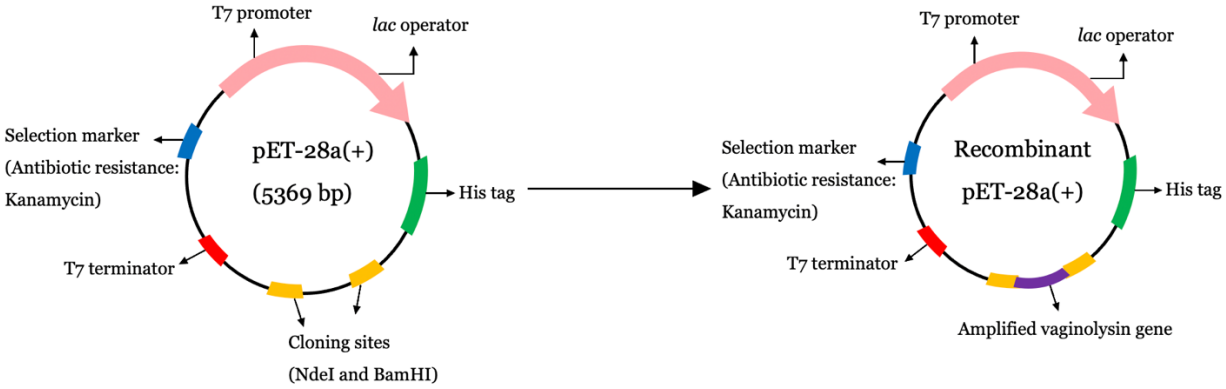


Figure 4.1 Schematic of recombinant plasmid construction.

4.3 Results and discussion

4.3.1 *G. vaginalis* genomic DNA extraction and purification

The concentration of *G. vaginalis* genomic DNA was measured to be 456.8 ng/μL (Figure 4.2). The ratio of absorbance at 260 nm and 280 nm was measured to be 1.92, which is an acceptable result given that a ratio of around 1.8 is generally accepted as pure for DNA. The purified genomic DNA can be used as template in genetic amplification of the VLY gene.

4.3.2 VLY gene cloning

4.3.2.1 DNA gel electrophoresis and DNA purification after gene amplification

According to GenBank, the VLY gene contains 1551 base pairs (bp). As is shown in Figure 3, four bright bands were visualized at around 1.5 kb by ultraviolet light. The band position corresponds to 1551 base pairs, indicating that the VLY gene has been amplified using all four pairs of primers successfully (Figure 4.3).

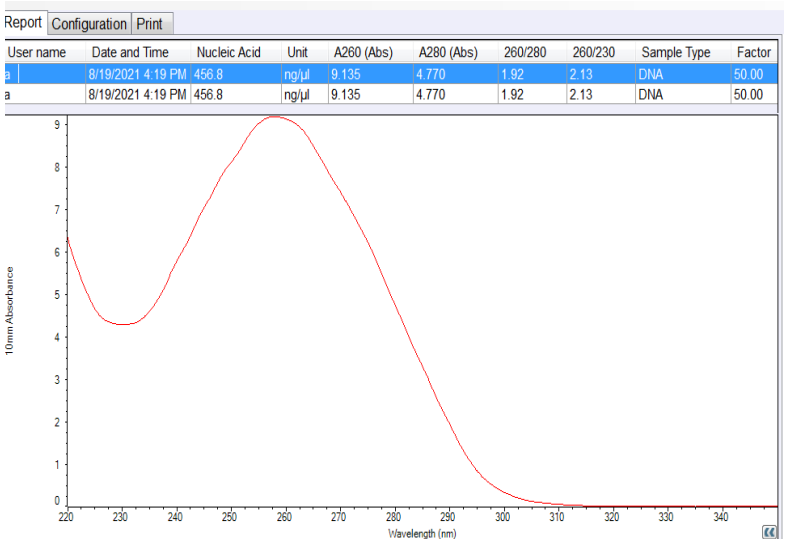


Figure 4.2 *G. vaginalis* genomic DNA concentration measured by Nanodrop™2000 spectrophotometer.

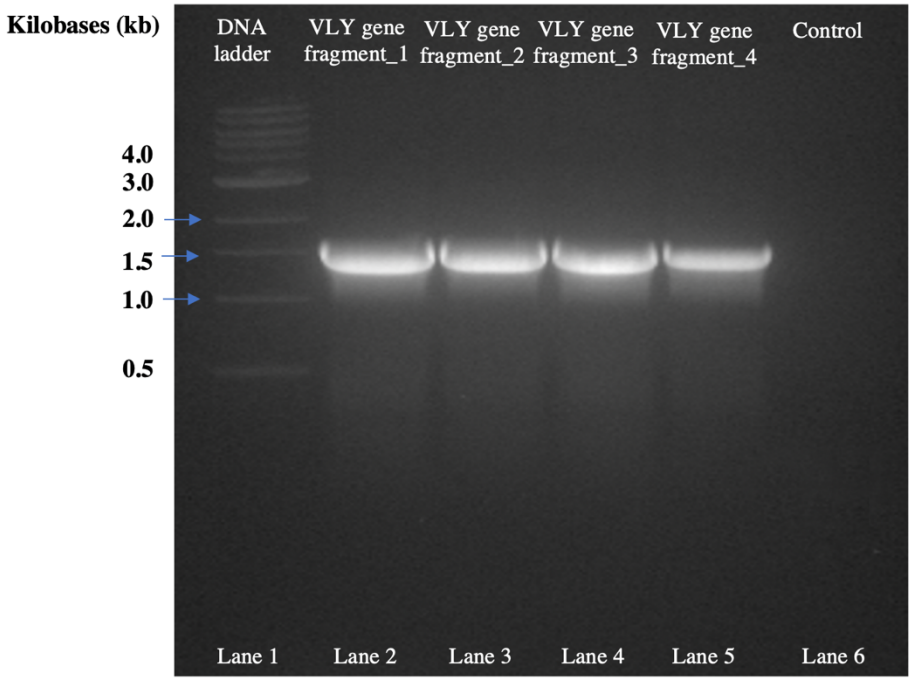


Figure 4.3 Agarose gel electrophoresis of DNA samples. Lane 2-lane 5 are the gene fragments amplified using primer pair 1, 2, 3, and 4 separately. Lane 6 is the control group using primer pair 1 without genomic DNA template.

The concentrations of the purified VLY gene fragment_1, VLY gene fragment_2 and VLY gene fragment_3 were measured before restriction digest (Table 4.10).

Table 4.10 DNA concentration and A260/A280 ratio after gel extraction.

DNA Samples	Concentration (ng/μL)	A260/A280 ratio
VLY gene fragment_1	82.6	1.91
VLY gene fragment_2	100.2	1.85
VLY gene fragment_3	90.5	1.95
VLY gene fragment_4	93.6	1.87

4.3.3 Construction of recombinant protein expression system

4.3.3.1 DNA gel electrophoresis and DNA purification after restriction digest

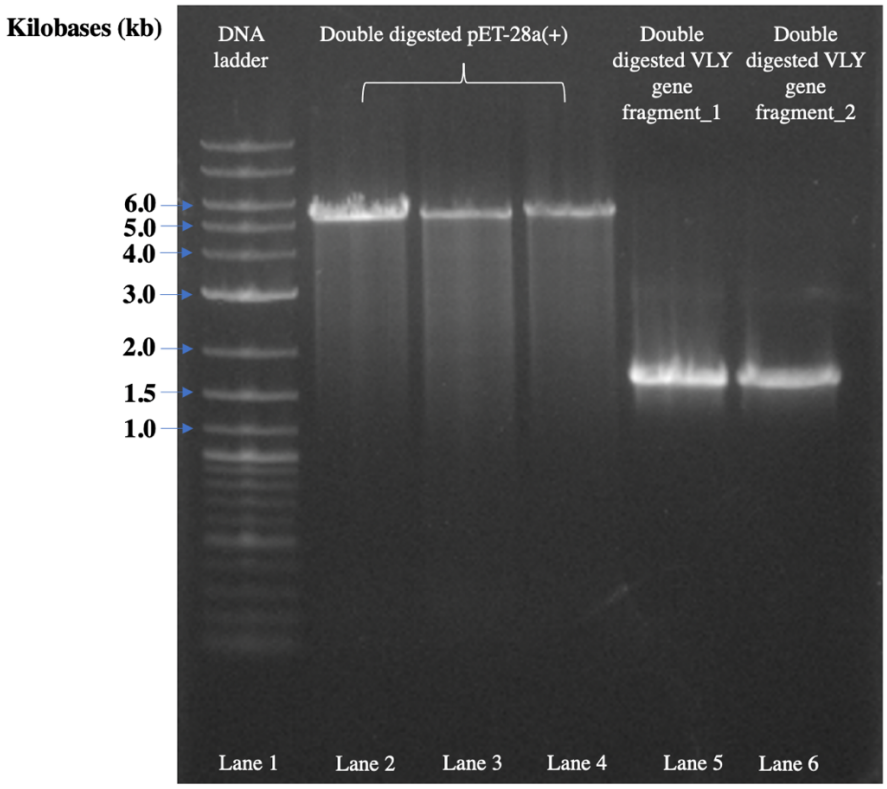


Figure 4.4 Agarose gel electrophoresis of double digested DNA samples. Lane 2-lane 4 are the double digested gene fragments of vector pET-28a(+) (the linearized plasmid vector). Lane 5 and 6 are double digested VLY gene fragment_1 and double digested VLY gene fragment_2, respectively.

Table 4.11 DNA concentration and A260/A280 ratio after gel extraction.

DNA Samples	Concentration (ng/µL)	A260/A280 ratio
Double digested VLY gene fragment_1	23.5	2.04
Double digested VLY gene fragment_2	14.2	2.02
Double digested pET-28a(+)	22.6	2.07

The DNA samples from lane 2 to lane 4 were combined before purification (Table 4.11). It is common that the DNA recovery is relatively low after gel extraction, and the purity is not ideal judging from the A260/A280 ratio. However, the relatively low purity does not negatively affect subsequent reactions much and thus the result is acceptable. The double digested VLY gene fragment_1 was used to ligate with the linearized pET-28a(+).

4.3.3.2 Transformation of the recombinant plasmid into a cloning host

Transformation into 5-*α* competent *E. coli* cells

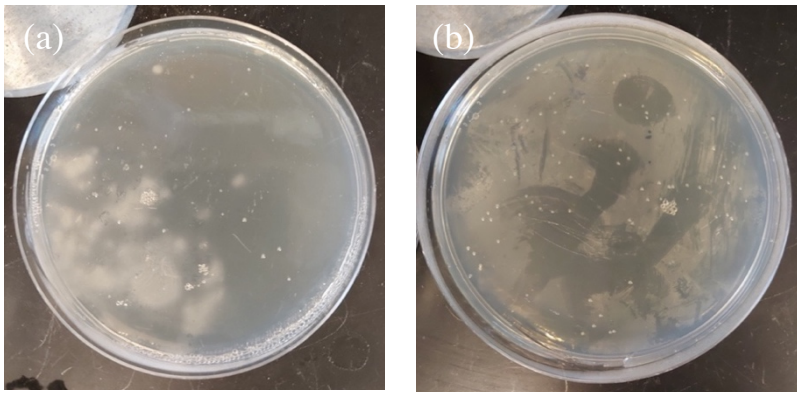


Figure 4.5 (a) The 5-α *E. coli* colonies grown on the LB selection plate (containing 50 μg/mL Kanamycin); (b) The 5-α *E. coli* colonies (concentrated) grown on the LB selection plate (containing 50 μg/mL Kanamycin).

Colony PCR validation and DNA gel electrophoresis

As is shown in Figure 4.6, four bright bands were visualized between 1.5 kb and 2 kb, corresponding to the VLY gene sequence inserted into the vector pET-28a(+), which indicates that transformation into 5-*α E. coli* cells was successful. The reason why the total number of DNA base pairs exceeds 1551 is that the amplified gene fragment also includes some sequences that are carried by the vector itself.

The recombinant plasmid DNA was isolated from 5-α *E. coli* cells and purified to be further transformed into BL21 (DE3) competent *E. coli* cells and BL21-CodonPlus (DE3)-RIPL competent *E. coli* cells, respectively.

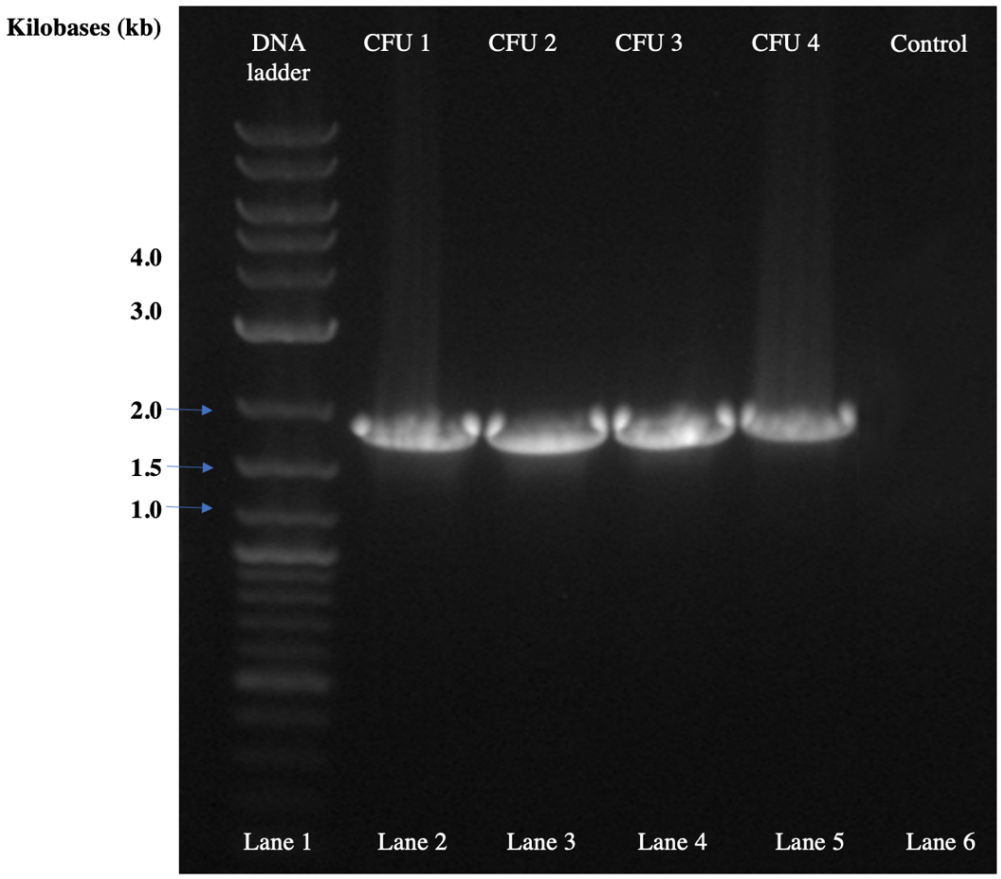


Figure 4.6 Agarose gel electrophoresis of VLY gene fragments amplified using T7 primers. Lane 2-Lane 5 are the amplified DNA fragments using four CFUs scratched from the selection plates as PCR template. Lane 6 is the control group using T7 primers without template.

Table 4.12 Plasmid DNA concentration and A260/A280 ratio after isolation and purification.

DNA Samples	Concentration (ng/μL)	A260/A280 ratio
Plasmid DNA isolated from 5-α *E. coli* cells	93.8	1.85

Transformation into BL21 (DE3) competent *E. coli* cells

The CFUs of BL21 (DE3) *E. coli* cells grown on the selection plates were much fewer and bigger compared to those of 5-α *E. coli* cells.

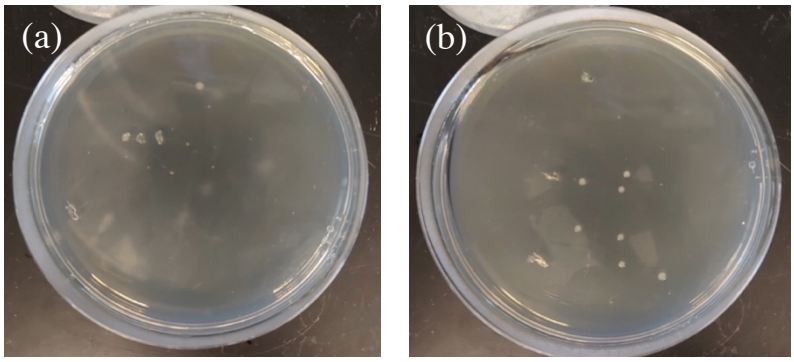


Figure 4.7 (a) The BL21 (DE3) *E. coli* colonies grown on the LB selection plate (containing 50 μg/mL Kanamycin); (b) The BL21 (DE3) *E. coli* colonies (concentrated) grown on the LB selection plate (containing 50 μg/mL Kanamycin).

Colony PCR validation and DNA gel electrophoresis

Of five CFUs scratched from the transformed LB selection plates, only three CFUs were validated (Figure 4.8). The three validated CFUs were inoculated into LB medium (containing 50 μg/mL Kanamycin) and then preserved for recombinant VLY expression.

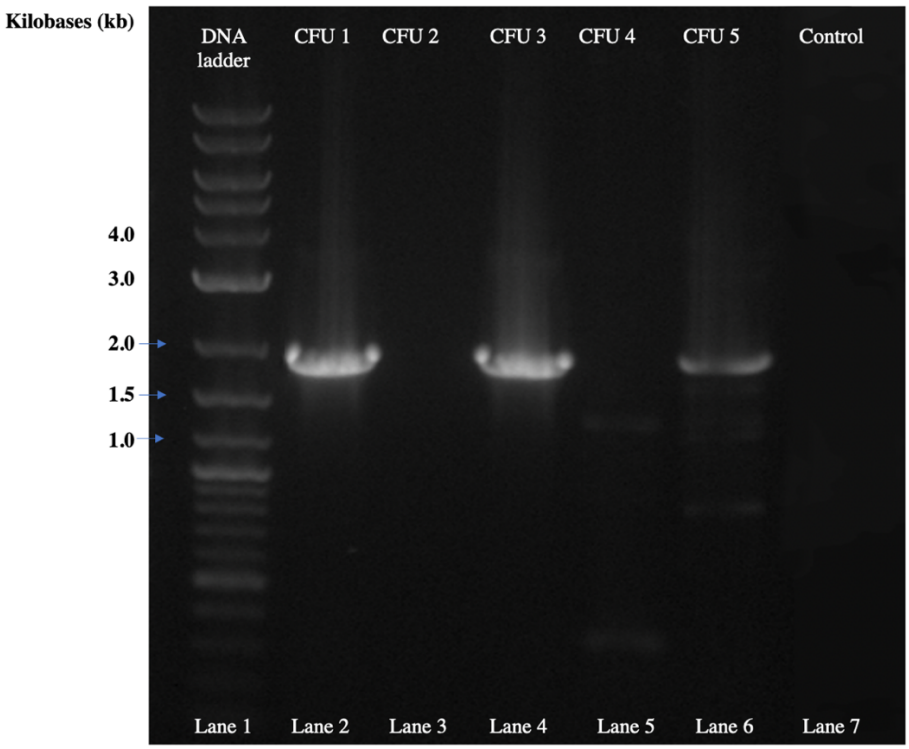


Figure 4.8 Agarose gel electrophoresis of VLY gene fragments amplified using T7 primers. Lane 2-Lane 6 are the amplified DNA fragments using five CFUs scratched from the selection plates as PCR template. Lane 7 is the control group using T7 primers without template.

Transformation into BL21-CodonPlus (DE3)-RIPL competent *E. coli* cells

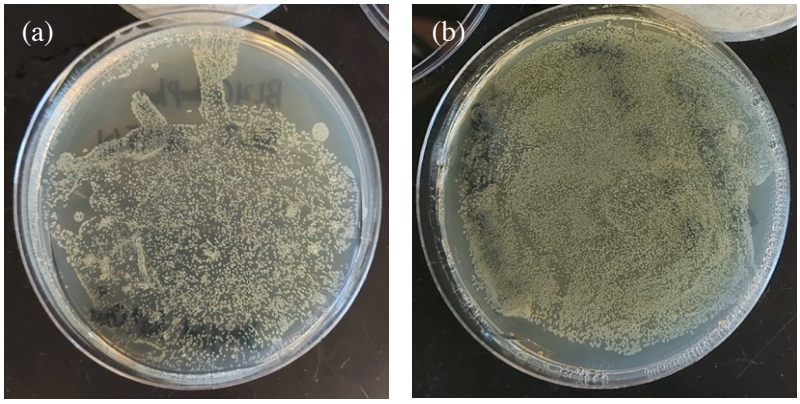


Figure 4.9 (a) The BL21-CodonPlus (DE3)-RIPL *E. coli* colonies grown on the LB selection plate (containing 50 µg/mL Kanamycin and 50 µg/mL chloramphenicol); (b) The BL21-CodonPlus (DE3)-RIPL *E. coli* colonies (concentrated) grown on the LB selection plate (containing 50 µg/mL Kanamycin and 50 µg/mL chloramphenicol).

Colony PCR validation and DNA gel electrophoresis

All eight CFUs were validated (Figure 4.10). The validated CFUs were inoculated into LB medium (containing 50 μg/mL Kanamycin and 50 μg/mL chloramphenicol) and then preserved for recombinant VLY expression.

4.3.4 DNA sequencing of the recombinant plasmid

The plasmid DNA product isolated from *E. coli* cells was further confirmed by sequencing, indicating that the recombinant bacterial expression system had been successfully constructed. The sequence landmarks of the recombinant pET-28a(+) vector are identified in Figure 4.11. Basically, the upstream of the vector contains the T7 promoter and an adjacent *lac* operator sequence that is believed to suppress uninduced expression. Translation is initiated from a Shine-Dalgarno (SD) sequence which binds to the ribosome. The VLY gene sequence to be expressed is cloned downstream of the coding sequence for a poly-histidine fusion tag (His_6), between the two restriction enzyme cutting sites for NdeI and BamHI, so that the recombinant VLY can be purified using nickel sepharose resin due to the high affinity of nickel (II) ions and histidine groups.

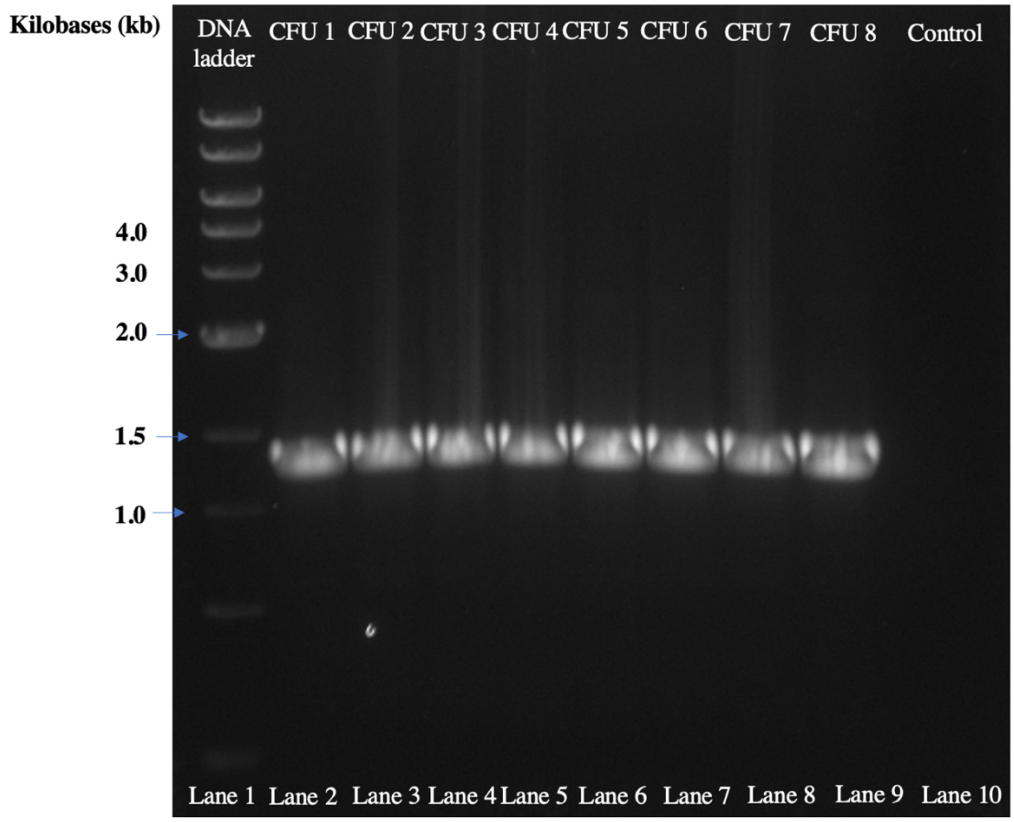


Figure 4.10 Agarose gel electrophoresis of VLY gene fragments amplified using T7 primers. Lane 1 is the ladder. Lane 2-9 are the amplified DNA fragments using eight CFUs scratched from the selection plates as PCR template. Lane 10 is the control group using T7 primers without template.

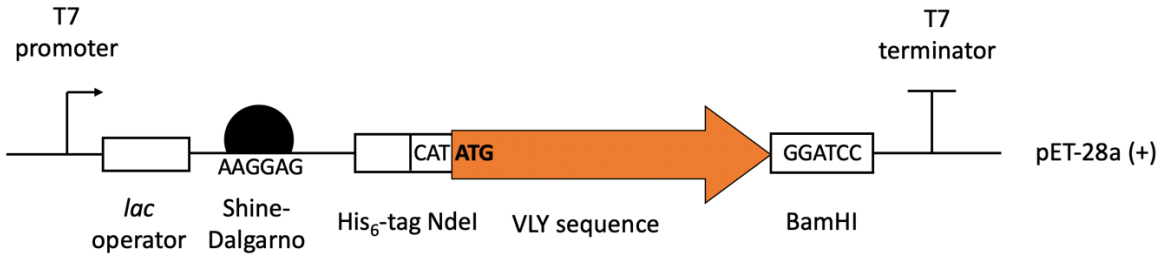


Figure 4.11 Schematic of the recombinant pET-28a(+) vector with the inserted VLY gene sequence.

Chapter 5 Recombinant VLY expression and purification

5.1 Materials

HisTrap™ high performance column (Cytiva 17-5247-01) was purchased from Sigma Aldrich. 10x Tris/glycine/SDS electrophoresis buffer, 2x Laemmli sample buffer, Bio-Safe™ Coomassie stain, 4-15% Mini-PROTEA®TGX™ protein gels, precision plus protein™ dual color standards (10-250 kDa) and 2-mercaptoethanol were purchased from Bio-Rad. Imidazole was purchased from Sigma Aldrich. RQ 1 RNase-free DNase (Promega) was purchased from Thermo Fisher Scientific. Color prestained protein standard (10-250 kDa) was purchased from New England Bio Labs Inc. Bugbuster® protein extraction reagent and Bugbuster® Master Mix were purchased from Sigma Aldrich. Coomassie brilliant blue R-250 was purchased from TCI. Sorbitol was purchased from Sigma Aldrich. Tris base, sodium chloride, sodium phosphate and EMPIGEN® BB detergent (30% solution) were purchased from Sigma Aldrich. Phosphate buffered saline (PBS, 1x, pH 7.2) was purchased from Wisent Bio Products.

5.2 Methods

5.2.1 Induction of recombinant VLY expression within the *E. coli* vector

5.2.1.1 Induction of recombinant VLY expression within BL21(DE3) *E. coli* cells

The preserved BL21 (DE3) *E. coli* cells carrying the recombinant pET-28a(+) vector were thawed on ice and inoculated into 5 mL LB medium (containing 50 μg/mL Kanamycin). The cells were incubated at 37 °C and 250 rpm overnight. The cells (1 mL) were transferred into 50 mL LB broth (containing 50 μg/mL Kanamycin) and the culture was incubated at 37 °C and 250 rpm until its

growth reached the exponential phase (OD_{600} = 0.6). The culture was then induced with 0.1 mM IPTG and incubated at different temperatures (20 °C, 30 °C) and 250 rpm for different time periods (18 hours, 20 hours).

5.2.1.2 Induction of recombinant VLY expression within BL21-CodonPlus (DE3)-RIPL *E. coli* cells

The preserved BL21-CodonPlus (DE3)-RIPL *E. coli* cells carrying the recombinant pET-28a(+) vector were thawed on ice and plated on a LB agar plate (containing 50 µg/mL kanamycin and 50 µg/mL chloramphenicol) by streaking. The plate was incubated at 37 °C overnight. One CFU was picked from the plate and inoculated into 3 mL LB medium (containing 50 µg/mL kanamycin and 50 µg/mL chloramphenicol). The culture was incubated at 37 °C and shaken at 250 rpm overnight. The cells (2.5 mL) were transferred into 50 mL of fresh LB broth (without the selection antibiotic). The culture was incubated at 37 °C and shaken at 250 rpm until its growth reached the exponential phase (OD_{600} = 0.5-0.6) before being induced with different concentrations of IPTG (0.1 mM, 0.5 mM, 1 mM) and 0.5 M sorbitol, incubated at different temperatures (20 °C, 37 °C), and shaken at 250 rpm for different time periods (2 hours, 20 hours). Another 50 mL culture without adding IPTG was incubated under identical conditions to serve as the non-induced group.

Alternatively, a slightly modified heat shock method was applied to improve soluble VLY production. Briefly, the culture was scaled up to 150 mL and was incubated at 37 °C and 250 rpm to reach an OD_{600} of 0.7. Then the culture was heated to 47 °C and then induced with 0.5 mM IPTG. The culture was kept at the temperature and shaken at 200 rpm for 20 minutes before it was incubated at 20 °C and shaken at 250 rpm for 20 hours.

5.2.2 *E. coli* cell lysis

Physiological saline was prepared by dissolving 8.5 g sodium chloride in 1000 mL Milli-Q water before cell lysis. After induction, *E. coli* cells were washed twice with physiological saline and collected by centrifugation at 8,000 g for 10 min.

5.2.2.1 Ultrasonication method

The *E. coli* cells were sonicated for 5 s on/off for different time periods and at different amplitude using an ultrasonicator (Qsonica S-4000). Then, the cell lysate was placed in a bath sonication (Sper Scientific 100004) for 15 minutes to reduce the viscosity.

5.2.2.2 Bugbuster® lysis method

E. coli cells were lysed by two methods using the BugBuster® reagent.

a. The cells were weighed after centrifugation. The BugBuster® protein extraction reagent (5 mL) was added per gram of the wet cell paste to resuspend the cells. A 1 mg/mL lysozyme solution was added and the mixture was gently vortexed to mix well. The mixture was incubated on a rotating mixer for 20 minutes at room temperature. To reduce viscosity, RQ 1 RNase-free DNAse (50 u/mL) and $MgCl_2$ (5 mM) were added and the mixture was incubated for 15 minutes at room temperature.

b. The cells were weighed after centrifugation. The BugBuster® Master Mix (5 mL) was added per gram of the wet cell paste to resuspend the cells in the presence of protease inhibitor cocktail (1:200 diluted). The mixture was then incubated on a rotating mixer for 30 minutes at

room temperature. The insoluble fraction was isolated from the soluble fraction by centrifugation at 16,000 g for 20 minutes at 4 °C.

5.2.3 Column purification of soluble recombinant VLY

A series of elution buffers were prepared prior to column purification. Imidazole (34 .0 g) and sodium chloride (29.2 g) were dissolved in 1 L PBS (1x, pH 7.2) to reach a final concentration of 500 mM imidazole and 500 mM sodium chloride. The pH of the buffer was adjusted to 7.4 with 37% hydrochloric acid. Then, the buffer was serially diluted to 200 mM, 100 mM, 60 mM, and 20 mM of imidazole while keeping the sodium chloride concentration constant. Alternatively, imidazole (34.0 g), sodium chloride (29.2 g), and Tris (6.1 g) were dissolved in 1 L Milli-Q water to reach a final concentration of 500 mM imidazole, 500 mM sodium chloride, and 50 mM Tris. The pH of the buffer was adjusted to 7.4 with 37% hydrochloric acid. Then, the buffer was serially diluted to 300, 70, and 20 mM of imidazole while keeping the sodium chloride and Tris concentration constant. All buffers were filtered using a 0.45 μm PES filter after pH adjusted to 7.4.

The soluble fraction was purified using HisTrap™ HP (Cytiva). Before being loaded onto the column, the sample was pretreated by passing through a 0.45 μm PES filter. The column was washed with 5 mL Milli-Q water and equilibrated with binding buffer (20 mM imidazole, 500 mM sodium chloride) at a flow rate of 1 mL per minute. The pretreated sample was then applied slowly and the flow-through was collected. Then, the column was eluted with wash buffer (60 mM or 70 mM imidazole, 500 mM sodium chloride) and a series of elution buffers containing 500 mM

sodium chloride and 100, 200, 300 and 500 mM imidazole, respectively. The corresponding eluted samples were collected separately.

5.2.4 Purification of inclusion bodies using the Bugbuster® reagent

The insoluble fraction harvested by centrifugation at 16,000 g for 20 minutes at 4 °C was purified with the BugBuster® Master Mix. Briefly, the pellets were resuspended in the same volume of 1:10 diluted BugBuster® Master Mix that was used to resuspend the original cell paste in the presence of protease inhibitor cocktail (1:200 diluted) to obtain an even suspension so that contaminating proteins could be solubilized and removed. The suspension was then centrifuged at 5,000 g for 15 minutes at 4 °C to spin down the IBs. Then, the IBs were resuspended in 1:10 diluted BugBuster® Master Mix (10 mL per gram of original cell paste), washed three times and collected by centrifugation at 5,000 g for 15 minutes at 4 °C.

5.2.5 Protein gel electrophoresis

Sodium dodecyl sulfate polyacrylamide gel electrophoresis (SDS-PAGE) was performed to separate the protein mixture produced by *E. coli* cells. The SDS loading buffer was prepared by mixing 2x Laemmli sample buffer with β-mercaptoethanol at a volume ratio of 19:1. SDS samples were prepared by mixing the samples with SDS loading buffer at a volume ratio of 1:1 prior to heating the samples at 95 °C for 10 minutes. Coomassie blue staining solution was prepared by dissolving 0.5 g Coomassie R250 in 225 mL ethanol, 50 mL acetic acid and 225 mL Milli-Q water.

The samples were loaded onto the Mini-Protean®TGX™ gel and the gel was run at 100 V for 80 minutes in the presence of 1x Tris-glycine-SDS electrophoresis buffer. Then, the gel was

washed with Milli-Q water three times within 10 minutes to remove the electrophoresis buffer before soaking in 50 mL Coomassie blue staining solution for 1 hour. The gel was rinsed with Milli-Q water and destained until the background was nearly clear. The gel image was captured by the iBright™ Imaging System FL1500 (Invitrogen).

5.2.6 Solubilization and column purification of inclusion body

The solubilization buffer was prepared by dissolving sodium phosphate (40 mM) and sodium chloride (300 mM) in 10 mL 30% Empigen BB® solution. The pH of the buffer was adjusted to 7.4 with 37% hydrochloric acid. Imidazole (3.4 g), sodium phosphate (8.2 g) and sodium chloride (1.76 g) were dissolved in 100 mL of 1:4 diluted 30% Empigen BB® solution to reach a concentration of 500 mM imidazole, 40 mM sodium phosphate, 300 mM sodium chloride, and 25 mM Empigen BB®, with pH adjusted to 7.4 before passing through a 0.45 μm PES filter. Then, the buffer was serially diluted to 300 mM, 60 mM, and 20 mM of imidazole while keeping the sodium chloride, sodium phosphate, and Empigen BB® concentration constant. All buffers were filtered using a 0.45 μm PES filter after pH adjusted to 7.4.

The IBs harvested by centrifugation were resuspended in 4 mL solubilization buffer and incubated at 4 °C for 3 hours with gentle shaking. Insoluble materials were removed by centrifugation at 18,000 g for 30 minutes at 4 °C. The solubilized IBs were purified using HisTrap™ HP.

5.3 Results and discussion

5.3.1 Induction within BL21(DE3) *E. coli* cells

BL21 (DE3) and its derivatives were used since they are the most popular strains for heterologous protein expression. Even if the engineered strain and the plasmid vector are fixed, it is pretty clear that there are numerous combinations of cultivation and induction strategies that facilitate high-level production of recombinant protein. As such, certain important factors including culture temperature, inducer concentration, culture additive, culture time have been studied in this thesis.

Specifically, a two-phase culture was used in this study. The *E. coli* cells were first cultured at 37 °C for the purpose of fast and robust growth, and then were cultured at reduced temperature after induction to decrease cell growth and promote soluble protein expression. In the first phase, the growth of BL21 (DE3) *E. coli* cells could reach mid-log phase with an OD_{600} value at around 0.6 within 2 hour 20 minutes, although there were minor differences among different batches of cultures. In the second phase, BL21 (DE3) *E. coli* cells were cultured at 30 °C and 20 °C separately for 20 hours with 0.1 mM IPTG.

Before cell lysis, cells were washed with physiological saline to eliminate potential impurities introduced by the nutrients in LB broth, which might complicate the subsequent purification process. Once the cell membrane is ruptured, the inter-cellular materials including chromosomal DNA are released, leading to a high viscosity of the lysate. Thus, reducing viscosity of the lysate is a crucial step in this process as it is hard to purify the sample by column chromatography due to high column pressure and stubborn bubbles that remain due to the high viscosity.

Therefore, three methods of cell lysis were applied to lyse BL21 (DE3) *E. coli* cells and release their internal contents and obtain the crude lysate containing VLY. For ultrasonication methods, two amplitudes (Table 5.1) were tried for 30 minutes and 15 minutes separately followed by a 15-minute bath sonication to reduce the viscosity by shearing DNA, but these methods failed. The resulting cell lysate was very turbid with quite a few sediments left after centrifugation, which might be an indication of incomplete cell lysis. Moreover, a 5-fold dilution of the cell lysate failed to reduce the viscosity. Similarly, bath sonication had limited effect for reducing the viscosity. Since it is very hard to select an amplitude and sonication time that would be suitable to ensure that the cells are completely disrupted, this method had a poor efficiency. The second method is to use the BugBuster® reagent, a tris-buffer based formulation of mixed detergents, to achieve cell wall perforation without denaturing the protein. Lysozyme was added to the cell lysate to aid protein extraction by hydrolyzing N-acetylmuramide linkages in the peptidoglycan layer of the cell wall, whereas DNase and $MgCl_2$ were added to break down DNA and thus help reduce viscosity. The chemical method was found to be more efficient in lysing the cells than the mechanical method, although the viscosity of the lysate was not reduced significantly even with the addition of DNase and $MgCl_2$. Alternatively, the BugBuster® Master Mix containing rLysozyme™ and Benzonase® Nuclease was used to lyse cells in a simpler way. The resulting cell lysate was much less viscous even without too much dilution. Therefore, this method was kept for the following studies.

Table 5.1 Ultrasonication method to lyse cells.

Ultrasonication procedures		
Step 1 Ultrasonication		Step 2 Bath sonication
Amplitude	Time	Time
50	30 minutes	15 minutes
70	15 minutes	15 minutes

16 cultures of *E. coli* cells were induced, cultivated, lysed and purified using different combinations of strategies (e.g., host strain type, culture volume, temperature, inducer concentration, additives, etc.) to optimize recombinant VLY expression. The details of the 16 cultures were summarized in Table 5.2.

Table 5.2 Summary of *E. coli* cell culture conditions for recombinant VLY expression.

Culture number	Host strain	Culture volume	Phase 1 cultivation	Phase 2 cultivation	Additive concentration	Inducer (IPTG) concentration	Cell lysis method	Purification	SDS-PAGE gel image
1	BL21 (DE3)	50 mL	37°C, 250 rpm OD_{600} = 0.6	30°C, 250 rpm, 20 hours	N/A	0.1 mM	Ultrasonication method and BugBuster® reagent lysis method	Purified with imidazole (60 mM, 100 mM, 200 mM and 500 mM)	Figure 5.1
2				20°C, 250 rpm, 20 hours			BugBuster® Master Mix reagent lysis method (in the presence of 1:200 diluted protease inhibitor cocktail)	Purified with imidazole (60 mM, 200 mM and 500 mM)	Figure 5.2 and 5.3
3								N/A	Figure 5.2
4								Purified with imidazole (60 mM, 200 mM and 500 mM)	Figure 5.2 and 5.3
5								N/A	

6	BL21-CodonPlus (DE3)-RIPL		37°C, 250 rpm OD_{600} = 0.5-0.6	37°C, 250 rpm, 2 hours		1 mM			Figure 5.4
7									
8						N/A			
9				20°C, 250 rpm, 20 hours		0.1 mM		The insoluble materials after cell lysis purified with BugBuster® Master Mix reagent	Figure 5.5
10						1 mM			
11						0.5 mM			
12						N/A			
13		150 mL				N/A		N/A	Figure 5.7
14					0.5 M sorbitol	1 mM		Purified with imidazole (70 mM, 300 mM and 500 mM)	
15								N/A	Figure 5.8
16				47°C, 250 rpm 20 minutes; 20°C, 250 rpm, 20 hours	N/A	0.5 mM		Purified with imidazole (70 mM, 300 mM and 500 mM)	

The approximate molecular weight (MW) of VLY is 57 kDa. However, there was no target band between 72 kDa and 55 kDa in all lanes in the protein gel image (Figure 5.1), indicating that there was no recombinant VLY production. The thick bands in lane 2 and the relatively faint bands in lane 4 further confirmed that the ultrasonication method performed poorly at lysing cells. Technically, most proteins expressed by BL21 (DE3) *E. coli* cells are soluble, and thus should stay in the supernatant instead of the insoluble cell debris. Therefore, the cell debris were further lysed by the BugBuster® reagent to obtain load 2, which contained more soluble proteins as is shown in the gel image. In general, the cell lysates were very viscous even after dilutions and addition of DNase and $MgCl_2$, resulting in clogging problems in the column purification process. More important, there was no band in lanes 7 or 8, where the target protein carrying the hexahistidine fusion tag should have eluted.

In order to optimize VLY expression, three cultures of BL21 (DE3) *E. coli* cells were cultivated at a lower temperature (20 °C) for 20 hours. Here, all cultures were lysed with the BugBuster® Master Mix and all cell lysates were not purified by HisTrap™ HP. This time, SDS-PAGE was run to verify if cell lysis was complete and if there was VLY production. All three lanes of cell debris contained very faint bands indicating that the cell debris contained a negligible amount of insoluble materials and that cell lysis using BugBuster® Master Mix worked well (Figure 5.2). Moreover, of the three lanes, there were two lanes containing a thin band between 72 kDa and 55 kDa, suggesting possible VLY expression. However, protein band tailing was observed from all three lanes of supernatants probably due to the high concentration of the load and thus it was hard to identify if there was actually soluble VLY produced.

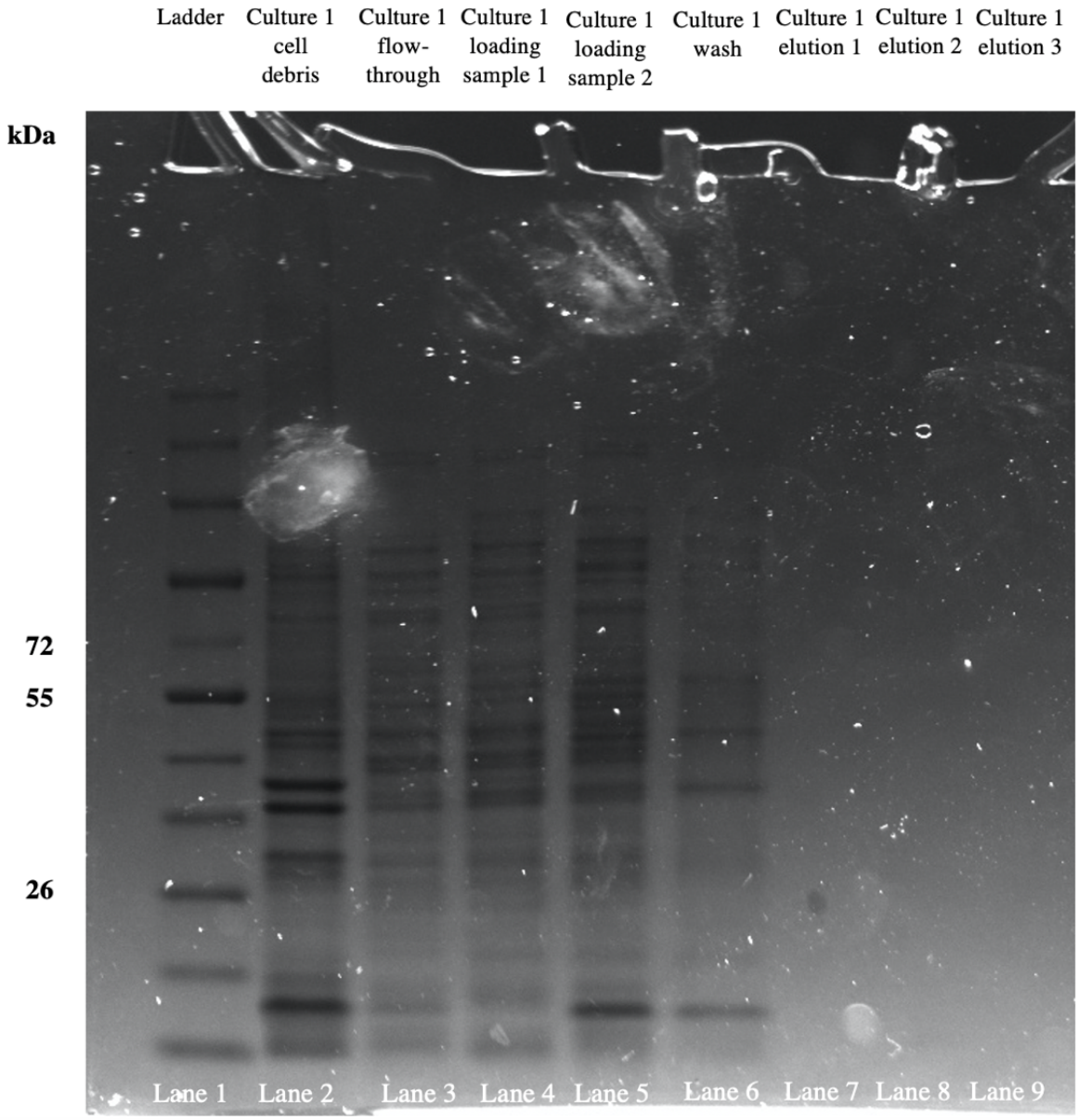


Figure 5.1 SDS-PAGE gel image. BL21 (DE3) *E. coli* cells were induced with 0.1 mM IPTG at 30 °C for 20 hours. The cells were lysed by ultrasonication and BugBuster® reagent separately. Cell debris is the resuspended pellets after spinning down the lysate harvested by ultrasonication method at 16,000 g for 20 minutes at 4 °C. Loading sample 1 is the supernatant from the cell debris. Loading sample 2 is the supernatant from cell debris lysed with BugBuster® reagent (DNase and $MgCl_2$ added). Flow-through is the elute from the column with no imidazole present. Wash is the elute from the column with 60 mM imidazole. Elution 1, 2 and 3 are the elutes of Culture 1 from the column with 100 mM imidazole, 200 mM imidazole and 500 mM imidazole respectively.

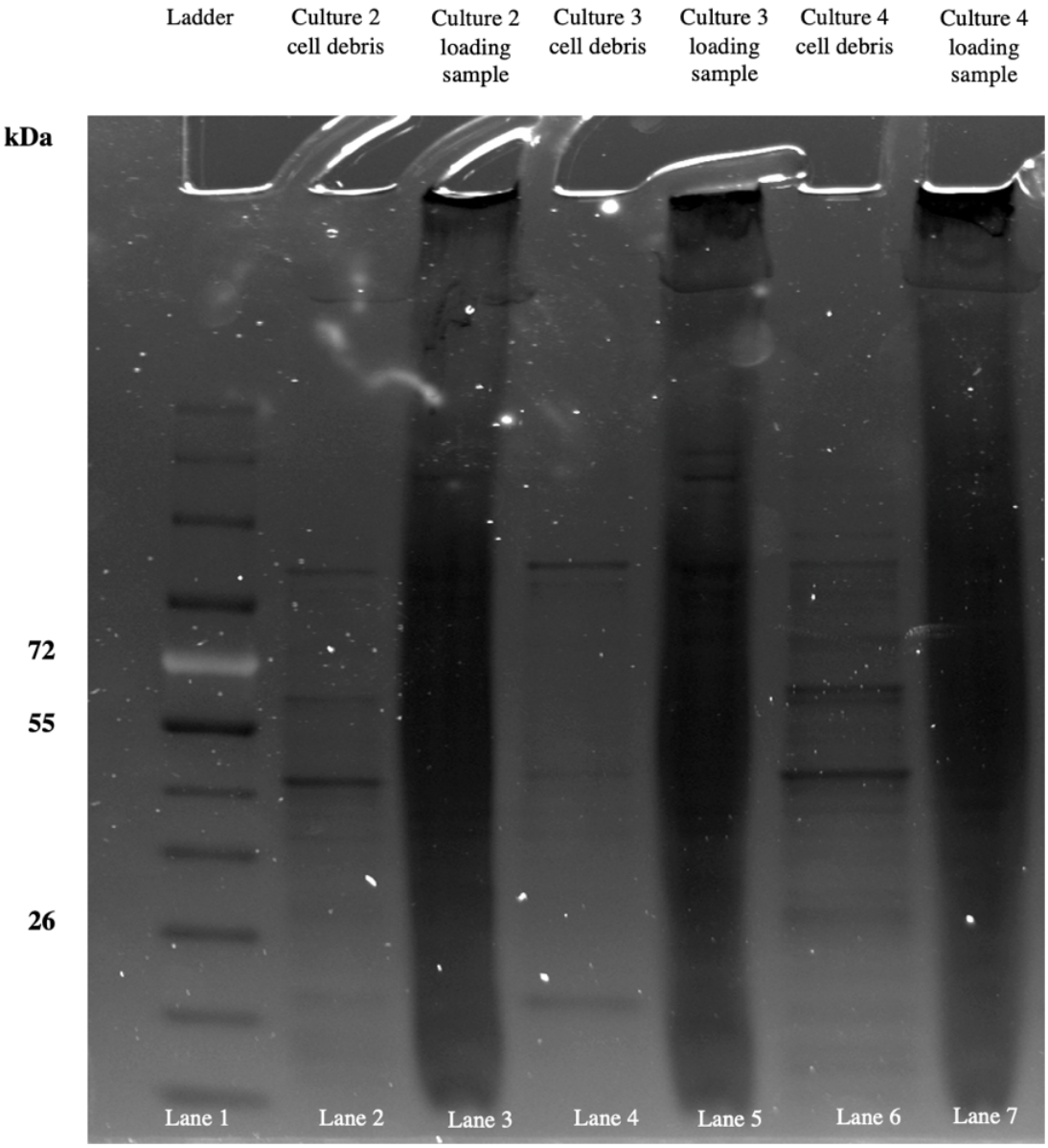


Figure 5.2 SDS-PAGE gel image. Three cultures of BL21 (DE3) *E. coli* cells were induced with 0.1 mM IPTG at 20 °C for 20 hours. The cells were lysed by BugBuster® Master Mix. Cell debris is the resuspended pellets after spinning down the lysate at 16,000 g for 20 m minutes at 4 °C. Loading sample is the supernatant from the cell debris.

Consequently, the supernatants from the cell debris of cultures 2 and 4 were diluted before loading them onto the gel and purified by HisTrap™ HP to see if the soluble VLY protein was

produced. As shown in Figure 5.3, the bands from the diluted supernatants were clearly visualized. However, there were no obvious bands between 72 kDa and 55 kDa in the supernatant lanes. In addition, very faint bands were identified in lanes 5 and 10, which suggested that the imidazole concentration of elution 1 was not high enough to elute other protein impurities.

In conclusion, there was no successful production of VLY within BL21 (DE3) *E. coli* cells after a couple of parallel studies with different cultivation conditions. As such, more efforts were invested in the VLY gene sequence itself as well as the host strain. Generally, there are two reasons for expression failure: protein toxicity and codon bias, both of which are possible in this study. As VLY is a toxin secreted by *G. vaginalis*, it can interfere with the normal proliferation and homeostasis of *E. coli* cells. Given that BL21 (DE3) is the most common host used for heterologous protein expression without special functions, it might not be the most suitable host for expressing VLY. Furthermore, rare codon analysis was performed using GenScript Codon Analysis Tool for the VLY gene sequence. It turns out that the Codon Adaptation Index (CAI) is 0.68, whereas the ideal CAI is between 0.8 and 1.0. This indicates that the codons in the VLY gene is significantly different from those of the host, leading to the depletion of the internal tRNA pools of normal *E. coli* cells, i.e., codon bias. When codon bias occurs, protein expression may be terminated early, leading to protein expression failure. Another finding about the VLY gene sequence is that the density of rare codons at the beginning is very high (the CAI for the first 60 base pairs is only 0.6).

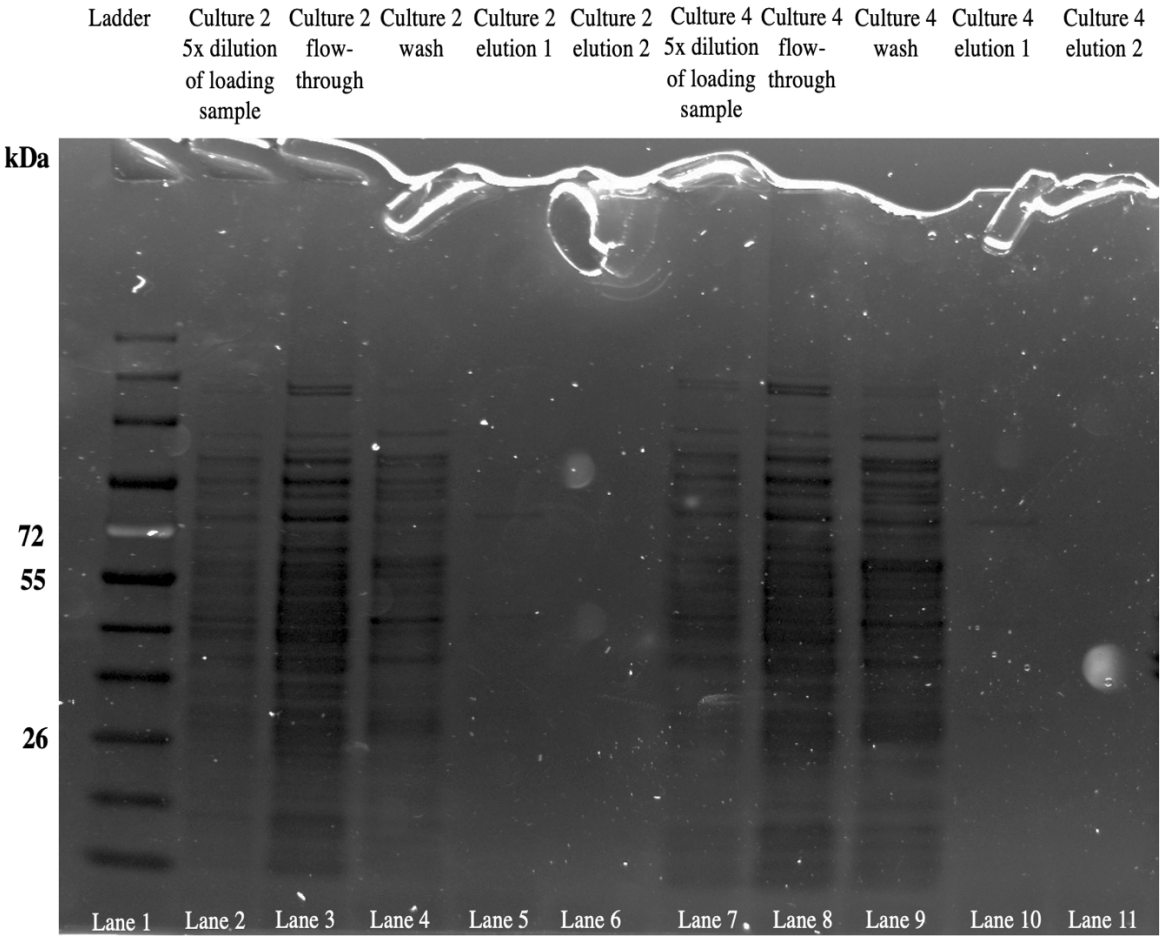


Figure 5.3 SDS-PAGE gel image. Three cultures of BL21 (DE3) *E. coli* cells were induced with 0.1 mM IPTG at 20 °C for 20 hours. Two of the cultures were lysed with BugBuster® Master Mix and purified using HisTrap™HP. Loading sample is the supernatant from the cell debris diluted 5 fold. Flow-through is the elute from the column with no imidazole present. Wash is the elute from the column with 60 mM imidazole. Elution 1 and 2 are the elutes from the column with 200 mM imidazole and 500 mM imidazole respectively.

One possible solution is codon optimization followed by gene synthesis, although this is not recommended for this study. Although changing synonymous codons helps improve translational efficiency and protein expression to some extent, it can be detrimental. Some negative effects that have been reported include improper protein folding and function, protein instability, translation inhibition, and mRNA instability. Therefore, codon optimization might not be the

optimal strategy for increasing protein expression. Instead, extra efforts should be put into the host system selection to enable a successful expression.

Host organism optimization is a more feasible choice in this study. Compared to conventional BL21 strains, BL21-CodonPlus (DE3)-RIPL strains were selected to address the problem of codon bias because they carry a ColE1-compatible, pACYC-based plasmid that contains extra copies of genes which encode the tRNAs (*argU*, *ileY*, *leuW*, *proL* tRNA genes) that most frequently limit heterologous protein translation in *E. coli*.

Reconstruction of pET-28a(+)-based recombinant plasmid by deleting signal sequence is another option. Signal peptide can affect recombinant VLY expression if it jams up the General Secretory System (Sec) of *E. coli* and thus saturates the system capacity. In addition, the rare codon density is extremely high in the sequence of the signal peptide as demonstrated by the CAI. As a result, it would be beneficial for protein expression once the sequence was removed. More important, mature VLY does not have the signal peptide as the peptide will be cleaved off by signal peptidase immediately after protein translocation into the periplasm in the real case.

5.3.2 Induction within BL21-CodonPlus (DE3)-RIPL *E. coli* cells

Compared to BL21 (DE3), the differences among CFUs of BL21-CondonPlus (DE3)-RIPL are more significant. Thus, for the following studies, each culture was grown from each distinct CFU. The culture time for reaching mid-log phase varied among different cultures, ranging from 1 hour 50 minutes to 2 hours 20 minutes. Then the cells were cultured at 37 °C for 2 hours with 1 mM IPTG. Protease inhibitor cocktail was added during cell lysis to protect VLY from possible protease degradation.

It was found that decreasing culture time after induction is not optimal. First, much fewer cells were harvested from the culture compared to previous studies (0.33 g cell paste per 50 mL culture), with less than 0.15 g cell paste collected per 50 mL culture. Secondly, fewer cells can lead to less protein production, which is also confirmed by the SDS-PAGE gel image showing protein bands that were all very thin (Figure 5.4). However, a breakthrough was that there were bands identified between 72 kDa and 55 kDa from the cell debris samples of all induced cultures. It was very likely that one of these bands represented VLY, as there was no band observed at the same position from the non-induced sample.

The phenomenon that all target bands were from insoluble cell debris indicates that VLY is expressed in the form of IBs without proper folding and conformation and is most likely not water-soluble. The milk-like broth of the *E.coli* cell lysate was also an indicator of IB formation. Generally, proteins tend to aggregate into IBs, when there is a high-level expression of the recombinant protein which exceeds the capacity of the host in managing post-translational modification and folding. According to previous work, decreasing the protein production rate can help avoid protein misfolding and thus mitigate IB formation. This is most easily achieved by reducing culture temperature and inducer concentration.

Three concentrations of IPTG were used for VLY expression with culture temperature reduced to 20 °C (Figure 5.5). It was found that the inducer concentration does not have a significant impact on improving the expression of the soluble protein in this study, and that decreasing the culture temperature does not make much difference, either. But increasing culture time does help produce more protein.

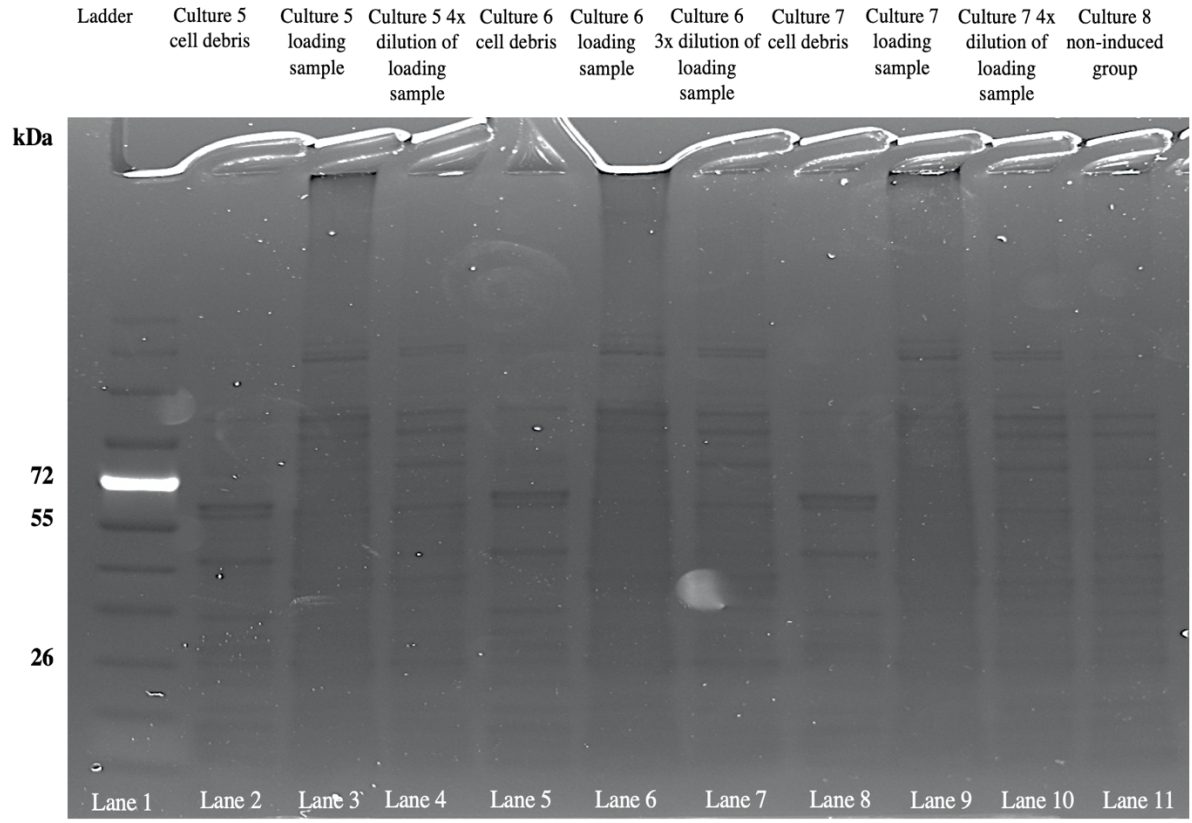


Figure 5.4 SDS-PAGE gel image. Four cultures of BL21-CondonPlus (DE3)-RIPL *E. coli* cells were induced with 1 mM IPTG at 37 °C for 2 hours. The cells were lysed with BugBuster® Master Mix in the presence of 1:200 diluted protease inhibitor cocktail. Culture 8 was kept at control group without adding IPTG while keeping other conditions the same with other three cultures.

IBs were also solubilized and purified for the purpose of obtaining soluble VLY, although refolding *in vitro* might be involved later considering the potential inactivity of IBs themselves. IBs were first solubilized with 30% Empigen BB®, an amphoteric surfactant, and then passed through the column with an elution buffer containing a mild concentration (25 mM) of Empigen BB®. The assumption was that the solubilized IBs would bind to the nickel (II) ions leading to their coupling with the resin through its exposed his-tag and thus would elute with imidazole. But it

turned out that there were hardly any bands visualized on the protein gel, indicating that collecting soluble VLY through IB solubilization was impossible (Figure 5.6).

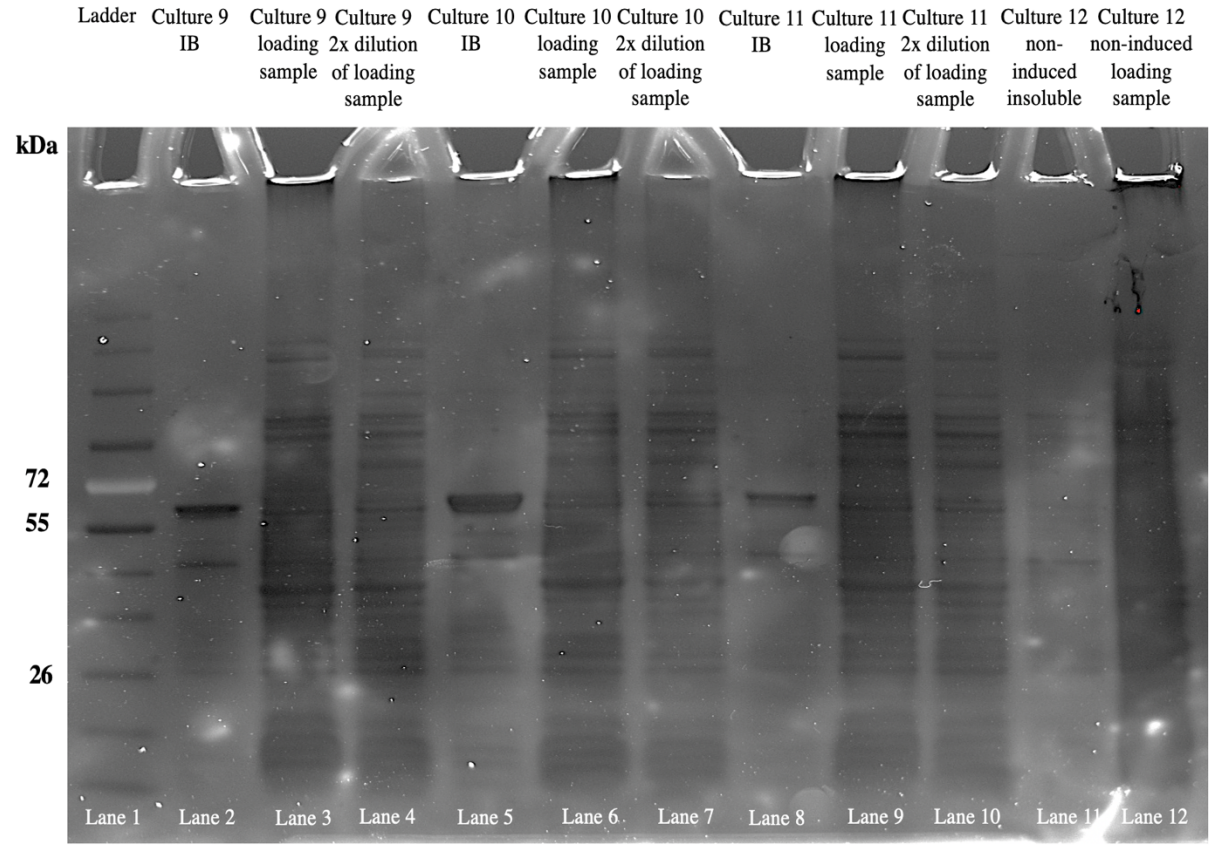


Figure 5.5 SDS-PAGE gel image. Culture 9 was induced with 0.1 mM IPTG at 20 °C for 20 hours. Culture 10 was induced with 1 mM IPTG at 20 °C for 20 hours. Culture 11 was induced with 0.5 mM IPTG at 20 °C for 20 hours. Culture 12 was cultivated at 20 °C for 20 hours without adding IPTG. The insoluble materials spun down at 16,000 g for 20 minutes at 4 °C were purified with BugBuster® Master Mix before loaded onto the gel (culture 9, 10 and 11). The non-induced soluble is the cell debris after cell lysis of culture 12. The non-induced load is the supernatant from the cell debris of culture 12.

Finally, IB solubilization was abandoned due to the many challenges associated with its solubilization. For example, even if IBs are solubilized successfully, it is highly likely that the protein lacks activity and does not have the function we need, as there is a chance that the buffer

denatures the protein during the solubilization process. In addition, *in vitro* refolding of IBs hardly succeeds, making it impossible for active protein recovery. Hence, we tried to improve soluble VLY expression by introducing sorbitol and heat shock cultivation before induction, hoping that these methods could help correct protein folding and promote the formation of soluble protein. Meanwhile, we also increased the culture volume from 50 to 150 mL and concentrated the elution samples from the HisTrap™HP column before loading samples on the protein gel to make the trace amount of soluble VLY detectable if any. Unfortunately, the two experiments failed, too, as there was no soluble fraction corresponding to the target protein neither in the cell lysates nor in the solution that eluted with 300 mM imidazole (Figure 5.7 and Figure 5.8).

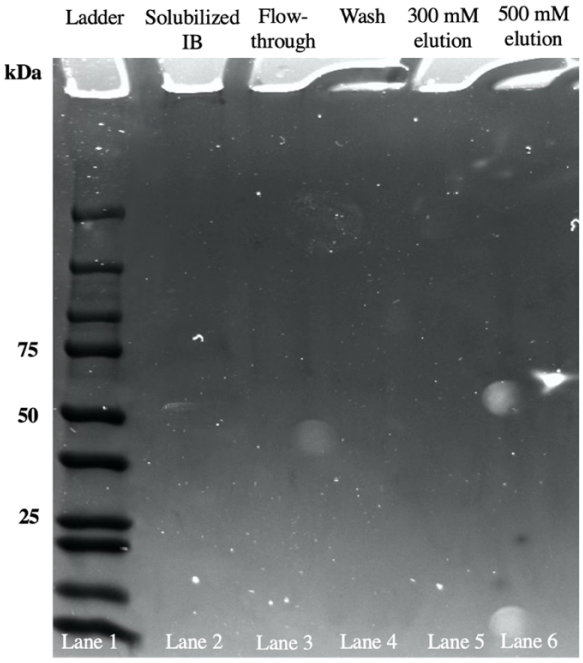


Figure 5.6 SDS-PAGE gel image. The culture was induced with 1 mM IPTG at 20 °C for 20 hours. After cell lysis, the IBs were collected, solubilized, and purified using HisTrap™HP. Flow-through is the elute from the column with no imidazole present. Wash is the elute from the column with 60 mM imidazole and 25 mM Empigen BB®. Elution 1 and 2 are the elutes from the column with 300 mM imidazole and 500 mM imidazole with 25 mM Empigen BB®, respectively.

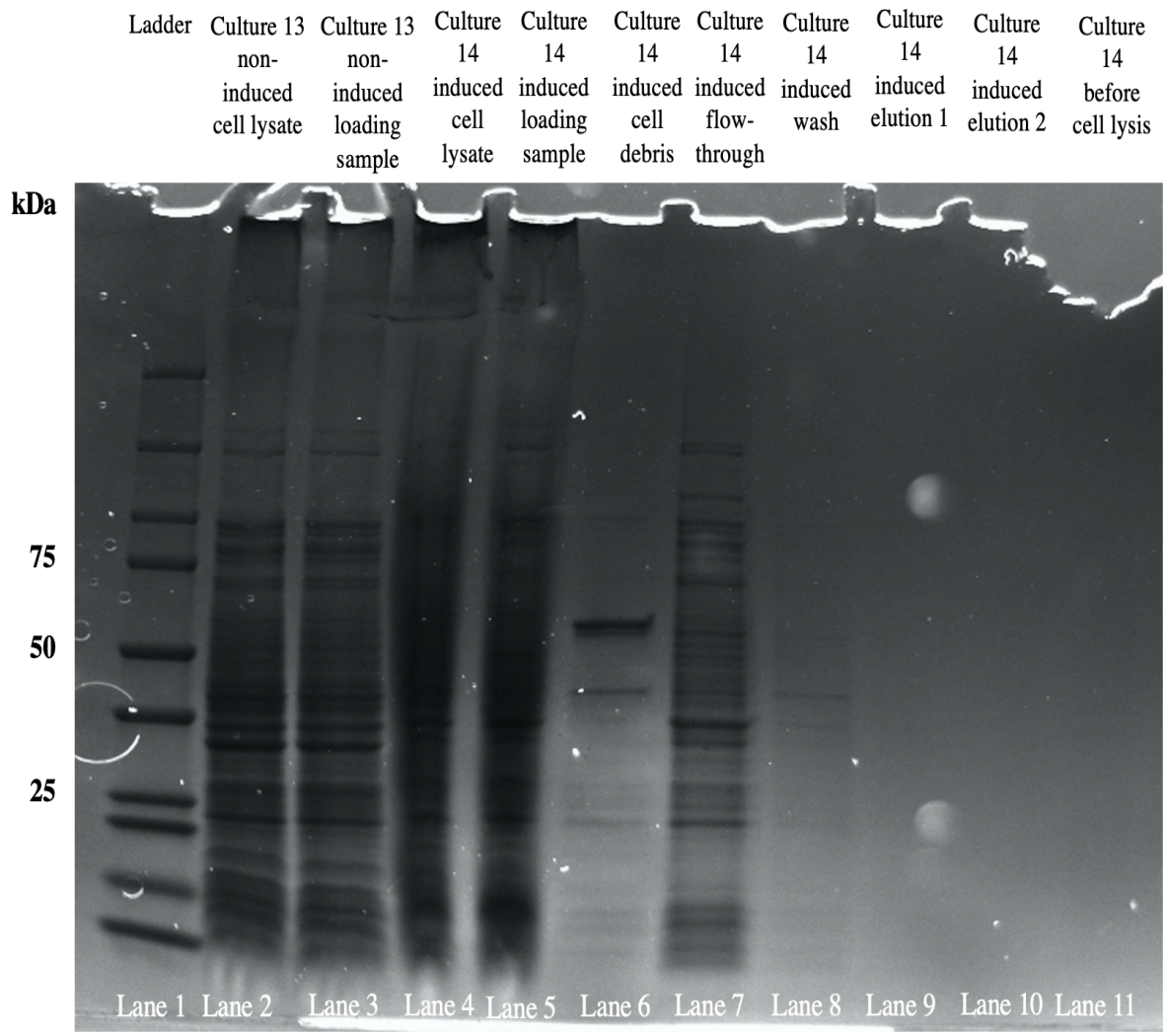


Figure 5.7 SDS-PAGE gel image. Culture 13 was set as non-induced control group. Culture 14 (150 mL) was induced with 1 mM IPTG and 0.5 M sorbitol at 20 °C for 20 hours. Culture 14 induced cell lysate is the mixture harvested after lysed with BugBuster® Master Mix. Culture 14 induced load is the supernatant from the cell debris. Culture 14 induced flow-through is the elute from the column with no imidazole present. Culture 14 induced wash is the elute from the column with 70 mM imidazole. Culture 14 induced elution 1 is the elute from the column with 300 mM imidazole. Culture 14 induced elution 2 is the elute from the column with 500 mM imidazole. Culture 14 before cell lysis is the supernatant from the 150 mL cell culture.

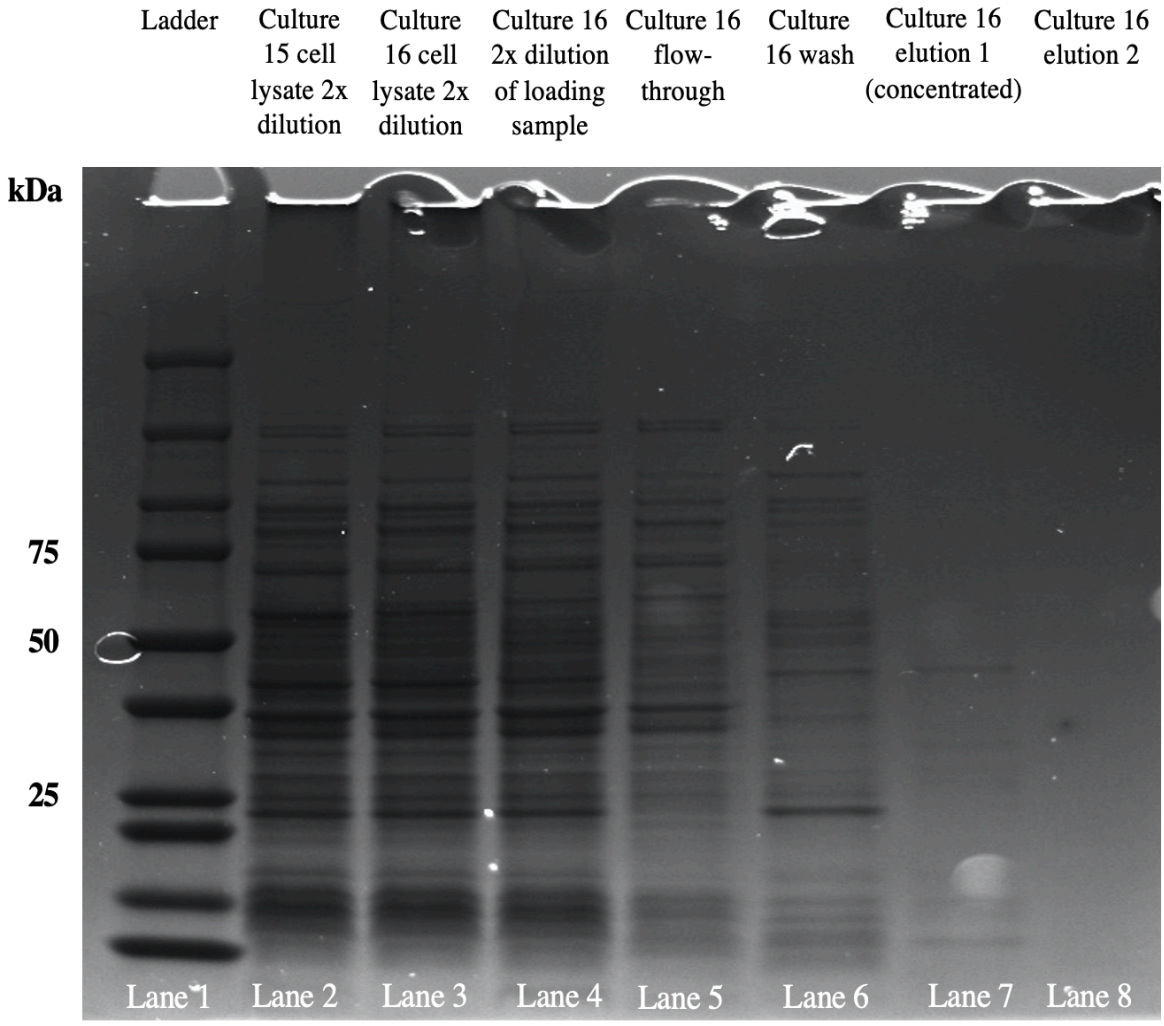


Figure 5.8 SDS-PAGE gel image. Culture 15 was induced with 0.5 mM IPTG and incubated at 20 °C for 20 hours as control. Culture 16 was induced with 0.5 mM IPTG at 47 °C for 20 minutes before incubated at 20 °C for 20 hours. Culture 16 cell lysate 2x dilution is diluted mixture harvested after lysed with BugBuster® Master Mix. Culture 16 2x dilution of loading sample is the supernatant from the cell debris. Culture 16 flow-through is the elute from the column with no imidazole present. Culture 16 wash is the elute from the column with 70 mM imidazole. Culture 16 elution 1 is the concentrated elute from the column with 300 mM imidazole. Culture 16 elution 2 is the elute from the column with 500 mM imidazole.

Chapter 6 Conclusions and future directions

In this study, a bacteria-responsive drug release platform aimed at treating BV has been successfully developed. For the first part of the work, we prepared and characterized liposomes encapsulating calcein, and then evaluated its responsiveness to bacteria. The conclusions are summarized below:

i) Four formulations of liposome encapsulating calcein were prepared via the polyol dilution method, which is facile, non-toxic, and applicable in women vagina. A series of optimizations in formulation design (initial calcein amount, total lipids, and sonication time) and purification methods (centrifugation, ultrafiltration, and dialysis) were performed to determine an optimal protocol. The optimized EE was calculated to be 10 – 15%.

ii) The prepared liposomes had an average diameter of around 300 nm with a relatively narrow size distribution (the PDI value ranging from 0.25 to 0.28). The average zeta potential of the liposomes is around -60 mV. All the results indicate that the preparation method is reliable, and that the liposomes can remain stable due to electrostatic repulsions.

iii) Four liposome formulations demonstrated their responsiveness to *G. vaginalis* and inertness to *L. crispatus*. In the presence of the *G. vaginalis* supernatant, the liposomes were capable of achieving sustained calcein release during 3 – 5 days, while in the presence of *L. crispatus*, the liposomes showed negligible calcein release. However, the average cumulative calcein release of the experiments slightly varied among the four formulations, ranging from 46.7% $\pm$ 0.5% to 51.8% $\pm$ 0.2%, which might be attributed to the difference in the molar ratio of CHOL. We speculate that the amount of calcein released increases as the amount of CHOL

increases, because VLY produced by *G. vaginalis* can insert into the liposome membrane and create pores in the presence of CHOL, resulting in calcein release.

This is the first time that a toxin secreted by the primary pathogen of BV is used to trigger drug release. We have proved that this platform has great potential to achieve on-demand therapy for BV relapse prevention and treatment without concerns of excess dosing. To make the platform applicable in the real treatment, we also need to quantify the responsive release before the real drug loading so that the formulation can be evaluated in terms of the therapeutic efficacy. Consequently, the solution is to express the recombinant VLY in the *E. coli* expression system and use it as standard to quantify VLY produced by *G. vaginalis*.

The second part of the work dealt with the recombinant VLY expression within the engineered *E. coli*. cells. However, a successful strategy has not been developed yet to get the purified recombinant VLY. The results and conclusions we have got so far are summarized below before further studies are required:

i) A recombinant protein expression system was successfully constructed. The VLY gene was amplified and then cloned into pET-28a(+), followed by transformation into BL21(DE3) and BL21-CodonPlus (DE3)-RIPL *E. coli* cells. The results of colony PCR and DNA sequencing showed that the VLY gene was successfully inserted into the plasmid vector.

ii) The expression of the recombinant soluble VLY failed. We have done a series of optimizations in expression conditions including using different host strains and changing induction/cultivation strategies. Unfortunately, VLY was expressed in an aggregated form (IBs) without proper three-dimensional structure and biological activity. We also tried to harvest the soluble fraction by solubilizing the IBs, but we did not get the expected result.

In the future, more efforts should be put into improving the soluble recombinant VLY expression. And we think that there are several possible solutions. The first one is to reconstruct the recombinant protein expression system by cloning the signal sequence-deleted VLY gene into the plasmid vector, because the signal peptide at the N-terminal is likely to negatively affect VLY expression within *E. coli* cells. The second option is to change the host strain, as the current BL21-CodonPlus (DE3)-RIPL strain may have caused the formation of VLY aggregates.

It is important to obtain purified VLY to further evaluate our drug delivery system. On the one hand, with the purified VLY we can further confirm the drug release mechanism by studying VLY-responsive liposome release profiles. On the other hand, utilizing the purified VLY as standard can help obtain the real drug release kinetics, e.g., determining the sensitivity of the platform. In this case, we can better adapt the liposome formulations to control the drug release level in accordance with the target therapeutic concentration of the actual antibiotic.

Letters of Copyright Permissions



Front Cell Infect Microbiol. 2020; 10: 168.
Published online 2020 Apr 24. doi: 10.3389/fcimb.2020.00168
PMCID: PMC7193744
PMID: 32391287

Gardnerella vaginalis as a Cause of Bacterial Vaginosis: Appraisal of the Evidence From *in vivo* Models

Sydney Morrill,[1,2] Nicole M. Gilbert,[2,3,4] and Amanda L. Lewis[1,2,3,*]

▸ Author information ▸ Article notes ▾ Copyright and License information Disclaimer

Copyright © 2020 Morrill, Gilbert and Lewis.

This is an open-access article distributed under the terms of the Creative Commons Attribution License (CC BY). The use, distribution or reproduction in other forums is permitted, provided the original author(s) and the copyright owner(s) are credited and that the original publication in this journal is cited, in accordance with accepted academic practice. No use, distribution or reproduction is permitted which does not comply with these terms.

References

1. Peebles, K.; Velloza, J.; Balkus, J. E.; McClelland, R. S.; Barnabas, R. V., High global burden and costs of bacterial vaginosis: a systematic review and meta-analysis. *Sex. Transm. Dis.* **2019,** *46* (5), 304-311.

2. Palmeira-de-Oliveira, R.; Palmeira-de-Oliveira, A.; Martinez-de-Oliveira, J., New strategies for local treatment of vaginal infections. *Adv. Drug Del. Rev.* **2015,** *92*, 105-122.

3. Amsel, R.; Totten, P. A.; Spiegel, C. A.; Chen, K. C. S.; Eschenbach, D.; Holmes, K. K., Nonspecific vaginitis: diagnostic criteria and microbial and epidemiologic associations. *Am. J. Med.* **1983,** *74* (1), 14-22.

4. Keane, F.; Ison, C. A.; Noble, H.; Estcourt, C., Bacterial vaginosis. *Sex. Transm. Infect.* **2006,** *82 Suppl 4*, iv16-18.

5. Bradshaw, C. S.; Sobel, J. D., Current treatment of bacterial vaginosis-limitations and need for innovation. *J. Infect. Dis.* **2016,** *214 Suppl 1*, S14-20.

6. Faught, B. M.; Reyes, S., Characterization and treatment of recurrent bacterial vaginosis. *J Womens Health (Larchmt)* **2019,** *28* (9), 1218-1226.

7. Leyva-Gómez, G.; Del Prado-Audelo, M. L.; Ortega-Peña, S.; Mendoza-Muñoz, N.; Urbán-Morlán, Z.; González-Torres, M.; González-Del Carmen, M.; Figueroa-González, G.; Reyes-Hernández, O. D.; Cortés, H., Modifications in vaginal microbiota and their influence on drug release: challenges and opportunities. *Pharmaceutics* **2019,** *11* (5), 217.

8. Morrill, S.; Gilbert, N. M.; Lewis, A. L., *Gardnerella vaginalis* as a cause of bacterial vaginosis: appraisal of the evidence from *in vivo* models. *Front. Cell. Infect. Microbiol.* **2020,** *10*, 168.

9. Machado, A.; Cerca, N., Influence of biofilm formation by *Gardnerella vaginalis* and other anaerobes on bacterial vaginosis. *J. Infect. Dis.* **2015,** *212* (12), 1856-1861.

10. Castro, J.; Cerca, N., BV and non-BV associated *Gardnerella vaginalis* establish similar synergistic interactions with other BV-associated microorganisms in dual-species biofilms. *Anaerobe* **2015,** *36*, 56-59.

11. Castro, J.; Machado, D.; Cerca, N., Unveiling the role of *Gardnerella vaginalis* in polymicrobial bacterial vaginosis biofilms: the impact of other vaginal pathogens living as neighbors. *ISME J.* **2019,** *13* (5), 1306-1317.

12. Randis, T. M.; Zaklama, J.; LaRocca, T. J.; Los, F. C.; Lewis, E. L.; Desai, P.; Rampersaud, R.; Amaral, F. E.; Ratner, A. J., Vaginolysin drives epithelial ultrastructural responses to *Gardnerella vaginalis*. *Infect. Immun.* **2013,** *81* (12), 4544-4550.

13. Schellenberg, J. J.; Patterson, M. H.; Hill, J. E., *Gardnerella vaginalis* diversity and ecology in relation to vaginal symptoms. *Res. Microbiol.* **2017,** *168* (9-10), 837-844.

14. Zilnyte, M.; Venclovas, C.; Zvirbliene, A.; Pleckaityte, M., The cytolytic activity of vaginolysin strictly depends on cholesterol and is potentiated by human CD59. *Toxins (Basel)* **2015,** *7* (1), 110-128.

15. Pleckaityte, M., Cholesterol-dependent cytolysins produced by vaginal bacteria: certainties and controversies. *Front. Cell. Infect. Microbiol.* **2019,** *9*, 452.

16. Ragaliauskas, T.; Pleckaityte, M.; Jankunec, M.; Labanauskas, L.; Baranauskiene, L.; Valincius, G., Inerolysin and vaginolysin, the cytolysins implicated in vaginal dysbiosis, differently impair molecular integrity of phospholipid membranes. *Sci. Rep.* **2019,** *9* (1), 10606.

17. Dingsdag, S. A.; Hunter, N., Metronidazole: an update on metabolism, structure-cytotoxicity and resistance mechanisms. *J. Antimicrob. Chemother.* **2018,** *73* (2), 265-279.

18. Falagas., M. E.; Gorbach., S. L., Clindamycin and metronidazole. *Med. Clin. North Am.* **1995,** *79* (4), 845-867.

19. Tomas, M.; Palmeira-de-Oliveira, A.; Simoes, S.; Martinez-de-Oliveira, J.; Palmeira-de-Oliveira, R., Bacterial vaginosis: standard treatments and alternative strategies. *Int. J. Pharm.* **2020,** *587*, 119659.

20. Joesoef, M. R.; Schmid, G. P.; Hillier, S. L., Bacterial vaginosis: review of treatment options and potential clinical indications for therapy. *Clin. Infect. Dis.* **1999,** *28*, S57-65.

21. Tidbury, F. D.; Langhart, A.; Weidlinger, S.; Stute, P., Non-antibiotic treatment of bacterial vaginosis—a systematic review. *Arch. Gynecol. Obstet.* **2021,** *303* (1), 37-45.

22. Nelson, A. L., Comprehensive overview of the recently FDA-approved contraceptive vaginal ring releasing segesterone acetate and ethinylestradiol: a new year-long, patient controlled, reversible birth control method. *Expert Rev. Clin. Pharmacol.* **2019,** *12* (10), 953-963.

23. das Neves, J.; Bahia, M. F., Gels as vaginal drug delivery systems. *Int. J. Pharm.* **2006,** *318* (1-2), 1-14.

24. Perioli, L.; Ambrogi, V.; Venezia, L.; Pagano, C.; Ricci, M.; Rossi, C., Chitosan and a modified chitosan as agents to improve performances of mucoadhesive vaginal gels. *Colloids Surf. B. Biointerfaces* **2008,** *66* (1), 141-145.

25. Xu, S.; Cavera, V. L.; Rogers, M. A.; Huang, Q.; Zubovskiy, K.; Chikindas, M. L., Benzoyl peroxide formulated polycarbophil/carbopol 934P hydrogel with selective antimicrobial activity, potentially beneficial for treatment and prevention of bacterial vaginosis. *Infect. Dis. Obstet. Gynecol.* **2013,** *2013*, 909354.

26. Singh, V. K.; Anis, A.; Banerjee, I.; Pramanik, K.; Bhattacharya, M. K.; Pal, K., Preparation and characterization of novel carbopol based bigels for topical delivery of metronidazole for the treatment of bacterial vaginosis. *Mater. Sci. Eng., C* **2014,** *44*, 151-158.

27. Ibrahim el, S. A.; Ismail, S.; Fetih, G.; Shaaban, O.; Hassanein, K.; Abdellah, N. H., Development and characterization of thermosensitive pluronic-based metronidazole *in situ* gelling formulations for vaginal application. *Acta. Pharm.* **2012,** *62* (1), 59-70.

28. Patel, P.; Patel, P., Formulation and evaluation of clindamycin HCL *in situ* gel for vaginal application. *Int. J. Pharm. Invest.* **2015,** *5* (1), 50-56.

29. Ferreira, N. N.; Perez, T. A.; Pedreiro, L. N.; Prezotti, F. G.; Boni, F. I.; Cardoso, V. M. O.; Venancio, T.; Gremiao, M. P. D., A novel pH-responsive hydrogel-based on calcium alginate engineered by the previous formation of polyelectrolyte complexes (PECs) intended to vaginal administration. *Drug Dev. Ind. Pharm.* **2017,** *43* (10), 1656-1668.

30. Pavelic, Z.; Skalko-Basnet, N.; Jalsenjak, I., Characterisation and *in vitro* evaluation of bioadhesive liposome gels for local therapy of vaginitis. *Int. J. Pharm.* **2005,** *301* (1-2), 140-148.

31. Vanic, Z.; Hurler, J.; Ferderber, K.; Golja Gasparovic, P.; Skalko-Basnet, N.; Filipovic-Grcic, J., Novel vaginal drug delivery system: deformable propylene glycol liposomes-in-hydrogel. *J. Liposome Res.* **2014,** *24* (1), 27-36.

32. Machado, R. M.; Tomas, M.; Palmeira-de-Oliveira, A.; Martinez-de-Oliveira, J.; Palmeira-de-Oliveira, R., The vaginal sheet: an innovative form of vaginal film for the treatment of vaginal infections. *Drug Dev. Ind. Pharm.* **2020,** *46* (1), 135-145.

33. Tentor, F.; Siccardi, G.; Sacco, P.; Demarchi, D.; Marsich, E.; Almdal, K.; Bose Goswami, S.; Boisen, A., Long lasting mucoadhesive membrane based on alginate and chitosan for intravaginal drug delivery. *J. Mater. Sci. Mater. Med.* **2020,** *31* (3), 25.

34. Dobaria, N.; Mashru, R., Design and *in vitro* evaluation of a novel bioadhesive vaginal drug delivery system for clindamycin phosphate. *Pharm. Dev. Technol.* **2010,** *15* (4), 405-414.

35. El-Kamel, A.; Sokar, M.; Naggar, V.; Gamal, S. A., Chitosan and sodium alginate–based bioadhesive vaginal tablets. *AAPS PharmSci* **2002,** *4* (4), E44.

36. Verstraete, G.; Vandenbussche, L.; Kasmi, S.; Nuhn, L.; Brouckaert, D.; Van Renterghem, J.; Grymonpre, W.; Vanhoorne, V.; Coenye, T.; De Geest, B. G.; De Beer, T.; Remon, J. P.; Vervaet, C., Thermoplastic polyurethane-based intravaginal rings for prophylaxis and treatment of (recurrent) bacterial vaginosis. *Int. J. Pharm.* **2017,** *529* (1-2), 218-226.

37. Pathak, M.; Turner, M.; Palmer, C.; Coombes, A. G., Evaluation of polycaprolactone matrices for the intravaginal delivery of metronidazole in the treatment of bacterial vaginosis. *J. Biomater. Appl.* **2014,** *29* (3), 354-363.

38. Chu, L.; Gao, H.; Cheng, T.; Zhang, Y.; Liu, J.; Huang, F.; Yang, C.; Shi, L.; Liu, J., A charge-adaptive nanosystem for prolonged and enhanced *in vivo* antibiotic delivery. *Chem. Commun. (Camb.)* **2016,** *52* (37), 6265-6268.

39. Kalhapure, R. S.; Jadhav, M.; Rambharose, S.; Mocktar, C.; Singh, S.; Renukuntla, J.; Govender, T., pH-responsive chitosan nanoparticles from a novel twin-chain anionic amphiphile

for controlled and targeted delivery of vancomycin. *Colloids Surf. B. Biointerfaces* **2017,** *158*, 650-657.

40. Wang, J.; Chen, X. Y.; Zhao, Y.; Yang, Y.; Wang, W.; Wu, C.; Yang, B.; Zhang, Z.; Zhang, L.; Liu, Y.; Du, X.; Li, W.; Qiu, L.; Jiang, P.; Mou, X. Z.; Li, Y. Q., pH-switchable antimicrobial nanofiber networks of hydrogel eradicate biofilm and rescue stalled healing in chronic wounds. *ACS Nano* **2019,** *13* (10), 11686-11697.

41. Radovic-Moreno, A. F.; Lu, T. K.; Puscasu, V. A.; Yoon, C. J.; Langer, R.; Farokhzad, O. C., Surface charge-switching polymeric nanoparticles for bacterial cell wall-targeted delivery of antibiotics. *ACS Nano* **2012,** *6* (5), 4279-4287.

42. Zhou, Z.; Hu, F.; Hu, S.; Kong, M.; Feng, C.; Liu, Y.; Cheng, X.; Ji, Q.; Chen, X., pH-activated nanoparticles with targeting for the treatment of oral plaque biofilm. *J. Mater. Chem. B* **2018,** *6* (4), 586-592.

43. Xie, X.; Sun, T.; Xue, J.; Miao, Z.; Yan, X.; Fang, W.; Li, Q.; Tang, R.; Lu, Y.; Tang, L.; Zha, Z.; He, T., Ag nanoparticles cluster with pH‐triggered reassembly in targeting antimicrobial applications. *Adv. Funct. Mater.* **2020,** *30*, 2000511.

44. Li, J.; Ding, Z.; Li, Y.; Miao, J.; Wang, W.; Nundlall, K.; Chen, S., Reactive oxygen species-sensitive thioketal-linked mesoporous silica nanoparticles as drug carrier for effective antibacterial activity. *Mater. Des.* **2020,** *195*, 109021.

45. Liu, Y.; Naha, P. C.; Hwang, G.; Kim, D.; Huang, Y.; Simon-Soro, A.; Jung, H. I.; Ren, Z.; Li, Y.; Gubara, S.; Alawi, F.; Zero, D.; Hara, A. T.; Cormode, D. P.; Koo, H., Topical ferumoxytol nanoparticles disrupt biofilms and prevent tooth decay *in vivo* via intrinsic catalytic activity. *Nat. Commun.* **2018,** *9* (1), 2920.

46. Quek, J. Y.; Uroro, E.; Goswami, N.; Vasilev, K., Design principles for bacteria-responsive antimicrobial nanomaterials. *Mater. Today Chem.* **2022,** *23*,100606.

47. Yang, S.; Han, X.; Yang, Y.; Qiao, H.; Yu, Z.; Liu, Y.; Wang, J.; Tang, T., Bacteria-targeting nanoparticles with microenvironment-responsive antibiotic release to eliminate intracellular *Staphylococcus aureus* and associated infection. *ACS Appl. Mater. Interfaces* **2018,** *10* (17), 14299-14311.

48. Abdali, Z.; Logsetty, S.; Liu, S., Bacteria-responsive single and core-shell nanofibrous membranes based on polycaprolactone/poly(ethylene succinate) for on-demand release of biocides. *ACS Omega* **2019,** *4* (2), 4063-4070.

49. Xiong, M. H.; Bao, Y.; Yang, X. Z.; Wang, Y. C.; Sun, B.; Wang, J., Lipase-sensitive polymeric triple-layered nanogel for "on-demand" drug delivery. *J. Am. Chem. Soc.* **2012,** *134* (9), 4355-4362.

50. Ji, H.; Dong, K.; Yan, Z.; Ding, C.; Chen, Z.; Ren, J.; Qu, X., Bacterial hyaluronidase self-triggered prodrug release for chemo-photothermal synergistic treatment of bacterial infection. *Small* **2016,** *12* (45), 6200-6206.

51. Ayaz, P.; Xu, B.; Zhang, X.; Wang, J.; Yu, D.; Wu, J., A pH and hyaluronidase dual-responsive multilayer-based drug delivery system for resisting bacterial infection. *Appl. Surf. Sci.* **2020,** *527*, 146806.

52. Xiong, M. H.; Li, Y. J.; Bao, Y.; Yang, X. Z.; Hu, B.; Wang, J., Bacteria-responsive multifunctional nanogel for targeted antibiotic delivery. *Adv. Mater.* **2012,** *24* (46), 6175-6180.

53. Thamphiwatana, S.; Gao, W.; Pornpattananangkul, D.; Zhang, Q.; Fu, V.; Li, J.; Li, J.; Obonyo, M.; Zhang, L., Phospholipase A2-responsive antibiotic delivery via nanoparticle-

stabilized liposomes for the treatment of bacterial infection. *J. Mater. Chem. B* **2014,** *2* (46), 8201-8207.

54. Lin, A.; Liu, Y.; Zhu, X.; Chen, X.; Liu, J.; Zhou, Y.; Qin, X.; Liu, J., Bacteria-responsive biomimetic selenium nanosystem for multidrug-resistant bacterial infection detection and inhibition. *ACS Nano* **2019,** *13* (12), 13965-13984.

55. Pornpattananangkul, D.; Zhang, L.; Olson, S.; Aryal, S.; Obonyo, M.; Vecchio, K.; Huang, C. M.; Zhang, L., Bacterial toxin-triggered drug release from gold nanoparticle-stabilized liposomes for the treatment of bacterial infection. *J. Am. Chem. Soc.* **2011,** *133* (11), 4132-4139.

56. Sikder, A.; Chaudhuri, A.; Mondal, S.; Singh, N. D. P., Recent advances on stimuli-responsive combination therapy against multidrug-resistant bacteria and biofilm. *ACS Appl. Bio Mater.* **2021,** *4* (6), 4667-4683.

57. Chen, M.; Wei, J.; Xie, S.; Tao, X.; Zhang, Z.; Ran, P.; Li, X., Bacterial biofilm destruction by size/surface charge-adaptive micelles. *Nanoscale* **2019,** *11* (3), 1410-1422.

58. Ahmad, I.; Nawaz, N.; Darwesh, N. M.; Ur Rahman, S.; Mustafa, M. Z.; Khan, S. B.; Patching, S. G., Overcoming challenges for amplified expression of recombinant proteins using *Escherichia coli*. *Protein Expression Purif.* **2018,** *144*, 12-18.

59. Kaur, J.; Kumar, A.; Kaur, J., Strategies for optimization of heterologous protein expression in *E. coli*: roadblocks and reinforcements. *Int. J. Biol. Macromol.* **2018,** *106*, 803-822.

60. Sorensen, H. P.; Mortensen, K. K., Advanced genetic strategies for recombinant protein expression in *Escherichia coli*. *J. Biotechnol.* **2005,** *115* (2), 113-128.

61. Rosano, G. L.; Ceccarelli, E. A., Recombinant protein expression in *Escherichia coli*: advances and challenges. *Front. Microbiol.* **2014,** *5*, 172.

62. Davis, G. D.; Elisee, C.; Newham, D. M.; Harrison, R. G., New fusion protein systems designed to give soluble expression in *Escherichia coli*. *Biotechnol. Bioeng.* **1999,** *65* (4), 382-388.

63. Kapust, R. B.; Waugh, D. S., *Escherichia coli* maltose-binding protein is uncommonly effective at promoting the solubility of polypeptides to which it is fused. *Protein Sci.* **1999,** *8* (8), 1668-1674.

64. Tegel, H.; Tourle, S.; Ottosson, J.; Persson, A., Increased levels of recombinant human proteins with the *Escherichia coli* strain Rosetta (DE3). *Protein Expression Purif.* **2010,** *69* (2), 159-167.

65. Buchan, J. R.; Stansfield, I., Halting a cellular production line: responses to ribosomal pausing during translation. *Biol. Cell* **2007,** *99* (9), 475-487.

66. Hausser, J.; Syed, A. P.; Bilen, B.; Zavolan, M., Analysis of CDS-located miRNA target sites suggests that they can effectively inhibit translation. *Genome Res.* **2013,** *23* (4), 604-615.

67. Dresios, J.; Chappell, S. A.; Zhou, W.; Mauro, V. P., An mRNA-rRNA base-pairing mechanism for translation initiation in eukaryotes. *Nat. Struct. Mol. Biol.* **2006,** *13* (1), 30-34.

68. Mauro, V. P.; Chappell, S. A., A critical analysis of codon optimization in human therapeutics. *Trends Mol. Med.* **2014,** *20* (11), 604-613.

69. Bhatwa, A.; Wang, W.; Hassan, Y. I.; Abraham, N.; Li, X. Z.; Zhou, T., Challenges associated with the formation of recombinant protein inclusion bodies in *Escherichia coli* and strategies to address them for industrial applications. *Front. Bioeng. Biotechnol.* **2021,** *9*, 630551.

70. Oganesyan, N.; Ankoudinova, I.; Kim, S. H.; Kim, R., Effect of osmotic stress and heat shock in recombinant protein overexpression and crystallization. *Protein Expression Purif.* **2007,** *52* (2), 280-285.

71. Kim, Y. E.; Hipp, M. S.; Bracher, A.; Hayer-Hartl, M.; Hartl, F. U., Molecular chaperone functions in protein folding and proteostasis. *Annu. Rev. Biochem.* **2013,** *82*, 323-355.

72. Gupta, S. K.; Shukla, P., Advanced technologies for improved expression of recombinant proteins in bacteria: perspectives and applications. *Crit. Rev. Biotechnol.* **2016,** *36* (6), 1089-1098.

73. Sadeghian-Rizi T, E. A., Moazzen F, Yousefian H, Jahanian-Najafabadi A., Improvement of solubility and yield of recombinant protein expression in *E. coli* using a two-step system. *Res. Pharm. Sci.* **2019,** *14*, 400-407.

74. Ruan, A.; Ren, C.; Quan, S., Conversion of the molecular chaperone Spy into a novel fusion tag to enhance recombinant protein expression. *J. Biotechnol.* **2020,** *307* (Complete), 131-138.

75. Vu, T. T. T.; Jeong, B.; Yu, J.; Koo, B.-K.; Jo, S.-H.; Robinson, R. C.; Choe, H., Soluble prokaryotic expression and purification of crotamine using an N-terminal maltose-binding protein tag. *Toxicon* **2014,** *92*, 157-165.

76. Singh, A.; Upadhyay, V.; Upadhyay, A. K.; Singh, S. M.; Panda, A. K., Protein recovery from inclusion bodies of *Escherichia coli* using mild solubilization process. *Microb. Cell Fact.* **2015,** *14*, 41.

77. Murray, D. T.; Griffin, J.; Cross, T. A., Detergent optimized membrane protein reconstitution in liposomes for solid state NMR. *Biochemistry* **2014,** *53* (15), 2454-2463.

78. Patra, A. K.; Mukhopadhyay, R.; Mukhija, R.; Krishnan, A.; Garg, L. C.; Panda, A. K., Optimization of inclusion body solubilization and renaturation of recombinant human growth hormone from *Escherichia coli*. *Protein Expression Purif.* **2000,** *18* (2), 182-192.

79. Palmeira-de-Oliveira, R.; Duarte, P.; Palmeira-de-Oliveira, A.; das Neves, J.; Amaral, M. H.; Breitenfeld, L.; Martinez-de-Oliveira, J., Women's experiences, preferences and perceptions regarding vaginal products: results from a cross-sectional web-based survey in Portugal. *Eur. J. Contracept. Reprod. Health Care* **2015,** *20* (4), 259-271.

80. Kikuchi, H.; Yamauchi, H.; Hirota, S., A polyol dilution method for mass production of liposomes. *J. Liposome Res.* **2008,** *4* (1), 71-91.

81. Li, J.; Wang, X.; Zhang, T.; Wang, C.; Huang, Z.; Luo, X.; Deng, Y., A review on phospholipids and their main applications in drug delivery systems. *Asian J. Pharm. Sci.* **2015,** *10* (2), 81-98.

82. Liu, P.; Chen, G.; Zhang, J., A review of liposomes as a drug delivery system: current status of approved products, regulatory environments, and future perspectives. *Molecules* **2022,** *27*, 1372.